

DISS. ETH NO. 24812

**Development of remote-sensing based approaches to evaluate  
sugar beet responses to nematode stress**

A thesis submitted to attain the degree of

**DOCTOR OF SCIENCES of ETH ZURICH**

(Dr. sc. ETH Zurich)

presented by

**Samuel Joalland**

**Diplôme d'Ingénieur Agronome**

Montpellier SupAgro

Centre international d'études supérieures en sciences agronomiques

Born on 28.01.1988

citizen of France

Accepted on the recommendation of

Prof. Dr. Achim Walter, examiner

Dr. Claudio Screpanti, co-examiner

Dr. Frank Liebisch, co-examiner

Prof. Dr. Jeremie Lecoer, co-examiner

2017



---

“They did not know it was impossible so they did it”

**Mark Twain**



## Summary

Improving crop production through the use of better cultivars and sustainable crop management practices is a necessity to feed 9.7 billion people in 2050. To achieve this goal, high quality phenotypic data are required for breeding projects and crop protection programs. In the last decade, many non-invasive root phenotyping methods have been developed under controlled and field conditions. The main objective is the fast and accurate evaluation in a non-destructive manner of traits related to root architecture, root biomass or stress caused by soil borne disease for example. Current methods are usually very crop and platform specific. Most of them are restricted to greenhouse conditions and cannot be directly applied for high throughput breeding program or the discovery and development of new crop protection molecules.

In the present thesis, we used the sugar beet crop as a model plant. The organ of interest for yield is the storage root, which grows and develops over the whole vegetative stage. Sugar beet canopy rosette architecture is particularly suitable for aboveground phenotyping. In this work, we intended to contribute to the field of crop phenotyping by deeply investigating the use of indirect non-destructive methods to detect and identify the effects of a biotic stress occurring belowground: the beet cyst nematodes (BCN), on the plant growth. Different remote sensing methods have been used and compared against each other at different scales (greenhouse, semi-field and field), on different sugar beet cultivars, for their abilities to characterise the growth and status of the sugar beet roots under nematode infestation.

The use of top digital imaging in a controlled environment (greenhouse) showed great ability for plant biomass accumulation prediction. Under artificial and moderate nematode infestation, canopy area was of great interest to precisely estimate leaf and root biomass in the early sugar beet growth stages. Such trait allowed to discriminate BCN infested and non-infested susceptible plants already after the apparition of the first two true leaves. It confirmed that BCN stress delays the canopy growth. Canopy area appeared a suitable trait to evaluate the degree of inhibition of the sugar beet biomass accumulation.

In the semi-field, sugar beet plants could be grown under more natural field conditions until harvest while ensuring moderate and homogenous nematode infestation in particular microplots set-up with a sufficient confined volume of soil (150 l). The semi-field platform enabled the precise comparison of the abilities of digital imaging, spectrometry and

thermography to identify BCN damage and predict final sugar beet yield at different times during the growth. As expected, digital images were suitable during the early growth stages when leaves were not overlapping each other. Canopy area could be used to discriminate infested and non-infested plants on both nematode susceptible and tolerant cultivars and predict the final yield. Spectrometry and thermography showed benefit in the BCN stress identification at more advanced growth stages when the canopy was fully developed. Canopy temperature was higher for the nematode infested sugar beets, reflecting BCN effect on the root water uptake and transpiration rate of the plant canopy. Spectral data allowed to compute a large variety of spectral indices (SIs). Some of them such as chlorophyll index (CHLG), normalised difference vegetation index (NDWI) or health index (HI), related to chlorophyll content, water content and general plant stress respectively, were suitable to discriminate symptom types caused by nematodes on two types of cultivars over three years of experimentations. They also showed high correlations with final yield ( $R^2=0.48$  on average for the susceptible cultivar).

Among the three methods tested in the semi-field, digital imaging was the most promising one. Image acquisition and processing are fast and easy and the approach can be used as soon as sugar beet seedlings emerged from the soil. This is not the case for spectrometry and thermography approaches which have a low spatial resolution making difficult to extract accurate canopy information in the early growth stages. In addition, the use of advanced computer vision methods showed that more canopy traits could be extracted from top images. Single leaves could be identified and counted from two to eight leaf growth stage. Indirect evaluation of the leaf area revealed that both leaf apparition and leaf expansion rates were affected by nematodes. Use of *Fosthiazate* nematicide demonstrated that it was crucial and sufficient to protect sugar beet seedlings against nematode infestation during the first month of growth when the root system is small and weak. Under controlled nematode infestation conditions (greenhouse and semi-field), our results demonstrated the potential use of canopy area as a trait of interest for early evaluation of nematicide efficacy and for yield prediction.

Greenhouse and semi-field investigations were followed by an open-field study with a moderate nematode infested level. The response of several susceptible and tolerant cultivars from four different seed providers was evaluated. Field spectral measurements and thermal images were acquired and compared with unmanned aerial vehicle (UAV) hyperspectral measurements. SIs computed from the field spectral data and the UAV hyperspectral images confirmed results previously observed in the semi-field. Several SIs were able to detect stress

caused by BCN and discriminate the response of nematode susceptible and tolerant cultivars. Both spectral and hyperspectral tools led to similar results demonstrating that UAV hyperspectral imager has a great potential to replace ground phenotyping measurements and generate maps of nematode distribution and yield potential. Combination of SIs through the use of univariate decision trees made possible the precise classification of susceptible and tolerant cultivars and the differentiation of the cultivar genetic backgrounds (seed providers). Cultivar type classification could also be performed using canopy temperature, which was higher for the susceptible cultivars.

Overall, this PhD thesis presents an innovative approach for plant phenotyping research by focusing on a single plant model, comparing several tools at different scales and combining fundamental and applied research. The different methods investigated in the greenhouse, semi-field and field presented diverse abilities in detecting nematode symptoms, evaluating the sugar beet growth and predicting yield. The non-specificity of BCN symptoms makes the remote nematode identification alone not certain in the field. Remote measurements should always be combined with a reduced number of ground truth assessment (soil sampling) to confirm the diagnostic. Digital image has potential to be implemented under controlled conditions for nematicide screening while in the field UAV hyperspectral imager showed great abilities for nematode tolerance breeding programs and crop management optimization.





## Résumé

L'amélioration de la productivité des cultures par l'usage de meilleures variétés et de pratiques culturales durables est une nécessité pour nourrir 9.7 milliards d'habitants en 2050. Pour atteindre ce but, il est nécessaire d'avoir des données phénotypiques de bonne qualité pour les projets de sélection variétale et les programmes de protection des cultures. Dans la dernière décennie, de nombreuses méthodes non invasives de phénotypage des racines ont été développées en conditions contrôlées et en plein champ. L'objectif principal est l'évaluation rapide et précise, de façon non destructive, de traits liés à l'architecture racinaire, la biomasse racinaire ou le stress induit par des maladies du sol. Les méthodes actuelles sont généralement très spécifiques à une culture et un type de plateforme. Beaucoup d'entre elles sont restreintes à une utilisation en conditions contrôlées et ne peuvent être directement appliquées à des programmes de sélection variétale haut débit ou à la recherche et au développement de nouvelles molécules de protection des cultures.

Dans cette thèse, nous avons utilisé la betterave à sucre comme plante modèle. L'organe d'intérêt pour le rendement est la racine pivot qui se développe tout au long de la croissance de la plante. L'architecture en rosette du feuillage de la betterave à sucre est particulièrement appropriée pour le phénotypage de la partie aérienne. Cette thèse a pour but de contribuer au domaine du phénotypage des plantes en étudiant l'utilisation de méthodes indirectes non destructives pour détecter et identifier les effets du nématode à kyste de la betterave sur la croissance de la plante. Plusieurs méthodes de télédétection ont été utilisées et comparées à différentes échelles (serre, semi-field et plein champ), sur différentes variétés, pour leur capacité à caractériser la croissance et l'état des racines de betteraves infestées par des nématodes.

Les images digitales prises au-dessus de la canopée en conditions contrôlées (serre) ont offert de bons résultats pour la prédiction de l'accumulation de biomasse de la plante. Sous infestation artificielle et modérée de nématodes, le paramètre « surface de la canopée » est apparu très intéressant pour estimer précisément la biomasse des feuilles et des racines durant les premiers stades de croissance des plants de betterave. Ce type de trait a permis de différencier les plantes infestées et non infestées par les nématodes, et ce dès l'apparition des deux premières vraies feuilles. Cela a confirmé que le stress causé par les nématodes retarde le développement du feuillage. La surface de la canopée est donc un trait approprié pour évaluer le degré d'inhibition de l'accumulation de biomasse.

Dans le semi-field, les betteraves à sucre ont pu être cultivées dans des conditions naturelles, similaires au champ, jusqu'à la récolte, tout en assurant un niveau d'infestation de nématodes homogène et modéré dans les « microplots » de 150 l. Cette plateforme a permis de comparer précisément la faculté des images digitales, de la spectrométrie et de la thermographie à identifier les dommages causés par les nématodes à différents moments pendant le développement et à prédire le rendement final. L'utilisation des images digitales est très appropriée pendant les premiers stades de développement lorsque les feuilles ne se superposent pas. La surface de la canopée a pu être utilisée pour différencier les plantes infestées et non infestées sur des variétés susceptibles et tolérantes aux nématodes et pour prédire le rendement final. La spectrométrie et la thermographie se sont montrées plus adaptées pour l'identification du stress causé par les nématodes à des stades de croissance plus avancés lorsque la canopée est entièrement développée. La température du feuillage était plus grande pour les betteraves infestées par les nématodes, reflétant l'effet des nématodes sur le prélèvement d'eau des racines et la transpiration du feuillage. Les données spectrales ont permis de générer une grande diversité d'indices spectraux. Certains d'entre eux comme CHLG, NDWI ou HI, liés respectivement au taux de chlorophylle, au contenu en eau et au stress général de la plante, se sont montrés particulièrement adaptés pour discriminer les types de symptômes causés par les nématodes sur deux variétés de betteraves. Ces indices ont aussi montré des corrélations élevées avec le rendement final ( $R^2=0.48$  en moyenne pour la variété susceptible).

Entre les différentes méthodes testées dans le semi-field, l'imagerie digitale est apparue la plus prometteuse. L'acquisition et le traitement des images sont simples et rapides et cette approche peut être utilisée dès que les pousses de betteraves sortent du sol. Cela n'est pas le cas pour la spectrométrie et la thermographie qui ont une faible résolution spatiale, rendant difficile l'extraction précise des informations liées au feuillage dans les premiers stades de développement des betteraves. De plus, l'utilisation de méthodes avancées d'analyse d'images a démontré que plus de traits relatifs au feuillage pouvaient être extraits des images de la canopée. Chaque feuille peut être identifiée et comptée depuis le stade « deux feuilles » au stade « huit feuilles » de la betterave. L'évaluation indirecte de la surface de chaque feuille a montré que la vitesse d'apparition des feuilles ainsi que la surface étaient affectées par les nématodes. L'utilisation du nématicide *Fosthiazate* a démontré qu'il était important et suffisant de protéger le système racinaire contre les nématodes pendant le premier mois de développement lorsque les racines sont petites et vulnérables. En conditions d'infestation

contrôlées (serre, semi-field), nos résultats indiquent qu'il est possible d'utiliser la surface de la canopée comme trait d'intérêt pour l'évaluation de l'efficacité de différents nématicides et pour la prédiction du rendement.

Les expériences en serre et semi-field ont été suivies par un essai en plein champ modérément infesté de nématodes. La réponse de plusieurs variétés susceptibles et tolérantes provenant de quatre semenciers différents a été évaluée. Des mesures de spectrométrie et des images thermiques ont été prises et comparées avec des mesures hyperspectrales obtenues à l'aide d'un drone. Les indices spectraux calculés en utilisant les données du spectromètre au sol et les images hyperspectrales du drone ont confirmé les résultats précédents obtenus dans le semi-field. Plusieurs indices spectraux permettent de détecter le stress causé par les nématodes et différencier la réponse de variétés susceptibles et tolérantes aux nématodes. Les deux outils de spectrométrie et d'hyper spectrométrie ont révélé des résultats similaires démontrant que l'imagerie hyperspectrale embarquée sur un drone pouvait remplacer les mesures de phénotypage au sol et générer des cartes de distribution des nématodes et de prédiction du rendement. La combinaison d'indices spectraux à travers l'utilisation d'arbres de décision univariés a rendu possible la classification des variétés susceptibles et tolérantes (précision de 75%) ainsi que la différenciation des bases génétiques des différents semenciers. La classification du type de variété a aussi pu être faite en utilisant la température de la canopée. Les variétés susceptibles ont été plus affectées par les nématodes. La température de leur feuillage était plus élevée que pour les variétés tolérantes.

Dans l'ensemble, cette thèse présente une approche innovante du phénotypage des plantes en se focalisant sur une seule plante modèle, en comparant plusieurs outils à différentes échelles et en combinant recherche fondamentale et appliquée. Les différentes méthodes de phénotypage étudiées en serre, semi-field et en champ ont montré des aptitudes différentes pour la détection des symptômes causés par les nématodes, pour l'évaluation du développement de la betterave et pour la prédiction du rendement. La non-spécificité des symptômes rend difficile l'identification certaine des nématodes par les méthodes non invasives. En plein champ, les mesures non destructives devront toujours être combinées avec un petit nombre de mesures (échantillonnage du sol) pour pouvoir confirmer le diagnostic. Les images digitales ont le potentiel d'être utilisées en conditions contrôlées pour la sélection de nématicides alors qu'en plein champ, les images hyperspectrales peuvent être implémentées pour la sélection de variétés tolérantes aux nématodes et pour l'optimisation des pratiques culturales.



# Table of Content

Summary.....	v
Résumé .....	ix
Table of Content.....	xiii
<b>Chapter 1. General introduction.....</b>	<b>1</b>
1.1 Challenges in plant phenotyping .....	2
1.2 Sugar beet crop .....	3
1.3 Beet cyst nematodes.....	4
1.4 Root phenotyping – Challenges and methods .....	7
1.4.1 <i>Direct root characterisation: the “Shovelomics” approach</i> .....	7
1.4.2 <i>Direct “In situ” root visualization</i> .....	8
1.5 Shoot phenotyping for indirect root evaluation and BCN detection .....	9
1.6 Project Background – From the greenhouse to the field.....	10
1.7 The microplot semi-field platform in Stein.....	12
1.7.1 <i>Platform presentation</i> .....	13
1.7.2 <i>Environmental characterisation and experimental design optimization</i> .....	14
1.8 General objectives .....	15
<b>Chapter 2. Belowground biomass accumulation assessed by digital image based leaf area detection.....</b>	<b>17</b>
2.1 Abstract.....	18
2.2 Introduction .....	19
2.3 Material and methods.....	22
2.3.1 <i>Plant growing</i> .....	22
2.3.2 <i>Evaluation of plants</i> .....	22
2.3.3 <i>Image based phenotyping: Data acquisition and processing</i> .....	23
2.3.4 <i>Statistical data analysis</i> .....	24
2.4 Results.....	25
2.4.1 <i>Leaf biomass and digital canopy area</i> .....	25
2.4.2 <i>Relationship between leaf and beet biomass</i> .....	26
2.4.3 <i>Use of canopy area to evaluate beet biomass</i> .....	28
2.4.4 <i>Effect of nematode infestation on the canopy area and plant biomass</i> .....	28
2.4.5 <i>Nematode effects on sugar beet growth</i> .....	29

2.5	Discussion .....	31
2.6	Conclusion and outlook.....	34
2.7	Acknowledgment .....	34
<b>Chapter 3. Comparison of visible imaging, thermography and spectrometry methods to evaluate the effect of <i>Heterodera schachtii</i> inoculation on sugar beets...35</b>		
3.1	Abstract .....	36
3.2	Background.....	37
3.3	Methods.....	40
3.3.1	<i>Plant cultivation</i> .....	40
3.3.2	<i>Preparation of the soil and nematode inoculum</i> .....	41
3.3.3	<i>Evaluation of plants and nematodes</i> .....	42
3.3.4	<i>Visible imaging</i> .....	43
3.3.5	<i>Thermography</i> .....	43
3.3.6	<i>Spectrometry</i> .....	44
3.3.7	<i>Statistical data analysis</i> .....	46
3.4	Results.....	47
3.4.1	<i>Plant fresh weight and nematode population</i> .....	47
3.4.2	<i>Early stress detection using visible imaging</i> .....	48
3.4.3	<i>Canopy temperature evaluation using thermography</i> .....	50
3.4.4	<i>Nematode stress identification by a spectrometry approach</i> .....	51
3.4.5	<i>Phenotyping parameters and final data</i> .....	52
3.4.6	<i>Practical application of visible imaging for nematicide research</i> .....	53
3.5	Discussion .....	55
3.6	Conclusions .....	59
3.7	Acknowledgment .....	59
<b>Chapter 4. Application of a leaf segmentation method to detect stress caused by nematodes on sugar beet plants ..... 61</b>		
4.1	Abstract .....	62
4.2	Introduction.....	63
4.3	Material and methods .....	65
4.3.1	<i>Sugar beet growing</i> .....	65
4.3.2	<i>Image capture</i> .....	65
4.3.3	<i>Image analysis</i> .....	66
4.3.4	<i>Data analysis</i> .....	67

---

4.4	Results and discussion .....	68
4.4.1	<i>Evaluation of the algorithm</i> .....	68
4.4.2	<i>Identification of nematode stress</i> .....	69
4.5	Conclusions .....	72
4.6	Acknowledgment.....	72
<b>Chapter 5. Multi sensors approach for the evaluation of sugar beet cultivar tolerance to the Beet Cyst Nematode in the field.....</b>		<b>73</b>
5.1	Abstract.....	74
5.2	Introduction .....	75
5.3	Material and methods.....	78
5.3.1	<i>Experimental site</i> .....	78
5.3.2	<i>Experimental design</i> .....	78
5.3.3	<i>Plant and nematode evaluation</i> .....	79
5.3.4	<i>In field thermography and spectrometry</i> .....	80
5.3.5	<i>Hyperspectral imaging</i> .....	80
5.3.6	<i>Spectral vegetation indices</i> .....	81
5.3.7	<i>Statistical data analysis</i> .....	82
5.4	Results.....	84
5.4.1	<i>Spatial BCN distribution in the field</i> .....	84
5.4.2	<i>Beet fresh weight and nematode population</i> .....	85
5.4.3	<i>Thermography</i> .....	87
5.4.4	<i>Spectrometry and UAV hyperspectral imaging</i> .....	89
5.4.5	<i>Field spectrometer versus UAV hyperspectral imager</i> .....	92
5.4.6	<i>Multivariate analysis</i> .....	92
5.5	Discussion.....	96
5.6	Conclusions .....	100
5.7	Acknowledgment.....	100
<b>Chapter 6. General discussion .....</b>		<b>101</b>
6.1	Sugar beet phenotyping under controlled conditions .....	103
6.1.1	<i>Nematode stress detection</i> .....	103
6.1.2	<i>Applications in the research context – Challenges and opportunities</i> .....	106
6.2	Sugar beet phenotyping in the field .....	107
6.2.1	<i>Sugar beet cultivar characterisation and classification</i> .....	107
6.2.2	<i>Applications in the field – Challenges and opportunities</i> .....	108

6.3	Semi-field platforms for phenotyping tools development and crop modelling.....	110
6.4	Conclusion and outlook.....	111
<b>7.</b>	<b>List of abbreviations .....</b>	<b>113</b>
7.1	General abbreviations.....	113
7.2	Spectral indices .....	114
<b>8.</b>	<b>Literature .....</b>	<b>115</b>
<b>9.</b>	<b>Acknowledgement .....</b>	<b>135</b>
	<b>Curriculum vitae.....</b>	<b>137</b>



## **Chapter 1.**

### **General introduction**

## 1.1 Challenges in plant phenotyping

In the quest of ensuring sufficient crop production for the needs of a growing human population, crop improvement, crop protection and plant science in general play essential roles (Cobb et al. 2013). Advances in techniques such as next generation sequencing or genome editing enable breeders to increase the rate and efficiency of genetic amelioration (Araus and Cairns 2014). In addition, the optimization of crop management practices through an efficient use of crop protection products facilitates yield increase while ensuring sustainable agriculture (Pingali 2012, Dobermann and Nelson 2013). However, the lack of access to specific phenotyping capabilities limits our ability to evaluate traits related to plant growth, yield, abiotic or biotic stresses. This reduces the breeding efficiency and the rate of new development of crop protection technology (Araus and Cairns 2014). Thus, it is crucial to develop phenotyping approaches and platforms enabling the evaluation of multiple traits in a fast and accurate manner.

Plant phenotyping is the evaluation of specific plant traits resulting from an interaction of genetics (gene expression, gene regulation) and environmental influences. From a more practical perspective, plant phenotyping can be defined as “the application of automated, high throughput methods to characterise plant architecture and performance” (Walter et al. 2012). The plant phenotype includes a broad range of traits related to growth, architecture, yield, physiology, development, tolerance and resistance. Direct measurements of these complex traits are parameters like root morphology (Walter et al. 2009; Clark et al. 2011), plant biomass (Golzarian et al. 2011; Joalland et al. 2016), photosynthetic efficiency (Bauriegel et al. 2011), yield components (Duan et al. 2011), biotic or abiotic stress response (Rao et al. 2016). Recently, several tools or methods have been developed to investigate with accuracy, high throughput and in a non-destructive manner these parameters on a large variety of plant species, intending to replace labour intensive, time consuming and not always repeatable manual evaluation. Among them we can mention imaging technologies such as digital imaging, fluorescence imaging, thermal imaging, hyperspectral imaging, 3D imaging, laser imaging or X-ray computed tomography (Li et al. 2014). Some phenotyping tools are also based on non-imaging sensor systems such as specific reflectance or fluorescence sensors. While non-imaging sensors average the reflectance over a specific area, imaging sensors allow to consider spatial information. In recent years, imaging tools have increasingly replaced non-imaging applications. Many high throughput phenotyping platforms have been developed based on the combination of image based novel technologies and high throughput dynamic

controlled environment facilities (Granier et al. 2006; Jansen et al. 2009; Arvidsson et al. 2011; Rahaman et al. 2015). Despite the high precision and efficiency in the quantification of traits, these platforms lack of flexibility and their use is restricted to a certain crop grown under specific conditions. In order to consistently evaluate plant phenotypes over different scales and environments there is a need to develop effective and reliable methods that can be deployed across platforms. In the present thesis, several non-destructive phenotyping methods were tested at different scales on sugar beet using the disease pressure of beet cyst nematodes (BCN) as an illustrative use case.

## 1.2 Sugar beet crop

Sugar beet (*Beta vulgaris*) is a crop belonging to the family *Chenopodiaceae* mainly grown for sugar production (Franke 1997). The storage root contains a high concentration of sucrose (up to 20%). Today, all commercial varieties of sugar beets are hybrids that are selected for high sugar yield, disease resistance, low soil tare and resistance to bolting. In the United States, a large proportion of commercial sugar beets are genetically modified for resistance to the herbicide *Glyphosate* (Monsanto Company, MO, USA). Twenty percent of the world's supply of sugar is derived from sugar beet (FAO 2009). In 2014, the world production of sugar beets has been approximately 270 million tons grown on 4.5 million ha (FAO 2017). The EU is the world's leading producer with a production of 102 million tons of sugar beet in 2015, which represented around 50% of the global production (Eurostat 2015). In Europe, sugar beet is mostly grown in the Northern half under a temperate climate. The main producing areas are in northern France, Germany, the UK and Poland. The by-products of the sugar beet, such as pulp and molasses, give an additional 10% value (animal feed) to the value of the sugar (Rezbova et al. 2013). In addition, sugar beet yields more energy per hectare than any other crop, which make this crop a great option for production of bioenergy. Overall, sugar beet is a very profitable crop for growers and sugar producing companies.

From an evolutionary point of view, sugar beet is a biennial dicotyledonous plant. The crop stores sugar in the roots during the first growing season (vegetative development) and switches to reproductive development, once vernalised, during the second year. The roots are harvested at the end of the first year for sugar production. Different phases in sugar beet biomass allocation have been identified and described: an early phase of leaf-dominated growth is followed by a phase dominated by growth of the storage root that is followed then by a phase of sugar storage (Fig. 1.1) (Green et al. 1986).



**Figure 1.1. Phenological stage of sugar beet crop. Plant growth stages are defined according to the BBCH scale (Meier et al. 1993). Adapted from <https://www.cropscience.bayer.co.nz>.**

Therefore, sugar beet appears an interesting model plant for phenotyping since the organ of interest is developing during the whole vegetative period. In addition, during the vegetative development, single leaves appear individually and horizontally on a 5:13 phyllotaxis, which gives the sugar beet plant a “rosette” architecture (Stehlik 1938; Milford 1985b). The planophile leaf structure and the direct relationship between root and canopy development make the sugar beet crop highly suitable for remote sensing evaluation (Milford et al. 1988).

### 1.3 Beet cyst nematodes

The BCN *Heterodera schachtii*, first described in 1859 in Germany, is a microscopic soil borne pathogen, which can infect more than 200 different plant species in 23 families (Steele 1965; Harveson and Jackson 2008). Among them, BCN affects economically important crops such as cabbage, broccoli, radish and sugar beet. BCN is distributed worldwide and is the most important pest of sugar beet in Central Europe (Müller, 1999). It can cause significant sugar beet yield losses up to 60% (Biancardi et al. 2010).

BCN occurs in patches in the field and has a low mobility (Jones 1980; Avendano et al. 2004). When stimulated by optimal soil moisture (80 to 100% of the field capacity), temperatures (20 to 27 °C), compact soils and root exudates from a suitable host crop, second stage juveniles (J2s) hatch from the cysts (Fig. 1.2) (Glenn and Sivasithamparam 1990; Laemmlen 2010). After migrating through the soil, J2s enter the host roots and migrate intracellularly through

the root cortical cells toward the vascular cylinder to establish a feeding site to create a syncytium (Siddique et al. 2015; Gardner et al. 2015).

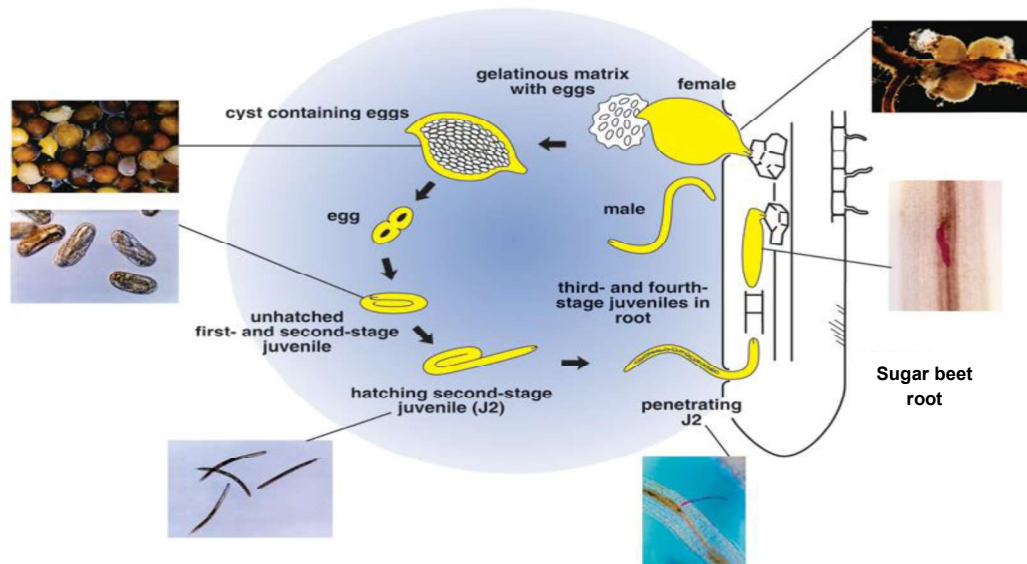


**Figure 1.2. BCN life cycle (adapted from Dirk Charlson, Iowa State University).**

Hatching, penetration and infection of the roots can occur within a few days (Cooke 1987). After three molts, J2s reach the adult stage. The sex of J2s is determined by environmental factors. Under favorable conditions in susceptible cultivars, female formation is promoted, whereas adverse conditions in resistant cultivars promote the development of males (Ellenby 1954). Male nematodes stop feeding in the roots and leave the feeding site to search for females to mate. After mating, hundreds of eggs will be produced inside the enlarged body of the females, which forms the protective cyst (Wyss et al. 1992). Cysts might stay attached to the roots or be released into the soil. The next generation of J2s can then hatch and colonise the roots. The development period of one generation of BCN depends on the prevailing meteorological conditions. For the completion of a whole cycle an accumulated temperature of 437 degree-days (Base soil temperature of 8°C), which corresponds on average to 4-6 weeks, is essential (Curi et Zmoray 1966). Soil physical properties also play a role in the life cycle. Soil texture and soil moisture contents influence nematode development (Cooke 1984). Under central European conditions, two to three life cycles can occur on average per year in the field (Müller 1979). In the strong-walled cyst, the eggs and larvae remain viable for more than 10 years.

Symptoms of belowground direct BCN damage include poor plant stands and reduction of the beet growth due to nutrient deficiency (Laemmlen 2010). Nematode infestation often leads to the appearance of many secondary roots to compensate for those infested (Decker 1969). BCN also cause aboveground symptoms like stunted growth, decreased chlorophyll content and wilting of the canopy due to water stress (Cooke 1987; Schmitz et al. 2006). These BCN damage reduce the overall tolerance or resistance of the sugar beet plant to other biotic or abiotic stresses.

In order to manage the damage caused by BCN, several farming practices are in use. The most common one is crop rotation with non-host crops. The use of so called “trap crops” such as white mustard or fodder radish has shown beneficial results in reducing the BCN population in the soil (Cooke 1991; Koch et al. 1999; Hafez and Sundararaj 2009), which allows for nematodes to hatch but does not allow for the establishment of good feeding sites. Other practices to avoid the multiplication of nematodes in the field involve early planting, use of chemical solutions (seed treatment or in-furrow application) or use of tolerant and resistant varieties. BCN tolerant cultivars can withstand nematode infestation and endure damage. They can have yield potential comparable with susceptible cultivars and a smaller yield drag in presence of nematodes (Anon 2016). However, most of the tolerant cultivars still increase the BCN population in the soil (final nematode population (pf) / initial nematode population (pi) = pf/pi reproduction rate ratio >1) (Reuther et al. 2017). Resistant cultivars do not support female development, which restricts BCN reproduction and therefore decrease the nematode population in the soil (Pf/Pi <1) (Wallace 1988; Davy de Virville and Person-Dedryver 1989; Stelter 1963, Kämpfe and Kerstan 1964). Their main disadvantage is the low yield potential, which makes them less attractive than tolerant cultivars in infested fields.

Dedicated strategies have been developed to identify BCN infested areas in the field. A first approach consists in evaluating whether the level of infestation in the field is above a given economical threshold thereby justifying specific nematode control methods. However, soil sample analysis are expensive and technically difficult because of the cluster distribution of BCN in the field (Evans et al. 2002; Wyse-Pester et al. 2002). Around 100 samples per hectare are required to achieve a reasonable estimation of the potential crop damage. In research and development of new crop protection technologies or new genotypes, studies consist in evaluating the efficacy of the solutions by looking at the number of nematodes in the soil and in the root and/or evaluating the impact on the final yield. This implies time consuming assessments of the sugar beet plants and for field trials to keep the trial up to harvest. The use

of non-destructive measurements would allow to early detect and quantify the nematode stress and predict the final yield, which will help the development of new solutions and the selection of the best countermeasures in the field. Thus, there is a need to develop reliable phenotyping methods that can be used either under controlled and field conditions to identify nematode symptoms on sugar beets.

## **1.4 Root phenotyping – Challenges and methods**

In earlier days, the normal way to test for improvements of the root system was to excavate or inspect root systems directly. Several traits could be evaluated precisely but assessments usually required destructive measurement and/or invasive tools disturbing the plant growth. There are two traditional techniques to directly study the root growth. They are based on direct root evaluation or visualization: the shovelomics approach and the direct in situ root visualization approach.

Root phenotyping is a specific case of plant phenotyping and is particularly difficult since roots are hidden in the ground (Walter et al. 2015). Although root system architecture is crucial for plant productivity, it has only received a little attention in the past few years in comparison to shoot phenotyping (Furbank and Tester 2011). More specifically, high throughput phenotyping for root pathogens is not as advanced as shoot phenotyping. This can be explained by the complexity of directly investigating the root system through the growing media (Zhu et al. 2011).

### **1.4.1 Direct root characterisation: the “Shovelomics” approach**

The term “Shovelomics” was first used by Trachsel et al. (2011) for the process of excavating plants from the field to evaluate the root system. In this destructive approach, plants are removed from their growing media before being evaluated. Several techniques can be used to analyse the roots such as rating, counting or imaging (Grift et al. 2011; Bucksch et al. 2014). Advanced shovelomics approaches use image analysis to extract traits of interest related to branching, root length and size (Colombi et al. 2015).

On sugar beets, such destructive methods are used to understand plant-pathogen interactions by weighing the roots, counting the number of white to brown cysts attached to the root surface, visually evaluating the number of compensatory secondary roots (“bearded” root symptom) and rating beet deformity (Cooke 1987; Hillnhütter et al. 2011).

The shovelomics method is very straightforward and accurate but it has the main disadvantage of being destructive and very time consuming. Its value still has to be demonstrated in delivering yield-related traits that cannot be measured at the canopy level (Walter et al. 2015).

#### **1.4.2 Direct “In situ” root visualization**

The second set of techniques used to directly investigate plant root systems consists in in-situ root visualization. Under controlled conditions, soil-free media such as paper rolls, gels or hydroponic solutions facilitate the evaluation of root length, branching or density with the use of visual rating or imaging devices (Tuberosa et al. 2002; Bengough et al. 2004; Watt et al. 2013; Le Marié et al. 2014). Soil based 2D- or 3D- methods such as rhizotrons (Devienne-Barret et al. 2006; Nagel et al. 2012; Mathieu et al. 2015; Paez-Garcia et al. 2015), X-ray tomography (Mooney et al. 2012; Pfeifer et al. 2015) or Nuclear magnetic resonance imaging (MRI) (Nagel et al. 2009; Schulz et al. 2013, Van Dusschoten et al. 2016) have also been developed to visualise and characterise the root system architecture in a real soil matrix. Several plant traits such as root length, root density or root diameter can be evaluated over time. These methods are non-destructive; roots can grow and develop in a real field soil media. Mini-rhizotrons have also been developed for the field. They consist of transparent plastic tubes inserted into the soil, in which a camera can be introduced to inspect the roots (Johnson et al. 2001). Electrical capacitance measurements in the field have shown results in the evaluation of the root biomass and root architecture (Chloupek et al. 2006; Dietrich et al. 2013).

MRI has been tested on sugar beet to evaluate several structural and functional traits on the root system and storage organ and to directly observe damage caused by nematodes on the roots such as excessive lateral root development and beet deformation (Jahnke et al. 2009; Metzner et al. 2014). Such technologies would allow to visualise cysts and syncytia of BCN (Hillnhütter et al. 2011).

Main disadvantages of these in-situ visualization methods are the disturbing effect of the apparatus on the roots, the small amount of soil used in rhizotrons, which does not allow to grow plants until harvestable stages, the small number of possible replicates in the case of X-ray tomography or RMI and the cost of the phenotyping tools. Thus, direct root phenotyping methods are not suitable for the cost effective and high throughput study of the nematode-plant interaction across environments (from the greenhouse to the field).



Since in sugar beet there is a strong link between number of nematodes and crop performance such as shoot development and root biomass accumulation (Seinhorst 1965; Cooke 1987; Franke 1997), I propose in this thesis, alternative methods to investigate the root system. These methods are based on the non-destructive observation of the belowground damage via the evaluation of the aboveground shoot performance.

### **1.5 Shoot phenotyping for indirect root evaluation and BCN detection**

Investigating roots using aboveground phenotyping parameters postulates the existence of high correlations between above and belowground part of the plants. Remote sensing methods have been widely used for non-destructive plant phenotyping in the lab and in the field. As described above, remote sensing technologies enable the characterisation of morphological or physiological traits on the plants such as plant biomass (Golzarian et al. 2011; Arvidsson et al. 2011), photosynthesis status, leaf canopy water status, canopy architecture or foliar disease. Such traits can be directly evaluated using leaf reflectance in various regions of the electromagnetic spectrum. It has been observed that any disturbance in the root induced by soil-borne pathogens like nematodes, induces changes in the chlorophyll or water content of the leaves (see for example (Cooke 1987; Schmitz et al. 2006)). Such changes lead to differences in leaf reflectance, which could be detected before they become visible. Thus, the close relationships between above and belowground parts of the sugar beet plants make them of interest for the indirect characterisation of the root system status and soil pathogen damage.

In 1927, first remote sensing black and white visible images of a cotton field were taken from an airplane to estimate damage and yield loss caused by the cotton rot (*Phymatotrichum omnivorum*) (Taubenhaus et al. 1929). Infrared images were first used to detect the burrowing nematode *Radolpholus similis* in citrus trees before visible symptoms could be observed (Norman and Fritz 1965). In the 70's, studies have been conducted using infrared images or spectroradiometers to detect symptoms caused by nematodes and root rot on cotton and avocado trees (Heald et al. 1972; Brodrick et al. 1971; Gausman et al. 1975). Most of the studies on the use of aerial images for the detection of soil-borne pathogen up to 1980 were summarised by Lee (1989). With the improvement of the remote sensing technologies, high precision could be achieved in the detection and quantification of nematode in the soil. Heath et al. (2000) used the Normalised difference vegetation index (NDVI) computed from a field spectrometer to predict the number of juveniles per gram of potato roots. Using narrowband

hyperspectral sensors, Nutter et al. (2002) built a map of the spatial distribution of soybean cyst nematode (*Heterodera glycines*) in soybean fields and predicted with high accuracy the initial nematode level and the final yield.

To our knowledge only few studies have been conducted on the detection of stress caused by *Heterodera schachtii* on sugar beets using non-destructive phenotyping methods. Schmitz et al. (2006) revealed the ability of remote sensing thermography at field level to detect small changes in the canopy temperature of BCN-infested susceptible sugar beets. This study confirmed results obtained by Berg (1980) who was able to discriminate BCN infested areas and non-infested ones in the field. NDVI computed from near range spectrometer showed high potential to evaluate the symptoms caused by BCN on sugar beet plants under controlled conditions (Hillnhütter et al. 2010). In field experiments, the use of specific SVIs to predict the final beet yield and the nematode population in the soil has also been reported using a field spectrometer and a drone hyperspectral imager (Hillnhütter et al. 2011). Thus, infrared thermography and spectrometry appear to be suitable phenotyping tools for the remote detection of belowground symptoms caused by BCN. However, these technologies require the use of expensive devices and complex data analysis methods.

Alternatively, standard visible / digital imaging technology can be used for sugar beet phenotyping. This technology is cheap since it uses low cost sensors and the devices are easy to handle and calibrate (Li et al. 2014). The projected shoot area of the plants, the canopy cover, is usually calculated and used as a parameter to predict shoot biomass in different plant species (Sher-Kaul et al. 1995; Smith et al. 2000; Mizoue et Masutani 2003). The canopy cover can be used to non-destructively assess early vigor-related traits (Mullan and Reynolds 2010; Grieder et al. 2015, Kirchgessner et al. 2017). Visible imaging combined with computer vision methods enables the analysis of several morphological and yield related traits (Duan et al. 2011; Hoyos-Villegas et al. 2014). Since shoot biomass is affected by nematodes, the use of the “digital canopy area” appears a suitable proxy to investigate the degree of stress caused by nematodes on the sugar beet plants during the early plant developmental stage.

## 1.6 Project Background – From the greenhouse to the field

Phenotyping methods investigated during the PhD project were tested at three different scales: Greenhouse, semi-field and field (Fig. 1.3). In modern breeding programs for new cultivars and in the screening cascade to discover and develop new chemical crop protection molecules, these three types of platforms play a crucial role. In the greenhouse, the

environment is fully controlled and monitored. Plants are usually grown for few days to few weeks in small pots or containers where the disease pressure can be controlled and monitored. Thousands of compounds against pathogens and diseases can be tested in the greenhouse every year. Conversely, in the field, plants are grown until harvest under realistic and uncontrolled conditions. Levels of infestation cannot be controlled, which makes field trial evaluation very complex but agronomically more relevant and realistic. The semi-field platform is a complementary type of platform in between the greenhouse and the field. Semi-field methods have first been developed for ecotoxicology studies (Schäffer et al. 2008) for the risk assessment of agrochemicals. Such platforms are generally built outdoor and comprise a rain shelter. Trials can be carried out directly in the ground, in pots or in specific growing systems.

Semi-field platforms are designed to combine advantages from the greenhouse and from the field (Schäffer et al. 2008). On one hand, the system allows the control of key parameters like soil type, soil moisture or disease pressure. On the other hand, the platform can be fully open and plants can be grown until harvest under realistic and complex field conditions (natural variability of temperature, relative humidity, sunlight) (Fig. 1.3).

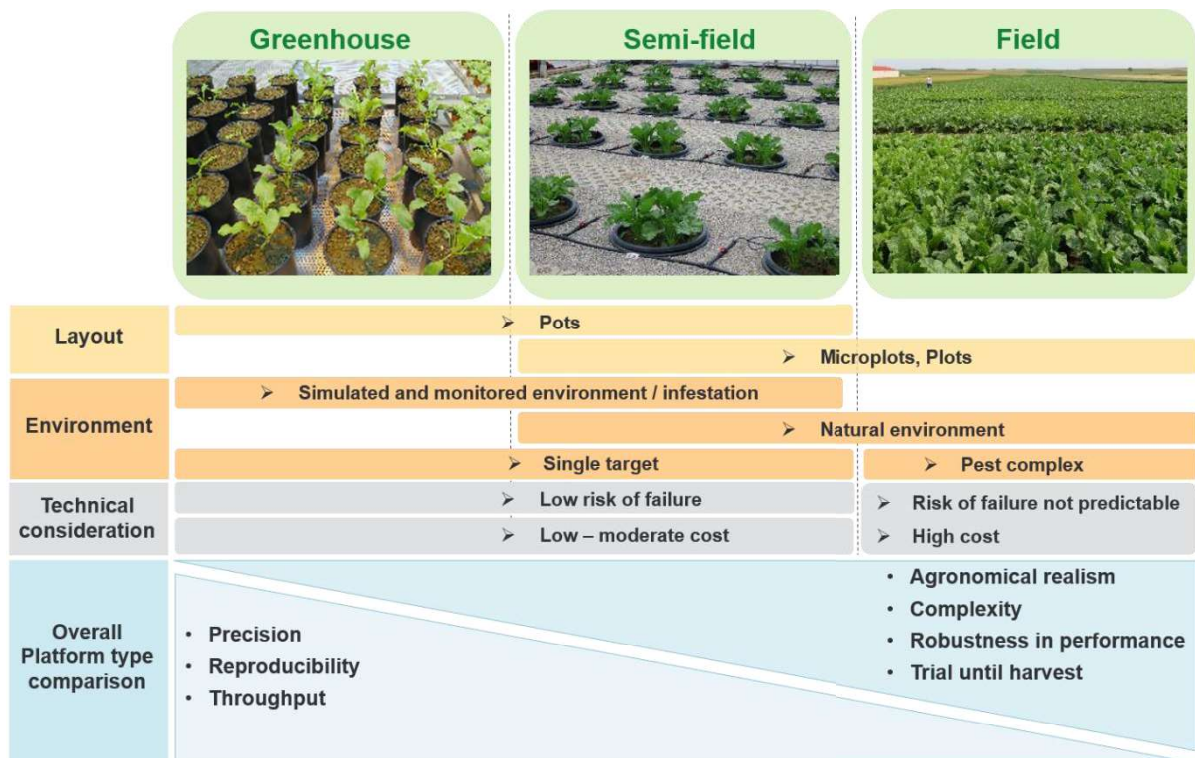


Figure 1.3. Comparison of greenhouse, semi-field and field platforms (Adapted from Schäffer et al. 2008).

The three types of platforms show different abilities for phenotyping method development. Greenhouse and semi-field platforms appear particularly suitable for primary investigations on the potential of different phenotyping methods in detecting the BCN pressure while field trials can be used for method validation under realistic and complex conditions. Both greenhouse and semi-field platforms enable the setup of accurate experiments and to easily perform measurements on growing plants.

In this PhD project, greenhouse investigations were carried out to evaluate the relationship between above and belowground parts of the sugar beet plants with and without nematode stress using digital images (Table 1.1). Semi-field studies were dedicated to the comparison of three non-destructive phenotyping methods to deeply investigate the root growth over time. Finally, field trial investigations were performed to validate the use of thermography and spectrometry under realistic conditions and open the doors for future applications. On the three platforms, the disease pressure of BCN was studied.

**Table 1.1. Overview of the three platforms used for sugar beet phenotyping.**

<b>Platform</b>	<b>Greenhouse</b>	<b>Semi-Field</b>	<b>Field</b>
<b>Volume of soil</b>	3L pots	150L microplots	Field plots
<b>Density of plants</b>	One plant per pot	Three plants per pot	100 000 plants per ha
<b>BCN infestation</b>	Artificial soil infestation	Artificial soil infestation	Natural soil infestation
<b>Duration of the trial</b>	7 weeks	3.5 months	5 months
<b>Phenotyping methods tested</b>	- Digital images	- Digital images - Thermography - Spectrometry	- Thermography - Spectrometry - Drone hyperspectral images
	<b>Chapter 2</b>	<b>Chapter 3 and 4</b>	<b>Chapter 5</b>

## 1.7 The microplot semi-field platform in Stein

Since substantial work has been performed on a microplot semi-field platform to compare the use of different phenotyping methods (Chapter 3 and 4) and since this platform will be used in the future with tests based on the approaches developed in this thesis, a precise description of this specific system is essential.

### 1.7.1 Platform presentation

A semi-field platform was developed by the Syngenta Seed Care Research group in Stein (Switzerland) in the past years. This platform aims to support the activities of screening and discovery of new solutions for crop protection, particularly for nematode control. The platform is 25 m long and 10 m wide and is protected by a rain shelter. The platform includes 70 microplots consisting of a pot in pot system (Fig. 1.4). One 150 cm<sup>3</sup> plastic container (65 cm diameter and 60 cm depth) is nested inside of another, with both recessed in the ground up to the rim to reduce fluctuation of soil temperature.



**Figure 1.4.** Overview of the Syngenta microplot semi-field platform (Stein, Switzerland).

Microplots are organised in ten columns and seven rows. The system allows the continuous monitoring of soil temperature and soil moisture. Three pots per column are equipped with two wireless soil moisture and temperature sensors (PlantCare Ltd, Switzerland) (one sensor at 10 cm depth and one at 35 cm depth). In total, sixty sensors were positioned on the platform. Each column was irrigated separately using an automated irrigation system connected to the soil moisture sensors. Eight weather stations were positioned following a grid sampling design on the semi-field platform at 50 cm high. Weather stations were equipped with a data logger (msr.ch) that recorded every hour the air temperature and the relative humidity.

This microplot system was inspired by the first semi-field experiment reported on nematodes using a system of microplot units (Pinkerton et al. 1989). This system allowed to study the spatial distribution of nematodes within the soil and plants. It also enabled to simulate field conditions with similar plant density and canopy conditions. In the last years, micro-plots

systems have been extensively used by research companies or institutes mainly for nematode or soil borne pathogens research.

### 1.7.2 Environmental characterisation and experimental design optimization

A full environmental characterisation has been performed on the microplot platform over four years of trials. Soil temperature sensors described above were used to map the soil temperature at 10 and 35 cm depth. Air temperature and relative humidity were also precisely characterised using the eight weather stations. In additions, seven photosynthetically active radiation (PAR) sensors (LI-COR Biosciences) were used to evaluate the light received on each individual microplot during the season as a function of the light received outside. Maps of soil temperature, air temperature, air relative humidity and PAR were built to evaluate the spatial variability of the environmental conditions on the microplot platform (Fig. 1.5).

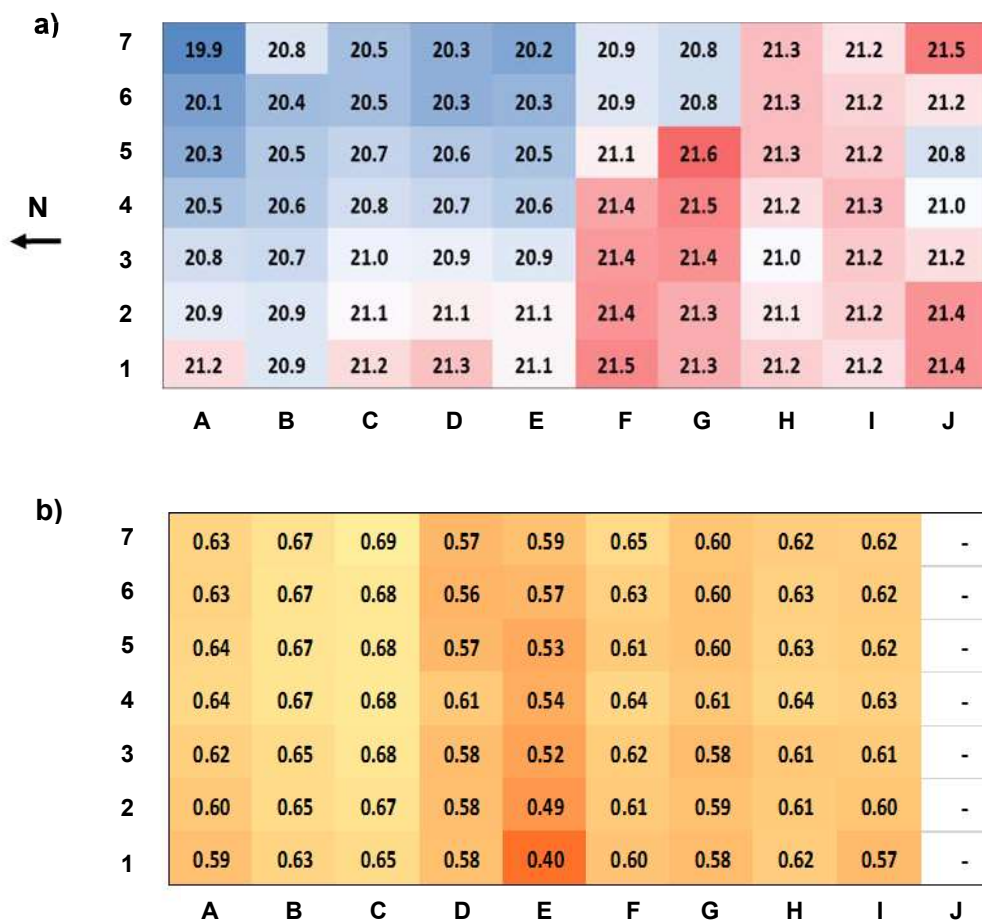


Figure 1.5. Maps of the a) average soil temperature ( $^{\circ}\text{C}$ ) at 10 cm depth during 2015 sugar beet trial (4<sup>th</sup> May to 27<sup>th</sup> August) and b) fraction of undisturbed PAR (outside of the shelter) received at 30 cm above ground.



Maps revealed the existence of a temperature gradient on the platform from North-East to South-West. On average there is 1.5°C difference between the two corners (Fig. 1.5a). This gradient can be explained by the semi-field structure. Plastic walls on the South part were generally closed, which limited airflow and increased temperature. In addition, another semi-field platform is located on the West side of the microplot reducing air circulation and increasing temperature on this side.

PAR evaluation showed that plants received, on average, 64% of the PAR they would receive outside. Light variability on the platform is mainly caused by the roof and walls of the platform that produce shadow on specific locations (Fig. 1.5b). Microplot E1 is located near the computer station and is prone to shading, which explains the low PAR received (40% of the outside PAR on average). The observed variability in temperature and light might have significant effects on the plant growth and therefore on the phenotyping measurements. This information has been used for the optimisation of the experimental design for the sugar beet trials and as co-factor for statistical analysis.

## 1.8 General objectives

The present thesis is aimed at investigating and comparing the ability of digital images, spectrometry and thermography to characterise the sugar beet growth over time and to detect stress caused by BCN on different cultivars. More specifically the objectives were to:

- Identify suitable parameters to detect symptoms of nematode damage on susceptible and tolerant cultivars
- Identify canopy-associated proxies to predict the final sugar beet yield
- Compare the potential of the methods to be used under controlled and field conditions for crop protection, breeding research and precision agriculture

This thesis thereby intended to contribute to the rapidly growing field of plant phenotyping by comparing the use of different methods on a single crops with a specific soil borne disease at three different scales of investigation (greenhouse, semi-field and field). While Chapter 2 is based on greenhouse results, chapters 3 and 4 focus on data obtained under semi-field conditions. Finally chapter 5 uses data acquired in a naturally infested field.

**Chapter 2** describes the use of top digital images to early evaluate the sugar beet root biomass and discriminate BCN infested and non-infested plants using the digital canopy area

parameter. These first results were obtained in the greenhouse. They confirmed the strong link between above and belowground part of the sugar beet plant and the opportunity to use the digital canopy area as a proxy for root growth.

**Chapter 3** presents a comparison of digital images, spectrometry and thermography to detect the stress caused by nematodes and predict the final sugar beet yield under semi-control conditions. It is based on two semi-field trials conducted with nematode susceptible and tolerant cultivars. Chapter 3 also demonstrates the ability of digital images to detect the effect of a nematicide very early and thereby shows the potential of digital imaging to be applied for the screening of new nematicides.

**Chapter 4** reports on an advanced use of nadir view digital images in the semi-field. It describes the ability of a computer vision method to identify and count sugar beet leaves from young seedlings. It shows the effect of nematode in delaying leaf appearance and decreasing leaf growth.

**Chapter 5** reports on the application of field spectroscopy, UAV hyperspectral imaging and thermography in the field to detect BCN stress, predict the final yield and rank the performance of several nematode susceptible and tolerant cultivars. The chapter also presents a comparison of field spectroscopy measurements with UAV hyperspectral measurements.

A general discussion of the presented topics is provided in **Chapter 6**.



## Chapter 2.

### Belowground biomass accumulation assessed by digital image based leaf area detection



Samuel Joalland, Claudio Srepani, Alain Gaume, Achim Walter

Plant and Soil (2016) 398: 257-266

Reprinted with permission from the peer-reviewed journal "Plant and Soil".

## **2.1 Abstract**

### **Aims**

Belowground plant biomass accumulation is facilitated by the photosynthetic capacity of the canopy. We investigated the hypothesis that a precise monitoring of leaf area development provides the potential to extrapolate to belowground biomass development and to assess the timing and the degree of an inhibition of the belowground biomass generation. Sugar beet seedlings and the retarding effect of beet cyst nematodes (BCN) were used as a model system.

### **Methods**

Thirty BCN infested plants and 30 non-infested plants were grown in three litre pots under greenhouse conditions. Top-view images of the plant leaf canopy were taken every two or three days. Leaf and beet biomass were measured at three different dates (32, 41 and 70 days after sowing (das)) by harvesting the plants.

### **Results**

Leaf dry weight and beet fresh weight were strongly correlated 32 and 41 das. The canopy area calculated was highly correlated with both leaf and beet biomass at 32 and 41 das, and was significantly reduced in the nematode infested plants from 22 to 60 das.

### **Conclusions**

Our results show the ability of canopy-imaging based approaches to evaluate plant biomass during the early developmental stages and to detect a delay in plant development caused by a below-ground stress such as nematodes.

## 2.2 Introduction

Plant phenotyping approaches have successfully shown that the analysis of total leaf area by imaging renders a valuable approximation of aboveground biomass (Leister et al. 1999; Granier et al. 2006; Jansen et al. 2009; Walter et al. 2015). It is unclear yet, to which extent the precise monitoring of total leaf area might be able to allow conclusions on belowground biomass generation. Although in young seedlings, the development of root and leaf biomass is closely correlated to each other, the question whether disturbances of belowground plant growth would impact leaf area development is not answered yet. A model plant, with which this topic could beneficially be addressed, is sugar beet.

Sugar beet is one of the most important crops and its yield is formed by the beet – a storage root that is initiated from an early developmental stage on. Often the development of the beet is affected seriously by soil borne pathogens such as plant-parasitic nematodes. Worldwide, they cause annually up to 20% or approximately 100 billion USD of financial losses on crops such as soybean, cotton, cereals, tuber crops, legumes, fruit and vegetables (Luc et al. 2005). Seinhorst (1965) modelled and demonstrated the strong link between numbers and types of nematodes and crop performance. The sugar beet cyst nematode (BCN) *Heterodera schachtii* occurs in patches in the field and has a low mobility. Briefly, when stimulated by optimal soil moisture (80 to 100% of the field capacity) and temperatures (20 to 23°C), second stage juveniles hatch from the cysts. After migrating through the soil to the host-plant roots, juveniles enter the roots and start establishing a feeding site which damages the vascular tissue. Hatching, penetration and infection of the roots can occur within a few days (Cooke 1987). Belowground symptoms include a reduction of the beet growth and the appearance of many secondary roots to compensate those infested by nematodes. BCN also cause diverse aboveground symptoms like stunted growth, decreased chlorophyll content and wilting of the canopy due to water stress (Cooke 1987; Schmitz et al. 2006). These visible symptoms in the foliage make BCN an appropriate target for non-destructive phenotyping method development.

Several methods to detect stress caused by nematodes have already been tested successfully on various crops. Most of them are based on imaging and non-imaging multi- and hyper spectral measurements with the calculation of spectral vegetation indices (SVI) (Heath et al. 2000; Laudien 2005; Nutter et al. 2002). Hillnhütter et al. (2012) demonstrated the potential of normalised difference vegetation index (NDVI) to evaluate the symptoms caused by BCN on

sugar beet plants under controlled conditions. Correlations of SVIs with other physiological or agronomical parameters (yield, nutrient supply) have also been reported for greenhouse and field experiments (Bajwa et al. 2010; Mahlein et al. 2010; Yang and Everitt 2002). However, spectrometry requires the use of complex and expensive devices and data analysis is generally time consuming. After pre-processing the data using reference measurements and percentage of soil coverage, more than sixty SVIs per spectrum can be calculated. In contrast, visible imaging technology uses low cost sensors which are easy to handle and to calibrate (Li et al. 2014). Such an approach only requires a standard digital camera and an image analysis software that allows for the calculation of suitable parameters such as canopy area.

Different methods using colour images have been investigated to characterise plant parameters like leaf morphology (Hoyos-Villegas et al. 2014), nitrogen status (Li et al. 2010), yield traits (Duan et al. 2011) or root architecture (Iyer-Pascuzzi et al. 2010). Only a few papers have described the use of visible images to directly estimate above-ground biomass of individual plants (Lukina et al. 1999; Paruelo et al. 2000). The projected shoot area of the plants is usually calculated and used as a parameter to predict leaf biomass (Sher-Kaul et al. 1995; Smith et al. 2000; Mizoue and Masutani 2003; Tackenberg 2007). HTPPheno (Plant Bioinformatics Group, Leibniz Institute of Plant Genetics and Crop Plant Research Gatersleben, Germany) and LemnaTech (LemnaTec, GmbH, Wuerselen, Germany) are examples of advanced imaged based phenotyping platforms that combine two plant pictures (top-view and side-view) to estimate the leaf biomass at high throughput (Hartmann et al. 2011; Golzarian et al. 2011). It is worth noting that the new image based methods allow a dynamic evaluation of plant growth to be carried out, facilitating a precise determination of time point of onset of stress (Jansen et al. 2009). Such approaches open new opportunities to gain a more precise evaluation of the impact of biotic stresses on plant growth, and specifically in the case of crops, also on any other trait related to the final yield. Practical applications are conceivable with respect to the evaluation of the effect of new chemical or biological control technologies or to support breeding programs for new nematode resistant varieties.

The overall aim of this study was to examine the potential of a single image based phenotyping method to discriminate nematode infested and non-infested sugar beet plants and to predict the beet biomass - as a key component of the final yield - in the early growing stages under greenhouse conditions. More specifically, the main objectives were to:

- (i) test the ability of top-view digital images to estimate the leaf biomass,
- (ii) examine the possible correlations between leaf and beet biomass, and
- (iii) evaluate the ability of top-view digital images to discriminate between nematode infested and non-infested plants and to quantify in a non-destructive manner the damage caused by nematodes.

## 2.3 Material and methods

### 2.3.1 Plant growing

Seeds of Sugar Beet (*Beta vulgaris*), cultivar Invicta (Syngenta AG, Switzerland), susceptible to BCN, were sown in 60 pots of three litres (10cm diameter, 15cm height) containing sandy loam soil (48% sand, 31% silt, 21% clay, pH 7.5, 4% O.M.). Seeds were pre-treated internally with a base treatment of *Thiram*, *Hymexazol*, *Thiamethoxame* and *Tefluthrine* (6+14+60+8 g<sub>ai</sub>/unit (one sugar beet unit is 100 000 seeds)) to avoid early insect attack and fungal disease. The experiment was conducted in controlled conditions (greenhouse) at 23/17 °C (day/night), a relative humidity of 75% ± 15% and a photoperiod of 12 hours per day. Plants were watered every day to keep the soil moisture at 90% of the field capacity.

Two treatments were prepared: (i) non-infested soil; and (ii) soil infested with cysts of *H. schachtii* establishing the equivalent of 600 eggs or larvae per 100 cm<sup>3</sup> of soil. Cysts were coming from greenhouse oil seed rape cultured in loess soil at the Syngenta research centre in Stein (Switzerland). Infested soil was prepared two hours before sowing by mixing the sandy loam soil with the infested loess soil containing the cysts. Pots were then filled with the mixture. Non-infested pots were filled likewise with sandy loam soil previously mixed with blank loess soil. Each treatment was replicated 30 times (60 pots in total). Three blocks were made with 10 BCN infested and 10 non-infested pots in a completely randomised design.

### 2.3.2 Evaluation of plants

Plant growth stages (GS) were defined according to the BBCH scale (Meier et al. 1993). At GS 16, 20 and 35 (corresponding to 32, 41 and 70 days after sowing (das) respectively), block number one, two and three were harvested. There were 20 plants per block (10 pots infested with BCN and 10 pots non-infested). For each plant, the fresh weight of beets was determined and the dry weight of leaves was calculated after a drying period of 48 hours in the oven at 70°C. Thermal time was calculated from air temperatures measured with a temperature sensor (Datenlogger MSR145, MSR Electronics GmbH, Hengart, Switzerland). A base temperature of 1°C was used for temperature summation.

### 2.3.3 Image based phenotyping: Data acquisition and processing

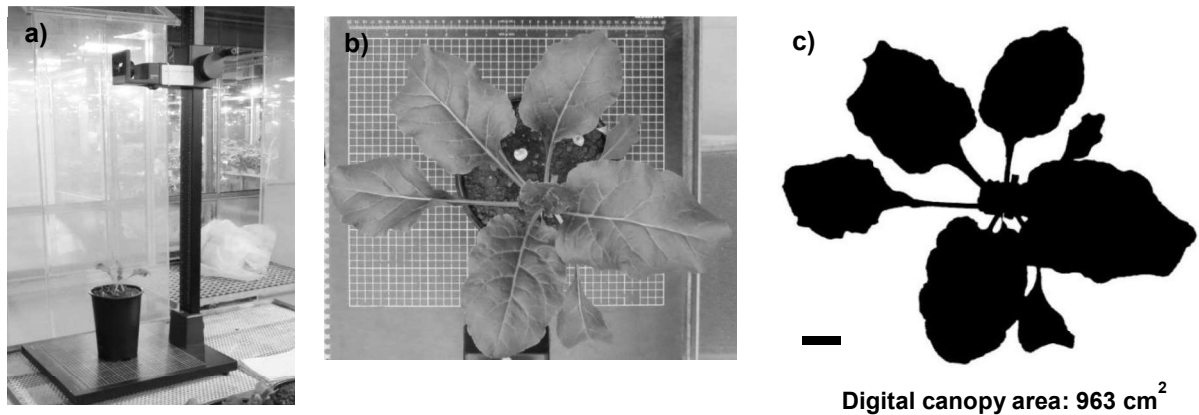


**Figure 1.** a) Frame for capturing images from the top of the sugar beet plant canopy. Images were taken from 0.8 m above plant canopy using automatic settings of the digital camera Canon S100. b) Top-view of a sugar beet plant at GS 20 (bar, 5cm). Image resolution is 0.2 cm<sup>2</sup> per pixel. c) Analysed image of a sugar beet plant at GS 20. Black area represents the plant canopy (bar, 5cm).

Visible images were captured from emergence to GS 20 every two or three days using a digital camera Canon S100 (Canon, Tokyo, Japan). In previous studies, we observed that, for sugar beet with a growth stage greater than 25, image analysis was not accurate in measuring the canopy area any longer due to pronounced overlapping of leaves, due to an alteration of leaf inclination angles and because pot size was beginning to limit plant growth. The camera was placed on a static monopod positioned on an easily movable trolley. Images were obtained from 0.8 m above plant canopy with a resolution of 0.2 cm<sup>2</sup>.pixel<sup>-1</sup> (Fig. 1a). Plants were handled by hand from the trolley to the monopod frame. Images were taken under low light using the automatic settings of the camera. Raw pictures (Fig. 1b) were processed using the software *ImageJ* (<http://rsb.info.nih.gov/ij/>). Images were split into three “colour channels” (R: red, G: green and B: blue). Each of these three layers was an 8-bit image. On each layer, pixels have a particular intensity which ranges from 0 to 255 (2<sup>8</sup>). A pixel with an intensity of 255 on each of the three bands will be white. The three “channel” images generated were then combined to accentuate greenness areas on the picture using the Excess Green Index (EGI) proposed by Woebbecke et al. (1995a):  $EGI = 2G - B - R$ . A threshold was then applied to segment the newly generated image. Pixels with intensities from 55 to 255 were considered “green pixels”. The total number of “green pixels” was calculated and subsequently re-scaled to obtain the final parameter “digital canopy area” expressed in cm<sup>2</sup> (Fig. 1c). This data acquisition and analysis were repeated for each plant, at each measurement date.

#### **2.3.4 Statistical data analysis**

The program *R* was used for analysis of the data. Beet fresh weight, leaf dry weight and canopy area of BCN infested and non-infested plants were tested for homogeneity of variance. They were then exposed to analysis of variance (ANOVA) at a probability level of 0.05 using the factor “nematode infestation”. Several linear regression models were used to quantify the relationship between beet fresh weight, leaf dry weight and canopy area.



## 2.4 Results

### 2.4.1 Leaf biomass and digital canopy area

Average leaf biomass and digital canopy area of infested and non-infested plants at different growth stages are shown in Table 1. No digital canopy area was computed at GS 35 because of leaf overlap and growth restrictions due to pot size. A significant reduction of shoot dry weight and digital canopy area was observed for the BCN infested treatment compared to the non-infested treatment at GS 16 and 20. Shoot dry biomass and digital canopy area varied similarly in the presence of BCN suggesting high correlations between both parameters. Magnitudes of shoot dry biomass and digital canopy area reductions caused by BCN are equal at GS 16 (35% reduction). At GS 20, BCN reduced the shoot dry weight by 63% and the digital canopy area by 56%. There was no significant reduction of the leaf biomass at GS 35.

**Table 1. Shoot dry biomass and digital canopy area of non-infested and BCN infested treatments at different growth stages. Numbers are means  $\pm$  standard error of the mean. Means with different letters are significantly different at 5% level.**

	Shoot dry biomass (g)			Digital canopy area (cm <sup>2</sup> )	
	GS 16	GS 20	GS 35	GS 16	GS 20
Non-infested	0.51 $\pm$ 0.03 <sup>a</sup>	2.04 $\pm$ 0.09 <sup>c</sup>	7.36 $\pm$ 0.3 <sup>e</sup>	238.3 $\pm$ 21.7 <sup>a</sup>	926.8 $\pm$ 35.3 <sup>c</sup>
BCN infested	0.33 $\pm$ 0.03 <sup>b</sup>	0.74 $\pm$ 0.1 <sup>d</sup>	6.83 $\pm$ 0.42 <sup>e</sup>	153.2 $\pm$ 22.2 <sup>b</sup>	407.7 $\pm$ 47.5 <sup>d</sup>

The correlation between digital canopy area and leaf biomass was high when data were pooled from GS 16 and 20 with and without nematodes ( $R^2=0.95$ ,  $n=40$ ,  $p<0.01$ , Fig. 2). The “canopy area” parameter allowed us to obtain a good estimation of the leaf biomass. Leaf dry weight estimation using canopy area was greater at GS 20 ( $R^2=0.97$ ,  $p<0.01$ ) than at GS 16 ( $R^2=0.84$ ,  $p<0.01$ ) because of the larger range of leaf dry weight at GS 20 which increased the linear correlation.

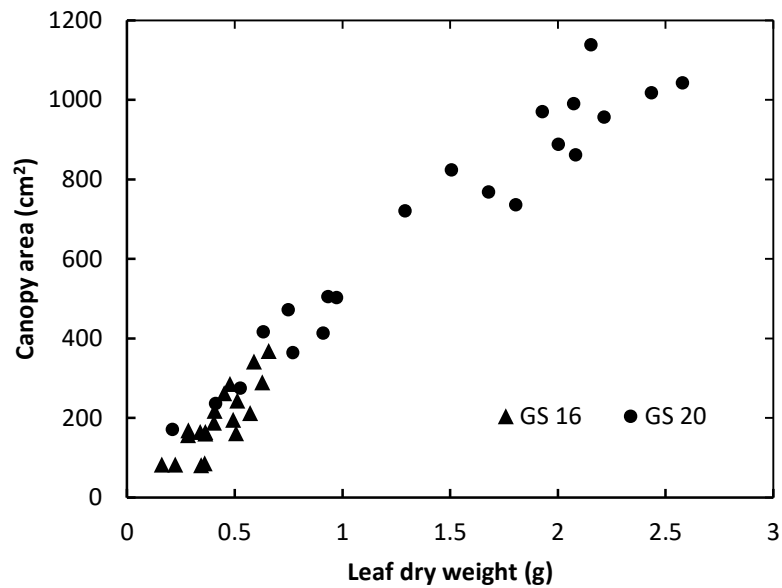
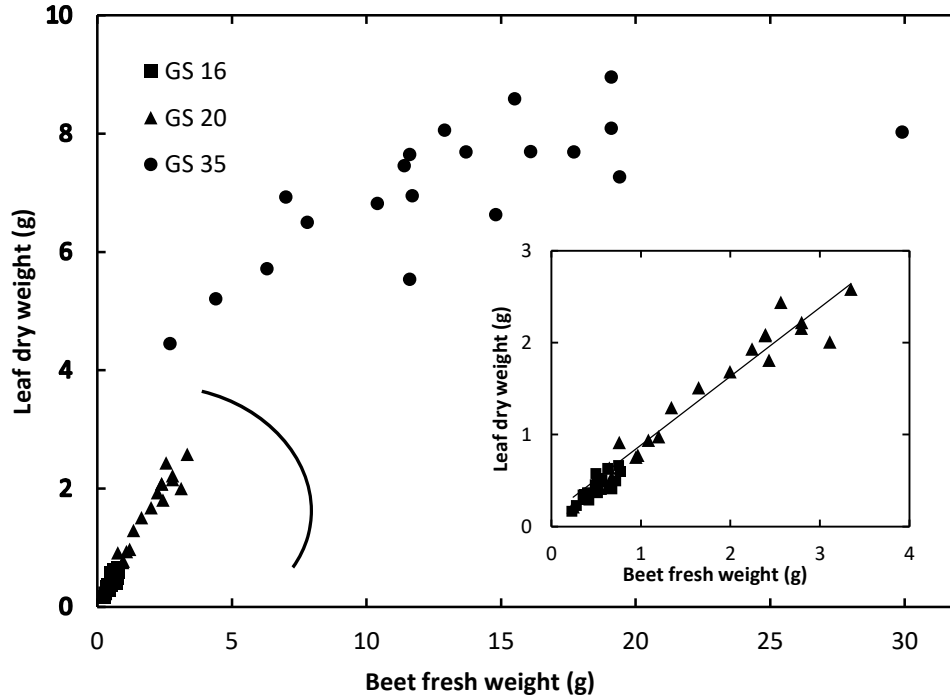


Figure 2. Canopy area as a function of the leaf dry weight. Plants were harvested at GS 16 and GS 20 respectively ( $n=40$ ,  $R^2=0.95$ ,  $p<0.01$ ).

#### 2.4.2 Relationship between leaf and beet biomass

The root fresh biomass of the sugar beet was correlated with the leaf dry biomass up to GS 20 (Fig. 3). At GS 20, leaf weight and beet weight were closely correlated ( $R^2=0.94$ ,  $p<0.01$ ). Correlation between above and below ground biomass was lower at GS 16 ( $R^2=0.68$ ,  $p<0.01$ ) and GS 35 ( $R^2=0.53$ ,  $p<0.01$ ).



**Figure 3.** Correlations between leaf dry weight and beet fresh weight at three different dates (n=60). Plant weights are expressed in grams.

Calculation of the ratio “leaf dry weight / beet fresh weight” allowed us to statistically distinguish two phases in the biomass allocation process (Table 2): a first phase including the growth stages GS 16 and GS 20, where the ratio was very similar (0.84) and a second phase with larger plants (GS 35) where the shoot/root ratio dropped to 0.66 which indicated a change in the biomass allocation ratio with a larger proportion allocated to the root system.

**Table 2.** Ratio between leaf dry weight and beet fresh weight at three times during the sugar beet growth. Means with different letters are significantly different at 5% level.

Growth stage	Ratio leaf dry weight / beet fresh weight
GS 16	0.85 <sup>a</sup>
GS 20	0.84 <sup>a</sup>
GS 35	0.66 <sup>b</sup>

During the early growth of sugar beet, calculation of the green canopy area from top-view images allowed us to evaluate the leaf biomass of the plant which was closely related to the beet biomass. Thus, it appeared interesting to investigate the ability of the canopy area to evaluate the beet fresh weight.

### 2.4.3 Use of canopy area to evaluate beet biomass

The correlation between plant biomass and canopy area was higher at GS 20 than at GS 16 (Table 3). As expected, correlations were greater between canopy area and leaf dry weight than between canopy area and beet fresh weight. However, the canopy area appeared closely correlated with the beet fresh weight ( $R^2=0.61$  at GS16 and  $R^2=0.87$  at GS 20) showing that it was possible to use the canopy area as a proxy to directly evaluate belowground biomass. The relationship between the canopy area and either leaf dry weight or beet fresh weight changed during the early growth of the sugar beet. Both the slope and the Y-intercept of the regression model were significantly different for the two dates ( $p<0.01$ ).

**Table 3. Coefficient of correlation ( $R^2$ ), slope, Y-intercepts and number of observations (n) for the linear model fit to the data of canopy area ( $\text{cm}^2$ ) and leaf dry weight / beet fresh weight. Both BCN and non-infested treatments were included in the analysis. For both leaf dry weight and beet fresh weight, there were significant differences in the slope and in the Y-intercept ( $p<0.01$ ) between GS 16 and GS 20.**

	Growth stage	Y intercept	Slope	$R^2$	n
Leaf dry weigh	16	-24.5	521.4	0.71	20
	20	116.2	395.9	0.94	21
Beet fresh weight	16	-16.4	416.3	0.61	20
	20	174.9	293.6	0.87	21

### 2.4.4 Effect of nematode infestation on the canopy area and plant biomass

The evolution of the canopy area from emergence to GS 20 (41 das) for both BCN infested and non-infested plants is represented in Fig. 4. The canopy area of infested sugar beet plants started to deviate from the canopy area of non-infested plants from an early developmental stage. At eleven days after sowing, a slight non-significant reduction of the canopy area ( $p=0.13$ ) was observed for the infested plants (10% lower than the non-infested plants). Canopy area allowed us to statistically discriminate BCN infested and non-infested sugar beets from 22 das with an average canopy area reduction of 29% for the infested plants (Fig. 4b). After 29 days of growth, there was a difference of more than 35% between the two treatments. The highest canopy area reduction (57%) was observed 35 das when leaves started to overlap each other. The minimum significant difference in digital canopy area detectable between the two treatments was 19% (29 das).

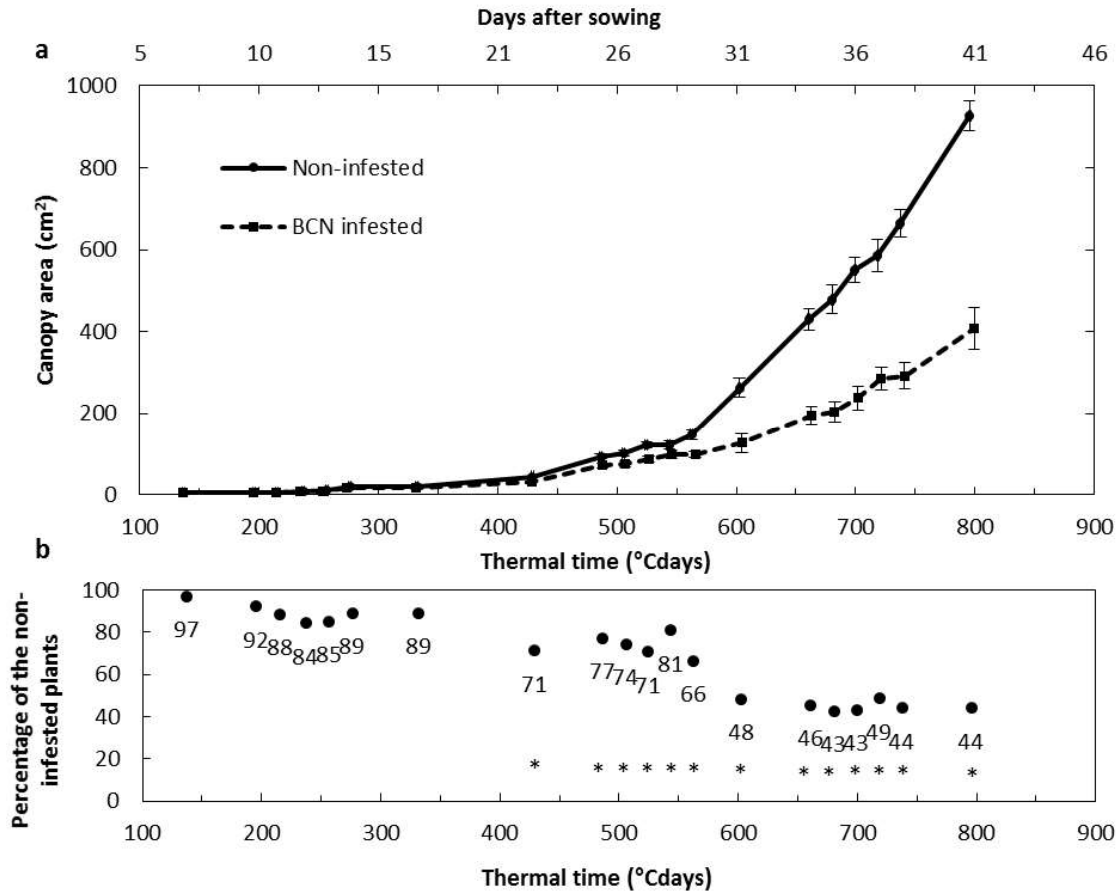


Figure 4. a) Canopy area as a function of the thermal time for BCN infested and non-infested plants (measurement points). Bars represent the standard error of the mean. b) Canopy area of BCN infested plants as a percentage of the non-infested plants. The star denotes significant differences ( $p < 0.05$ ) between canopy area of BCN infested and non-infested plants.

#### 2.4.5 Nematode effects on sugar beet growth

Statistically significant differences were observed in the beet fresh weight between non-infested and infested sugar beets at the three different dates (Fig. 5). The fresh weight of the beets of infested plants was reduced by up to 65% at GS 20 compared to the non-infested plants. A similar pattern was observed for the leaf dry weight with the exception of GS 35 with a leaf biomass reduction of only 8% which was not statistically significant. The fact that differences were not significant any longer at GS 35 can be explained by the specific layout used in this study. In three litre pots, after 70 days, the plant growth started to be limited by the available soil volume in the pot. Therefore, it is likely that, at this stage, infested plants were able to catch up in their development to non-infested plants and that both groups by then reached an asymptotic level of maximal leaf size.

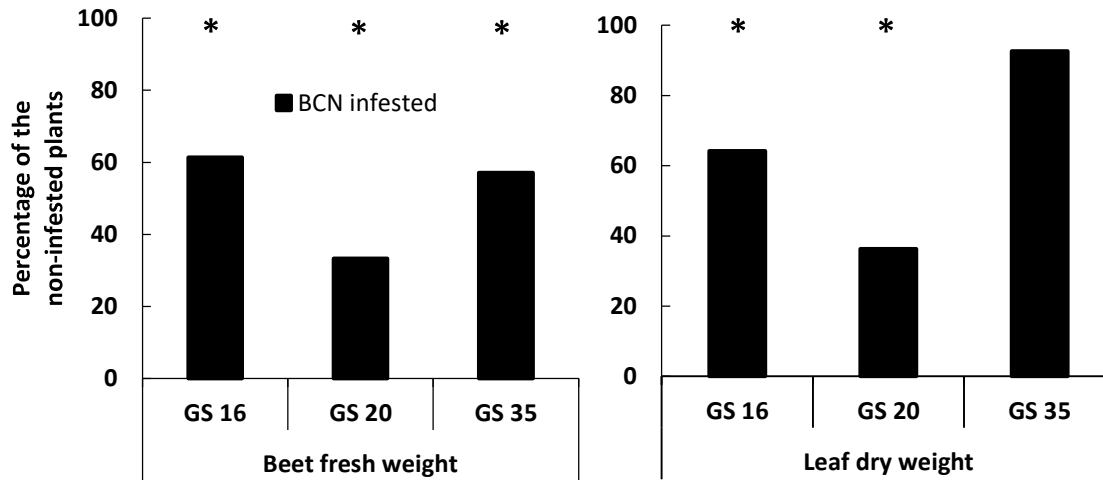


Figure 5. Average leaf dry weight and beet fresh weight as a percentage of the non-infested plants. The star denotes significant differences ( $p < 0.05$ ) between beet fresh weight and leaf dry weight of BCN infested and non-infested plants.

There was a highly linear relationship ( $R^2 = 0.92$ ,  $p < 0.01$ ) between the canopy area and the beet fresh weight of the plants when considering the two growth stages and the infested and non-infested treatments (Fig. 6). The identified relationship shows how canopy area can be used as promising proxy to estimate the beet fresh weight in the early growth stage of plants (GS 16 and GS 20) and furthermore to be able to differentiate between infested and non-infested plants.

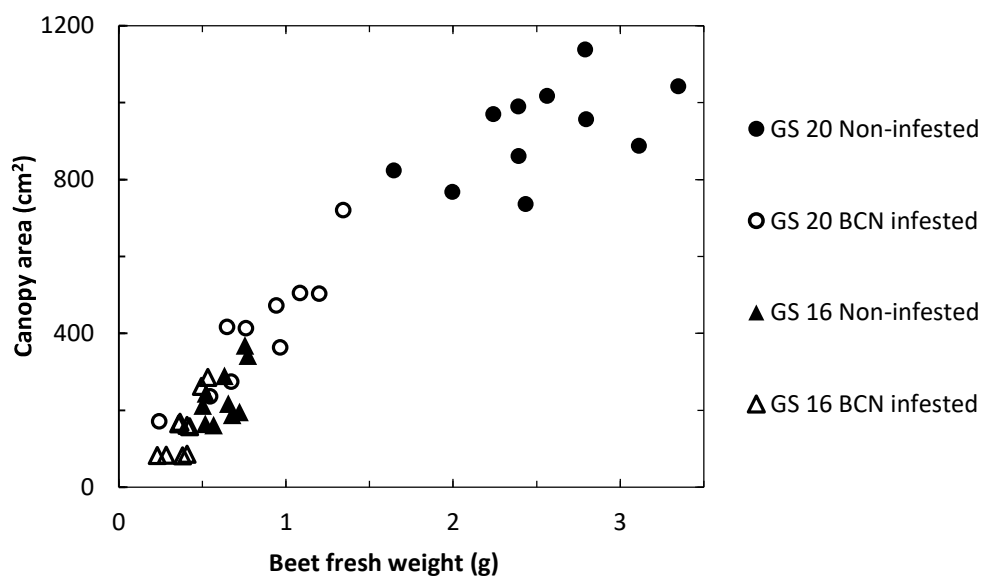


Figure 6. Relationship between canopy area and beet fresh weight for nematode infested and non-infested sugar beet plants at two different dates (GS 16 and GS 20) ( $n = 40$ ,  $R^2 = 0.95$ ,  $p < 0.01$ ).

## 2.5 Discussion

The results of this study demonstrated that a phenotyping system, based on visible images and a simple picture analysis algorithm was suitable to detect differences in plant biomass between nematode infested and non-infested sugar beets and to predict the sugar beet plant biomass early in the growing season under greenhouse conditions. The study also showed the advantage of using a dynamic approach by studying the increase of the digital biomass over time to detect the effect of nematode infestations. The reduction of beet biomass, leaf biomass and leaf area were in the same order of magnitude (60% at GS 16; 40% at GS 20), respectively. This indicates that the divergence of canopy area at 11 das could be an early sign of nematodes acting on the beets. Surprisingly the technique enabled us to statistically detect very early the nematode infestation effect which caused a delay in shoot development. Canopy areas of infested and non-infested sugar beet differed significantly for the first time at 22 das (29% difference) at GS 12 (two leaves well developed). Internal screening tests, using similar protocols, always showed a high level of nematode infestation in the roots. From 15 to 60 juveniles per root system, 14 days after sowing, are sufficient to cause a biological stress. Therefore, it is conceivable that imaging methods might provide an indication also in the field that certain patches of a field are affected by BCN – this would allow a more timely application of any countermeasures such as the use of specific nematicides. Use of crop rotation and of appropriate BCN tolerant sugar beet cultivars would also be suitable countermeasures.

The phenotyping method used in this study has the advantage of being consistent, fast and cheap. Pots were moved one by one on the phenotyping frame and the top-view picture was taken subsequently. Sixty canopy images were captured in 30 minutes and 15 minutes were necessary to extract the pictures, run the image analysis macro and generate the digital canopy area for the 60 plants. The whole methodology only requires a digital camera, a static frame to hold the camera and the free software *ImageJ* that make this system a low cost phenotyping approach. This approach could and will also be applied in the field in future studies with a few necessary adaptations. The main constraint in the field is the ever changing intensity and spectral composition of solar irradiance, which induces partial shadow on the plants during sunny weather conditions, making the green pixel analysis comparison inconsistent between different pictures. However, a specific framework could be built with oriented flaps that generate homogeneous shadow over the targeted soil area. In a field situation, several factors may also vary such as nutrients, soil moisture, soil temperature and soil compaction making the detection of nematodes more difficult using canopy area. This

technique would be particularly useful in a trial situation where environmental factors are characterised or controlled. For example, the method could help to evaluate the plant growth and detect the efficacy of new chemical or biological technologies to control BCN.

The sugar beet growth pattern mainly depends on the temperature (Milford et al. 1985; Granier and Tardieu 1998). The radial angle of the first leaves is close to  $0^\circ$  (horizontal leaves) and leaves appear individually on a 5:13 phyllotaxis (Stehlik 1938; Milford 1985b) which prevent leaves from overlapping each other before growth stage 25. This particular plant architecture allowed an accurate evaluation of the canopy area using top-view visible images and explains its high correlation with the leaf biomass in the early growth stages. This study showed how digital evaluation of aerial biomass of the sugar beet plant could be used to evaluate the belowground biomass generation within a certain degree of precision and in a non-invasive manner from the early growth stages. Scott et al. (1973) and Jaggard et al. (1983) showed that any delay in the emergence and early growth of the sugar beet plant significantly affected the final sugar beet yield which demonstrated the need for early biomass characterisation and prediction tools.

The present study showed a significant change in the biomass allocation ratio (between leaves and roots) between GS 16-20 and GS 35. Different phases in sugar beet biomass allocation are well known and this classical framework of the sugar beet plant development has been highlighted by Green et al. (1986): an early phase of leaf-dominated growth is followed by a phase dominated by growth of the storage root that is followed then by a phase of sugar storage. Milford et al. (1988) showed that the transitions between these phases are not occurring stepwise, but that the transitions occur gradually (Milford et al. 1988). Therefore, a prediction of beet biomass from leaf canopy growth is possible already early in plant development, since some storage and beet growth is occurring earlier than conceived in a classical framework of sugar beet development.

BCN causes important damage to sugar beets which results in specific symptoms such as differences in plant weight and canopy development (Cooke 1987; Herr 1996). The present study confirmed these observations. A large reduction of plant biomass was observed for the nematode-infested plants compared to the non-infested plants. BCN had an effect on the plant development and growth affecting the organogenesis (leaf appearance) and/or morphogenesis (leaf growth/expansion). Once nematodes start to infest the plant, a recovery process is initiated with a production of secondary roots (bearding) leading to a reduction of



leaf growth (delay in leaf appearance) and beet weight (Cooke 1987). In this study, the thermal time interval that separates the appearance of two successive leaves (phyllochron) as defined by Milford et al. (1985a) was significantly longer in presence of BCN (33°C days instead of 30°C days) which would slow down the early development of BCN infested plants compared to non-infested plants.

It is worth noting that the approach used in this study to discriminate nematode infested and non-infested plants was valid for a sugar beet cultivar which was classified as susceptible to nematodes and with an initial nematode infestation level higher than the damage threshold. The damage threshold of a BCN susceptible cultivar is usually between 200 and 300 eggs or larvae per 100 cm<sup>3</sup> of soil. In the present study, we used an infestation rate of 600 eggs or larvae per 100 cm<sup>3</sup> of soil which can be considered as a moderate infestation level. Further studies are needed to demonstrate whether this type of phenotyping approaches is valid across cultivars with a wide range of susceptibility to nematode attack. Moreover, as mentioned above, after this successful proof of principle, it will be important to test the validity of this approach in the field.

Other plant systems have to be assessed to determine the generality of this top-view digital image based phenotyping approach. We assume that such systems involving top-view images would be suitable to non-destructively monitor plant biomass of dicotyledonous crop species such as soybeans, sunflower, cotton or potato for instance. In such species, the early development of horizontal leaves following a spiral or alternate phyllotaxis is particularly suitable for top-view phenotyping. It will be interesting to evaluate on these crops whether measurements of digital canopy area at given growth stages under different belowground disturbances could be used to discriminate high from low potential yields compared to more advanced phenotyping methods (Ma et al. 2001; Wishart et al. 2014).

## 2.6 Conclusion and outlook

This study demonstrated that the use of digital images to characterise the canopy area of plants has a high potential to become a fast, cheap and reliable method to assess differences in belowground plant biomass caused by specific biotic or abiotic stresses. Sugar beet plants and the retarding effect of BCN were used to illustrate this phenotyping approach. The methodologies showed promising results in evaluating the speed of growth of sugar beet in the early growth stages and the impact of biotic stress on the crop development. This can represent an interesting tool to predict crop performance by looking at early crop parameters and evaluating the degree of inhibition of the plant biomass generation. However the described methodology presents some limitations, the main one is the described system which appeared suitable only for the early growth stages of the sugar beet (from emergence until GS 25). Multiple layers of leaves and overlapping could drastically reduce the accuracy of this method after GS 25. Further work will be required to investigate the ability of this system to evaluate directly the nematode pressure in the soil. Testing the potential implementation of this system at larger scale in the field on diverse sugar beet cultivars (susceptible, tolerant, and resistant to BCN) with different BCN infestation levels will be the next step to further develop the system.

## 2.7 Acknowledgment

We would like to thank Beat Reber for the technical support, Nuria Bonilla for the precious insights regarding this manuscript and Hubert Varella for statistical support. We also thank Brigitte Slaats, Domenica Jenni and Tobias Straumann for growing and providing the nematode inoculum. We are grateful to Norbert Wuest for the use of the greenhouse.

## Chapter 3.

### Comparison of visible imaging, thermography and spectrometry methods to evaluate the effect of *Heterodera schachtii* inoculation on sugar beets



Samuel Joalland, Claudio Screpanti, Frank Liebisch, Hubert Vincent Varella, Alain Gaume, Achim Walter

Plant Methods (2017) 13: 73

Reprinted with permission from the peer-reviewed journal "Plant Methods".

### 3.1 Abstract

#### Background

Phenotyping technologies are expected to provide predictive power for a range of applications in plant and crop sciences. Here, we use the disease pressure of Beet Cyst Nematodes (BCN) on sugar beet as an illustrative example to test the specific capabilities of different methods. Strong links between the above and belowground parts of sugar beet plants have made BCN suitable targets for use of non-destructive phenotyping methods. We compared the ability of visible light imaging, thermography and spectrometry to evaluate the effect of BCN on the growth of sugar beet plants.

#### Results

Two microplot experiments were sown with the nematode susceptible cultivar *Aimanta* and the nematode tolerant cultivar *Bluefox* under semi-field conditions. Visible imaging, thermal imaging and spectrometry were carried out on BCN infested and non-infested plants at different times during the plant development. Effects of a chemical nematicide were also evaluated using the three phenotyping methods. Leaf and beet biomass were measured at harvest. For both susceptible and tolerant cultivar, canopy area extracted from visible images was the earliest nematode stress indicator. Using such canopy area parameter, delay in leaf growth as well as benefit from a chemical nematicide could be detected already 15 days after sowing. Spectrometry was suitable to identify the stress even when the canopy reached full coverage. Thermography could only detect stress on the susceptible cultivar. Spectral Vegetation Indices (SVIs) related to canopy cover (NDVI and MCARI2) and chlorophyll content (CHLG) were correlated with the final yield ( $R=0.69$  on average for the susceptible cultivar) and the final nematode population in the soil ( $R=0.78$  on average for the susceptible cultivar).

#### Conclusion

In this paper we compare the use of visible imaging, thermography and spectrometry over two cultivars and two years under outdoor conditions. The three different techniques have their specific strengths in identifying BCN symptoms according to the type of cultivars and the growth stages of the sugar beet plants. Early detection of nematicide benefit and high yield predictability using visible imaging and spectrometry suggests promising applications for agricultural research and precision agriculture.

## 3.2 Background

The rapid development of sensitive tools for plant phenotyping allows the assessment of very complex traits such as root morphology, biomass, leaf characteristic, yield related traits, biotic and abiotic response (Mahlein et al. 2013; Liebisch et al. 2015; Walter et al. 2015). In most cases, phenotyping approaches are tested independently under a given scenario which does not facilitate the objective comparison of the methods tested. Often, the different methods are investigated at various scales (field or greenhouse) by following diverse protocols (cultivar, type and level of infestation, growth duration). Sugar beet is an interesting crop since the harvested organ develops vegetatively, thereby integrating environmental effects over time. It has recently been shown that beet development is reflected by aboveground development facilitating the use of shoot phenotyping procedures for yield estimation and disease effects (Joalland et al. 2016). On sugar beet, limited studies have been published which makes it difficult to evaluate the advantages and disadvantages of the different phenotyping approaches to characterise nematode symptoms.

Nematodes are soil borne parasites that occur naturally in soil. They cause annually up to 20% of yield losses in crops such as soybean, cotton, cereals, tuber crops, legumes, fruit and vegetables (Luc et al. 2005). Sugar beet is a root crop which is widely cultivated in Europe and North America for sugar production. The sugar beet cyst nematode *Heterodera schachtii* (Schmidt) is a major threat and can cause severe beet damage and compromise the final yield. It has been demonstrated that there is a strong link between number of nematodes and crop performance such as shoot development and root biomass accumulation (Seinhorst 1965; Cooke 1987).

In order to manage the damage caused by nematodes, dedicated strategies have been developed. A first approach consists of evaluating whether the level of infestation in the field is above a given economical threshold thereby justifying specific nematode control methods. However, soil sample analyses are expensive and technically difficult because of the cluster distribution of BCN in the field (Evans et al. 2002; Wyse-Peter et al. 2002). Thus, many samples per hectare are required to achieve a reasonable estimation of the potential crop damage.

To reduce costs and increase the spatial resolution of BCN soil pressure evaluation, non-destructive methods have been developed (Hillnhütter et al. 2010). It is worth noting that BCN occurs in patches in the field, has a low mobility, and causes diverse and rather generic visible aboveground symptoms, for example stunted growth, decreased chlorophyll content

and canopy wilting (Cooke 1987; Schmitz et al. 2006). All this makes BCN an appropriate target for non-destructive phenotyping method development. Several remote sensing methods to detect stress caused by nematodes have already been successfully tested on a variety of crops such as potato, soybean or sugar beet. These methods are mainly based on imaging and non-imaging multi- and hyper spectral measurements, with the calculation of spectral vegetation indices (SVIs) (Heath et al. 2000; Nutter et al. 2002; Laudien 2005).

Hillnhütter et al. (2012) demonstrated the potential of normalised difference vegetation index (NDVI) to evaluate the symptoms caused by BCN on sugar beet plants under controlled conditions. Use of specific SVIs to predict the final beet yield and the nematode population in the soil has also been reported in field experiments (Hillnhütter et al. 2011). Schmitz et al. (2004) showed the ability of remote sensing thermography at field level to detect small changes in the canopy temperature of BCN-infested sugar beet. Thus, thermography and spectrometry appear to be suitable phenotyping methods for the detection of belowground symptoms caused by BCN. However, these systems require the use of expensive devices and complex data analysis methods.

Alternatively, visible imaging technology can be used for sugar beet phenotyping. Such a technology is cheaper than the aforementioned technologies, since it uses low cost sensors and the devices are easy to handle and calibrate (Li et al. 2014). The projected shoot area of the plants is usually calculated and used as a parameter to predict shoot biomass in different plant species (Sher-Kaul et al. 1995; Smith et al. 2000; Mizoue and Masutani 2003; Tackenberg 2007). Particularly in sugar beet, the use of visible images showed very promising results in discriminating, at an early plant developmental stage, BCN-infested and non-infested plants in the greenhouse (Joalland et al. 2016). In this study, the “digital canopy area” parameter calculated was a suitable proxy for shoot and root biomass estimation during the first two months of growth.

Beside the need to identify damage caused by nematodes and to evaluate the degree of infestation in the field, the use of phenotyping tools plays a role in agricultural research and development activities aiming at the discovery and development of new solutions for nematode control. In most of the cases, the evaluation studies aimed at evaluating the efficacy of the solutions by looking at the impact on the final yield. This implies that trials need to be kept up to harvest and last three months or longer. Using non-destructive measurements to get early insights regarding the efficacy of new solutions (compounds or cultivars) on the

yield potential would allow to reduce the duration and costs of the trials, and to increase the testing cycles per year. Overall such new tools can have a substantial impact on the efficiency of compound screening or development of new cultivars.

The present study compares the ability of several traits (canopy area, canopy temperature and SVIs) obtained with three different phenotyping devices (visible imaging, thermography and spectrometry) to identify and characterise stress caused by BCN on sugar beet plants at the semi-field level. More specifically, the main objectives were to:

- (i) compare the ability of the three phenotyping methods to detect stress generated by BCN on nematode susceptible and tolerant sugar beet plants,
- (ii) evaluate the capability of the methods to predict sugar beet yield,
- (iii) evaluate the potential of visible imaging to detect benefit of a contact nematicide.

### 3.3 Methods

#### 3.3.1 Plant cultivation

Studies were conducted in 2014 and 2015 on a polytunnel area located in the Syngenta Research Centre in Stein (Switzerland). The area was equipped with a microplot system (Fig. 1a), which simulates real field conditions and allows to monitor the main environmental conditions. The experimental layout includes 70 microplots consisting of a pot in pot system. One 150 l plastic container (65 cm diameter and 60 cm depth) is nested inside of another, with both recessed in the ground up to the rim to reduce fluctuation of soil temperature.



**Figure 1. a) Overview of the semi-field platform with 70 microplots. b) Top view of a microplot 416 °Cd. White dots represent the three “sowing locations”.**

The nematode susceptible cultivar *Aimanta* (Syngenta AG, Basel, Switzerland) and the nematode tolerant cultivar *Bluefox* (Syngenta AG, Basel, Switzerland) were used in 2014 and 2015 trials, respectively. The soil used was non-sterile sandy loam (56% sand, 31% silt, 11% clay, pH 7.7, 2% O.M.). A commercial seed treatment consisting of *Thiram*, *Hymexazol*, *Thiamethoxame* and *Tefluthrine* (6+14+60+8 g<sub>ai</sub>/unit (one sugar beet unit is 100 000 seeds)) was applied to the seeds to avoid early insect attack and fungal disease. Six seeds were sown per microplot at three different locations (two seeds per location) (Fig. 1b). Two weeks after sowing, three seedlings were left in each microplot (one seedling kept per location) simulating a sowing density similar to the real sowing density adopted under field conditions (100 000 seeds per hectare).



### 3.3.2 Preparation of the soil and nematode inoculum

Cysts of *Heterodera schachtii* were cultured at the Syngenta research centre in Stein. Cysts were coming from greenhouse oilseed rape plants cultured in loess soil. Infested soil was prepared by mixing the sandy loam soil with the amount of infested loess soil to reach a final level of 600 eggs and juveniles (J2) per 100 cm<sup>3</sup> soil. Only the upper layer (corresponding to a volume of 40 litres) of each microplot was infested.

In the 2015 experiment, an additional treatment including soil infested with cysts of *H. schachtii* + *Fosthiazate* nematicide (ISK Bioscience Corporation, Concord, OH, USA) was added (Koyanagi et al. 1998). *Fosthiazate* was applied as granules of Nemathorin 10G product (Syngenta AG, Basel, Switzerland) at the same time as the soil infestation with a final rate of 30 kg.ha<sup>-1</sup>. A randomised complete block design with ten replicates was used in the two years. Experimental settings and main crop management operations are reported in Table 1.

**Table 1. Summary of the experimental settings and the farming operations during the two microplot experiments. °Cd represents the thermal time.**

	2014	2015
<b>Sugar beet Cultivar</b>	Nematode susceptible <i>Aimanta</i>	Nematode tolerant <i>Bluefox</i>
<b>Nematode infestation level</b>	600 eggs and J2 per 100 cm <sup>3</sup> of soil	600 eggs and J2 per 100 cm <sup>3</sup> of soil
<b>Treatments</b>	1) Non-infested 2) Nematode infested	1) Non-infested 2) Nematode infested 3) <i>Fosthiazate</i> treatment
<b>Sowing</b>	May 6 <sup>th</sup> 2014	May 4 <sup>th</sup> 2015
<b>Fertilizer application (Osmocote® granules)</b>	-	440 °Cd
<b>Insecticide application</b>	534, 1094 °Cd	857, 1419 °Cd
<b>Fungicide application</b>	1830 °Cd	2012 °Cd
<b>Harvest</b>	September 10 <sup>th</sup> (2200 °Cd - 127 das)	August 27 <sup>th</sup> (2190 °Cd - 115 das)

In both years, microplots were equipped with sensors to monitor air temperature ([www.msr.ch](http://www.msr.ch)) and soil moisture ([www.plant-care.ch](http://www.plant-care.ch)). Soil sensor technology is based on the microthermic measurements of soil moisture. Details of the environmental conditions are

shown in Fig. 2. Thermal Time (TT) expressed in degree days ( $^{\circ}\text{Cd}$ ) was calculated using air temperature as:  $TT = \sum_{if \geq 0} \left( \frac{T_{\max} + T_{\min}}{2} \right) - T_{\text{base}}$ , with  $T_{\text{base}}$  of  $1.1^{\circ}\text{C}$  (Holen and Dexter 1996).

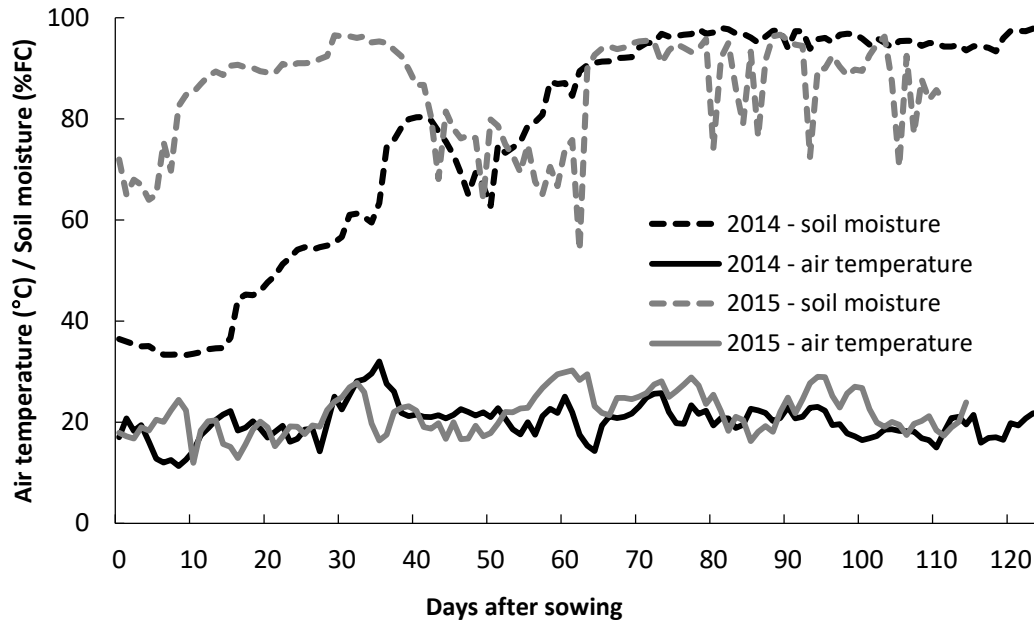


**Figure 2.** Evolution of daily average air temperature and soil moisture during 2014 and 2015 trials. Soil moisture is expressed as percentage of the field capacity (FC). The end of the lines corresponds to the respective harvest dates.

In 2015, soil moisture during the first 40 days was higher than in 2014. In both years, soil moisture conditions were sufficient to allow a homogenous growth of the seedlings. It is worth noting that high air temperatures were observed during the sugar beet emergence (between six and nine days after sowing) in 2015 ( $21^{\circ}\text{C}$  on average).

### 3.3.3 Evaluation of plants and nematodes

After harvest, fresh weight of beets was determined for each plant. Dry weight of the leaves was measured after a drying period of 72 h ( $70^{\circ}\text{C}$ ). Final nematode population was assessed by sampling 1000 g of soil. Soil sampling was performed between five and 20 cm depth in the middle of each pot. All the soil samples were subsequently sent to an external lab (ClearDetection, Wageningen, NL) for analysis of the number of cysts and number of eggs and larvae per  $100\text{ cm}^3$  of dry soil according to EPPO method 1/25 (<http://pp1.eppo.int/>). Plant growth stages (GS) were defined according to the BBCH scale (Meier et al. 1993).

### 3.3.4 Visible imaging

Canopy visible images were captured from seedling emergence up to 1300 °Cd every two or three days using a digital camera Canon S100 (Canon, Tokyo, Japan). The device was mounted on a mobile monopod and images were obtained from 1.8 m above plant canopy with a resolution of 0.0029 cm<sup>2</sup> pixel<sup>-1</sup>. The monopod was held vertically in order to have the camera centred in the middle of the pot. To optimise image processing, photos were captured, when possible, under cloudy conditions early in the morning using the automatic settings of the camera. 15 minutes were necessary to acquire the 70 images which prevented any changes in the illumination and therefore also the necessity for white balancing. Raw pictures (Fig. 3a) were processed using *ImageJ*, the Java-based open-source image processing and analysis program (<https://imagej.nih.gov/ij/>), following a workflow described by Joalland et al. (2016) based on an image segmentation proposed by Woebbecke et al. (1995a). This fast and non-invasive method allows to evaluate the “digital canopy area” (green area) at different times (Fig. 3b).

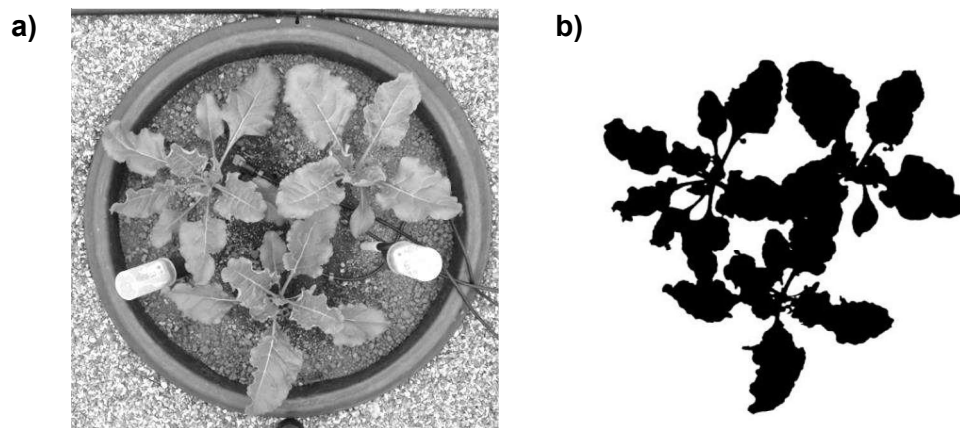
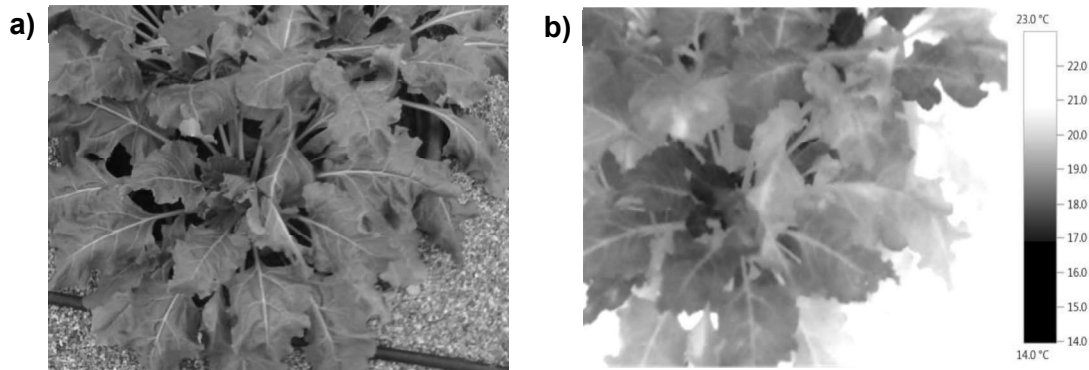


Figure 3. a) Raw visible image taken from the top b) Image after processing 534 °Cd (susceptible cultivar *Aimanta* in 2014).

### 3.3.5 Thermography

Thermal images were acquired using an infrared camera (Testo 885, Testo Ltd, UK). The thermal device was calibrated prior to taking pictures by setting up the emissivity to 96% and the reflected temperature compensation parameter to the current air temperature (Oerke and Steiner 2010). Pictures were then taken from the top of each pot in manual mode (autofocus off). Two images were automatically generated by the camera during the image acquisition;

one thermal image, in which pixels correspond to temperature value, and one visible image (Fig. 4a and 4b). A macro was specifically built on *ImageJ* to extract the canopy temperature by combining both thermal and visible images.



**Figure 4.** a) Visible and b) thermal images obtained simultaneously with the thermal camera 856 °Cd in 2015.

For each date and timing of measurement, the Vapour Pressure Deficit (VPD) was calculated according to the equation of Anderson (1936) using air temperature and relative humidity. VPD reflects the ability of the air to hold water and it reflects the transpirational demand.

### 3.3.6 Spectrometry

#### Data acquisition

Spectral measurements were performed several times during plant development (Table 2) with a non-imaging spectroradiometer (ASD FieldSpec® 4, Analytic Spectral Devices, Boulder, CO, USA) with a spectral range of 350-2500 nm. Spectra were acquired from the top of the microplots at a height of 1.20 m with a 25° field of view using a mobile dark box specifically designed for the microplot experiments. A 120 W halogen lamp (spotlight 120W, Kent, Lyon, France) was used to provide constant optimum illumination of the canopy inside the box during the measurements. The dark box and halogen lamp combination made the conditions of measurement consistent between microplots and between days.

Instrument optimization and reflectance calibration were performed using a Zenith Polymer® (SphereOptics, Germany) 99% reflectance target as white reference before the sample acquisition. Each sample scan represented an average of five reflectance spectra.

**Table 2. Summary of phenotyping measurements during the two studies. °Cd represents the thermal time.**

	2014		2015	
	data points #		data points #	
<b>Visible imaging</b>	33	Emergence to 1300 °Cd	33	Emergence to 1300 °Cd
<b>Thermal imaging</b>	3	935, 1446, 1485 °Cd	5	581, 599, 736, 856, 1347 °Cd
<b>Spectrometry</b>	1	1371 °Cd	6	404, 460, 599, 736, 978, 1618 °Cd

### Spectral vegetation indices

For each date of measurement and each microplot, a selection of 123 published SVIs was computed to reduce the data dimension. SVIs were calculated using ratios of several bands at different ranges of the spectrum. For each measurement date, a correlation matrix was built for the 123 SVIs using control non-infested and control infested treatments. Indices highly inter-correlated to each other (Pearson's correlation coefficient  $R > 0.8$ ) were grouped resulting in 20 groups. One SVI was then selected by group which resulted in a final selection of 20 SVIs per date. For the final study, eight SVIs were selected out of 20 following a discriminant analysis between non-infested and nematode infested treatments to reflect the broad range of traits for which the SVIs were initially developed (Table 3).

**Table 3. Selected SVIs, their respective equations, the aimed detection trait and references.**

SVIs	Equation	Traits	Reference
NDVI	$(R_{800} - R_{680}) / (R_{800} + R_{680})$	Biomass, coverage	Rouse et al. 1974
MCARI2	$(1.5[2.5(R_{800}-R_{670})-1.3(R_{800}+R_{550})]) / \sqrt{(2*R_{800}+1)^2-(6*R_{800}-5*\sqrt{R_{670}}-0.5)}$	LAI, coverage	Haboudane et al. 2004
780/700	$R_{780} / R_{700}$	Nitrogen content	Mistele et al. 2004
TGI	$-0.5[(W_{670}-W_{480})(R_{670}-R_{550})-(W_{670}-W_{550})(R_{670}-R_{480})]$	Chlorophyll content	Hunt et al. 2011
CHLG	$(R_{760}-R_{800}) / (R_{540}-R_{560})$	Chlorophyll content	Gitelson et al. 2006
PRI	$(R_{531}-R_{570}) / (R_{531}+R_{570})$	Stress	Gamon et al. 1992
NDWI1650	$(R_{840}-R_{1650}) / (R_{840}+R_{1650})$	Plant water status	Clay et al. 2006
HI	$(R_{534}-R_{698}) / (R_{534}+R_{698}) - R_{704} / 2$	Plant health	Mahlein et al. 2013

### 3.3.7 Statistical data analysis

The program R (R Development Core Team 2008) was used for analysis of the biological data. Beet fresh weight, leaf dry weight and canopy area of BCN infested and non-infested plants were tested for homogeneity of variance. They were then exposed to analysis of variance (ANOVA) at a probability level of 0.05 using the factor “nematode infestation”. Linear regression models were used to quantify the relationship between final beet fresh weight, nematode population and several phenotyping parameters. Regarding spectrometry data, a discriminant analysis was performed to identify, for each date of measurement, indices that allow to discriminate between control infested and non-infested treatments.

### 3.4 Results

#### 3.4.1 Plant fresh weight and nematode population

In both experiments, an artificial inoculation corresponding to 600 eggs and J2 per 100 cm<sup>3</sup> of soil led to a moderate pressure similar to what can be expected in field situations. Such nematode pressure significantly affected the final beet fresh weight (Table 4). In 2014, beet biomass of nematode infested treatment was reduced by 32% compared to the non-infested treatment for the susceptible cultivar *Aimanta*, whereas in 2015, the final beet biomass reduction was 11% for the tolerant cultivar. Final average leaf dry biomass of infested plants (39.4 g.plant<sup>-1</sup>) was significantly lower than that of non-infested plants (47 g.plant<sup>-1</sup>) for the susceptible cultivar (-16%) ( $p < 0.05$ ). This was not the case for the tolerant cultivar where no effect of BCN could be observed on the final leaf dry biomass.

As expected, almost no nematodes were found in the soil of non-infested treatments for both trials. Presence of negligible numbers of eggs and larvae can be explained by the non-sterile field soil that was used for these experiments. A larger number of nematodes was found in the infested pots in 2014 (on average 13535 eggs and larvae per 100 cm<sup>3</sup> soil) compared to 2015 (6950 eggs/larvae on average). The average pf (Final nematode population) / pi (Initial nematode population) ratio was 27 in 2014 and 11.5 in 2015.

**Table 4. Effect of BCN on final beet fresh weight and leaf dry weight of sugar beet plants. Non-infested and infested treatments are displayed for 2014 and 2015 experiments. Means with different letters are significantly different at 5% level.**

	Beet fresh weight (g)	Leaf dry weight (g)	Final nematode population (eggs/larvae per 100 cm <sup>3</sup> soil)
<b>2014 – susceptible cultivar <i>Aimanta</i></b>			
<b>Non-infested (control)</b>	1286.1 ± 30.0 <sup>a</sup>	47.0 ± 1.5 <sup>a</sup>	16.7 ± 14.3 <sup>a</sup>
<b>Nematode infested</b>	886 ± 49.0 <sup>b</sup>	39.4 ± 2.2 <sup>b</sup>	13535.0 ± 1552.0 <sup>b</sup>
<b>2015 – tolerant cultivar <i>Bluefox</i></b>			
<b>Non-infested (control)</b>	1230.7 ± 34.2 <sup>a</sup>	58.7 ± 1.2 <sup>a</sup>	50.0 ± 43.4 <sup>a</sup>
<b>Nematode infested</b>	1096.2 ± 42.3 <sup>b</sup>	60.0 ± 2.0 <sup>a</sup>	6950.0 ± 1236.2 <sup>b</sup>

For both susceptible and tolerant cultivars, final aboveground biomass was strongly correlated with the belowground biomass (Fig. 5). Linear regression in 2014 and 2015 resulted

in  $R^2$  of 0.82 and 0.74 respectively suggesting that leaf biomass is a good indicator of the beet biomass. The close relationship between above and belowground sugar beet biomass confirms the interesting use of non-destructive phenotyping tools to evaluate the status of the plant canopy over time. By measuring the canopy, the growth of the beet can be indirectly investigated.

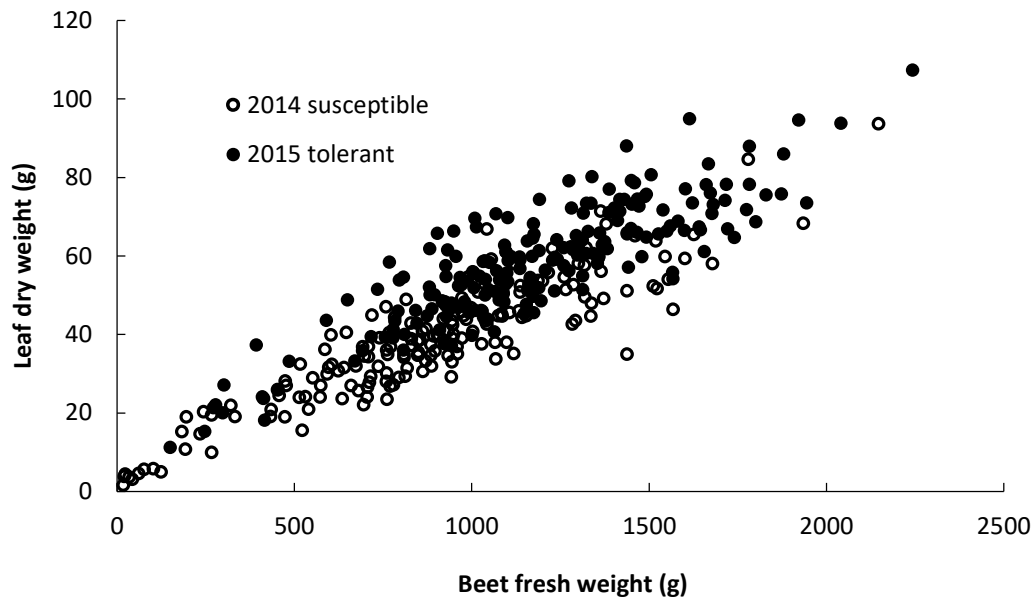


Figure 5. Final leaf dry weight as a function of the final beet fresh weight ( $n=381$ ,  $R^2=0.79$ ,  $p<0.01$ ).

### 3.4.2 Early stress detection using visible imaging

Evolution of the canopy area of infested sugar beets presented similar patterns for susceptible and tolerant cultivars (Fig. 6). Canopy areas of both varieties were strongly affected by BCN during the first 600 °Cd. From 600 to 1000 °Cd, canopy area differences between infested and non-infested plants decreased due to a combination of leaf overlapping and plant recovering. After 1000 °Cd, differences between infested and non-infested treatments were not visible anymore using the canopy area parameter.



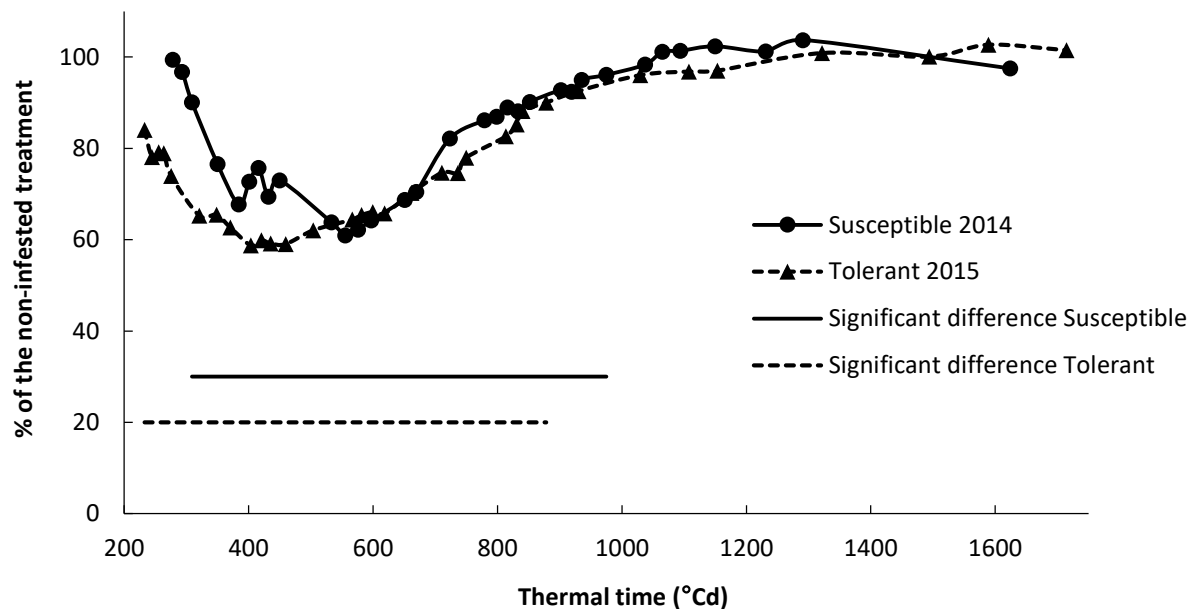


Figure 6. Evolution of the canopy area of infested susceptible and tolerant cultivars. Canopy area is expressed as a percentage of the non-infested treatment. Time periods where the difference in canopy area between infested and non-infested treatments are significant are represented on the figure ( $p < 0.05$ ).

Canopy area allowed the detection of the nematode stress that was applied and the statistically significant discrimination between infested and non-infested plants from 230 °Cd (GS 13) to 880 °Cd (GS 33) for the nematode tolerant cultivar *Bluefox* and from 335 °Cd (GS 14) to 995 °Cd (GS 35) for the susceptible cultivar *Aimanta* ( $p < 0.05$ ) (Fig. 6). This difference in the timing of the stress detection between the two years of trial was most likely caused by the low air temperatures during the first two weeks after sowing in 2014 (Fig. 2). This led to a slow and non-homogenous crop establishment and a low nematode pressure. The high variability in canopy area was reflected by the higher coefficient of variation observed (38% in 2014 and 18% in 2015). In summary, the visible imaging method was very sensitive in detecting the damaging effect of nematodes on aboveground plant growth already in very early stages (after the development of the third leaf 335 °Cd).

### 3.4.3 Canopy temperature evaluation using thermography

Table 5. Canopy temperature (°C) of non-infested and nematode infested treatments at different times during the season. a) Susceptible cultivar in 2014. b) Tolerant cultivar in 2015. Displayed, are the mean  $\pm$  standard error of each treatment. Different letters within each column indicate significant differences.

a)

Susceptible 2014	935 °Cd (57 das)	1446 °Cd (84 das)	1485 °Cd (86 das)
Date - Time	02/07 - 10:30	29/07 - 15:30	31/07 - 14:30
Vapour Pressure Deficit (kPa)	0.37	0.77	1.93
Non-infested	13.7 $\pm$ 0.3 <sup>a</sup>	18.6 $\pm$ 0.5 <sup>a</sup>	22.8 $\pm$ 0.4 <sup>a</sup>
Nematode infested	14.6 $\pm$ 0.2 <sup>b</sup>	19.5 $\pm$ 0.3 <sup>b</sup>	27.4 $\pm$ 0.6 <sup>b</sup>

b)

Tolerant 2015	581 °Cd (36 das)	599 °Cd (37 das)	736 °Cd (44 das)	856 °Cd (52 das)	1347 °Cd (74 das)
Date - Time	09/06 - 17:30	10/06 - 16:30	17/06 - 17:00	25/06 - 14:30	17/07 - 16:30
Vapour Pressure Deficit (kPa)	0.68	0.87	2.01	2.44	4.88
Non-infested	15.1 $\pm$ 0.1 <sup>a</sup>	17.7 $\pm$ 0.22 <sup>a</sup>	23.7 $\pm$ 0.46 <sup>a</sup>	23.3 $\pm$ 0.69 <sup>a</sup>	32.8 $\pm$ 0.79 <sup>a</sup>
Nematode infested	15.4 $\pm$ 0.09 <sup>b</sup>	18.1 $\pm$ 0.18 <sup>a</sup>	23.8 $\pm$ 0.41 <sup>a</sup>	24.5 $\pm$ 0.43 <sup>a</sup>	33.4 $\pm$ 0.75 <sup>a</sup>

In 2014, canopy temperature differed significantly between treatments throughout the whole observed period (Table 5). Always, canopy temperature of nematode infested plants was significantly higher than the canopy temperature of the non-infested plants. At 1446 °Cd, average canopy temperature of the non-infested treatment was 18.6 °C versus 19.5 °C for the infested treatment. For the susceptible cultivar, differences between the two treatments increase with increasing VPD.

In 2015, for the five dates of measurement, the canopy temperature of infested plants was on average 0.5 °C higher than the canopy temperature of the non-infested ones. However the difference was statistically significant only at 581 °Cd. There was no obvious correlation

between the differences in canopy temperature of the two treatments and the VPD for the tolerant cultivar.

It can be stated that such canopy temperature differences observed between treatments are caused by nematode stress and not by the environmental condition variability on the platform. In fact, the randomised complete block design of the experiment was set up according to an air temperature gradient which prevented any effect of air temperature variability on the canopy temperature comparison between nematode infested and non-infested treatments. Soil moisture was similar for all the pots at each measurement date.

#### 3.4.4 Nematode stress identification by a spectrometry approach

**Table 6. Selection of SVIs that allowed to statistically discriminate non-infested and nematode infested treatments. A comparison of means has been performed (t-test for independent samples) and the significant SVIs are displayed in the table. SVIs in bold discriminate treatments with a p-value lower than 5% and the others between 5% and 10%. SVIs were grouped according to the trait they are related to.**

	Thermal Time	Growth stage	Biomass	Chlorophyll	Water	Stress
2014	1371 °Cd	37	NDVI, 780/700	CHLG	NDWI1650	HI
	404 °Cd	15	NDVI, 780/700, MCARI2	PRI	-	HI
	460 °Cd	16	MCARI2, 780/700	PRI	-	HI
2015	599 °Cd	20	MCARI2	CHLG, PRI	-	HI
	736 °Cd	31	MCARI2	TGI	NDWI1650	HI
	978 °Cd	35	780/700	TGI	-	-
	1618 °Cd	39	-	PRI	-	-

In Table 6, indices are grouped according to their relevance in assessing plant biomass, chlorophyll content, water status and general stress. Among the different indices, those related to the biomass, chlorophyll and general stress resulted in better detection of the nematode infestation and damage at the different stages of the crop development. In 2015, from 404 °Cd to 736 °Cd (GS 15 to GS 31), SVIs mainly related to plant biomass such as NDVI or leaf area such as MCARI2 were significantly affected by nematodes which confirmed the previous observation concerning the canopy area. At more advanced stages (GS 31 to GS 39), differences could be detected on both susceptible and tolerant cultivars using the CHLG and

TGI respectively. The Health Index (HI), which was developed specifically for sugar beet, was particularly effective consistently across the two years of investigation and at different stages of crop development.

In the last measurement (1618 °Cd), sugar beet plants displayed additional symptoms of general stresses with early leaf senescence which affected the identification of sole nematode effects.

### 3.4.5 Phenotyping parameters and final data

Table 7. Pearson's correlation (R) between phenotyping variables at different dates and the fresh weight of the beet and final nematode population in the soil (n = 20, p<0.1).

	Thermal Time	Detection trait	Beet fresh weight	Final number of eggs/larvae per 100 cm <sup>3</sup> of soil
2014 - susceptible	935, 1446, 1485 °Cd	Canopy temperature	.	.
	-	Cumulative canopy area	0.32	.
		CHLG	0.80*	- 0.79*
	1371 °Cd	NDVI	0.59*	- 0.76*
		MCARI2	0.67*	- 0.78*
2015 - tolerant	581, 599, 736, 856, 1347 °Cd	Canopy temperature	.	.
	-	Cumulative canopy area	0.54*	.
	404 °Cd	HI	0.40*	- 0.60*
	460 °Cd	780/700	0.37*	- 0.71*
	599 °Cd	CHLG	0.41*	- 0.42*
		PRI	0.32	- 0.61*
	736 °Cd	TGI	0.36	- 0.51*
	978 °Cd	HI	0.37*	.

**Cumulative canopy area: Integral of the canopy area from sowing until the date when the plateau was reached (1300 °Cd in 2014 and 1100 °Cd in 2015). \* indicates significant correlations (p<0.1).**

Most of the SVIs in Table 6 were significantly correlated with beet fresh weight and final nematode population in the soil. Correlation coefficients were always higher for the susceptible cultivar compared to the nematode tolerant cultivar (Table 7). On average NDVI,

MCARI2 and CHLG were highly correlated with the beet fresh weight ( $R=0.69$ ) and the final nematode population ( $R=0.78$ ) for the susceptible cultivar. Cumulative canopy area which reflects the ability of the plants to absorb light over the season was significantly correlated with the final beet fresh weight in 2015 ( $R=0.54$ ,  $p<0.1$ ). In 2014, the weak correlation observed was not significant ( $R=0.32$ ). There was no significant correlation between cumulative canopy area and final BCN population in the soil. Canopy temperatures did not show any significant correlations with the final beet fresh weight and BCN population.

### 3.4.6 Practical application of visible imaging for nematicide research

In 2015, clear differences were observed in the canopy area between treatments during the first 35 days of plant development (Fig. 7). 244 °Cd (15 das), canopy area of *Fosthiazate* treated plants was 29% higher than canopy area of the nematode infested treatment. At this date, average canopy areas of non-infested and *Fosthiazate* treatments were statistically larger than the canopy area of nematode infested treatment (Fig. 8a). Evolution of canopy areas of non-infested and *Fosthiazate* treated plants showed similar pattern. Both treatments showed significantly higher canopy area compared to the nematode-infested treatment from 244 to 560 °Cd (GS 16) (Fig. 7).

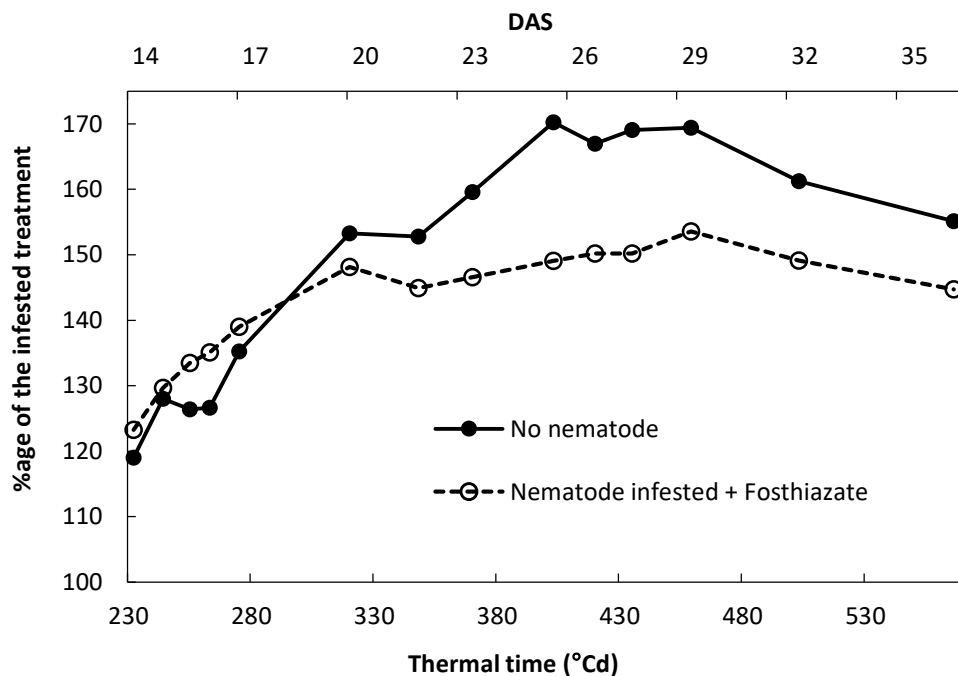


Figure 7. Canopy area of the non-infested and *Fosthiazate* treatments as a percentage of the nematode infested treatment ( $n=10$ ). Only the first 35 days of growth are represented. From 244 to

560 °Cd both non-infested and *Fosthiazate* treatments showed statistically significant higher canopy area than the nematode infested treatment ( $p < 0.05$ ).

The same trend was observed in the final sugar beet yield. *Fosthiazate* treatment showed significant benefit in the final beet fresh weight compared to the nematode infested treatment (+ 14%) (Fig. 8b). Early canopy area differences reflected the final sugar beet yield.

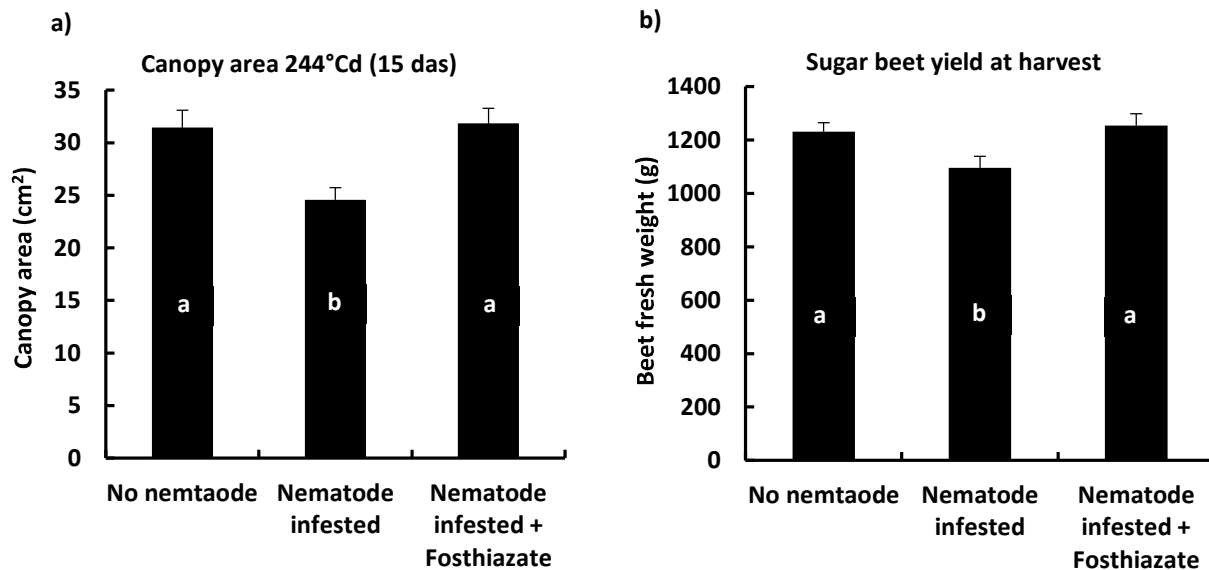


Figure 8. a) Average canopy area and b) final beet fresh weight of three treatments from 2015 trial ( $n=10$ ). Bars represent the standard error of the mean. Different letters indicate significant differences ( $p < 0.05$ ,  $n=10$ ).

### 3.5 Discussion

The present study compares three phenotyping techniques in the same experimental settings across two years and two sugar beet cultivars. A multi-sensor approach was found to be of advantage for continuous crop phenotyping or monitoring in experimental and field settings (Liebisch et al. 2015; Pfeifer et al. 2016). While more studies have been conducted under controlled greenhouse conditions (Hillnhütter et al. 2012; Joalland et al. 2016), this work was carried out outdoor by simulating conditions that are close to the real field situations comprising soil type, nematode infestation, plant density, duration of the crop cycle, plant canopy and root development. To the best of our knowledge, such a comparison of three phenotyping methods under outdoor conditions to characterise the sugar beet growth has not been published before.

During the two years of experimentation, the artificial nematode infestation successfully led to a yield reduction of 32% for the susceptible cultivar and 11% for the tolerant cultivar. These results are consistent with reports from other field and microplot studies (Cooke 1987; Herr 1996). Thus the microplot settings used in this study were successful to simulate a realistic timing of nematode infestations and crop damage. BCN multiplication was 2.5 times higher for the susceptible cultivar compared to the tolerant one. This order of magnitude is consistent with respect to the definition of “nematode tolerance” given by Trudgill (1991). The fact that no differences could be observed in the final shoot biomass for the tolerant cultivar can be explained by the ability of the nematode tolerant cultivar to endure nematode damage and recover during the second part of the growing season (Wallace 1988; Davy de Virville and Person-Dedryver 1989).

Visible imaging, thermography and spectrometry measurements enabled detection in a non-invasive, dynamic and objective manner of the effect of nematode infestation on sugar beet plants. Digital canopy area extracted from top-view visible images is a suitable tool to evaluate the effective plot-based canopy area. This parameter is taking account of different morphological components of the sugar beet such as the number of leaves, the area of the leaves and the plant architecture (Milford et al. 1985a). Canopy area appeared particularly suitable to dynamically characterise the early growth of the sugar beet plant from sowing to an advanced vegetative stage (GS 35). In a previous study carried out under greenhouse conditions, the “digital canopy area” parameter was identified as a proxy to estimate the shoot and root biomass of the sugar beets (Joalland et al. 2016). Such dynamic prediction of

leaf biomass using visible images was also reported and used for high throughput phenotyping on other crops under greenhouse conditions (Golzarian et al. 2011; Hartmann et al. 2011). In the present study we demonstrated that the digital canopy area can be adapted to, and is effective in, outdoor conditions by looking at clusters of plants simulating the natural seed density expected in real field conditions. Overall, the top down visible imaging method showed its strength in the early evaluation of the degree of growth inhibition of the plant biomass. The nematode tolerant cultivar did not prevent BCN affecting the early plant development. Surprisingly, in the early growth stages, the canopy area reduction was higher for the tolerant cultivar compared to the susceptible cultivar which indicates that the tolerance mechanism does not prevent early nematode damage (Trudgill 1992). Benefits in very early plant growth (244 °Cd) observed with the use of *Fosthiazate* showed the ability of a contact nematicide to protect the root by suppressing the first generation of J2 hatching from the cysts and to ensure yield benefit compared to the untreated plants (Woods et al. 1999).

Canopy temperature reflects plant water status, stomatal conductance and transpiration rate of the leaves (Inoue et al. 1990; Cohen et al. 2005; Oerke and Steiner 2010). It has been shown that nematodes strongly decrease water uptake of the roots which increases the stomatal resistance and consequently reduces the leaf evapotranspiration (Haverkort et al. 1991; Jones 2004). In 2014, significantly higher canopy temperatures were observed for the nematode infested sugar beets compared to the non-infested plants. These results are consistent with previous observations made by Schmitz et al. (2004) where a correlation between canopy temperature and nematode density was observed. Temperature difference between the two treatments increased with VPD. Infested susceptible plants had difficulties in cooling down their leaves when air conditions become constraining (VPD >1.5). Most likely, infested plants were not able to keep up the high transpiration rate because of nematode damage at root level which compromised water uptake. The tolerant cultivar *Bluefox* behaved differently. Tolerance mechanisms allow sugar beet plants to maintain their transpiration rate even under high VPD.

Spectrometry measurements allowed the calculation of SVIs that reflected specific agronomical or physiological traits such as chlorophyll content, water content, biomass or photosynthesis rate (Curran et al. 1991; Gitelson and Merzlyak 1996; Mahlein et al. 2012; Liebisch et al. 2014). The present study showed that specific SVIs allowed to differentiate between nematode infested and non-infested plants. Nematodes have an effect on different physiological parameters in both susceptible and tolerant cultivars. On the tolerant cultivar,



most symptoms occur during the first two months of growth whereas on the susceptible cultivar, symptoms persist at more advanced growth stages since the plants are not able to recover from the infestation. The 2015 experiment helped to associate a type of BCN stress with the growth stages or time period where it occurs. The performance of indices related to the biomass and chlorophyll content was variable depending on the growth stages and among them MCARI2, 780/700 and TGI were the most promising. A close relationship has been demonstrated between the value of TGI index and the leaf chlorophyll content on a variety of crops (Hunt et al. 2011, Constantin et al. 2015). Such effect of BCN decreasing the leaf chlorophyll content was also reported by Schmitz et al. (2006). Nematode effect on the leaf water content was low in the tolerant cultivar which confirmed the limited effect of nematodes (also observed with thermography) in reducing transpiration rate on a tolerant cultivar. Two SVIs appeared suitable from early growth stages (GS 15) to advanced stages (GS 39) in detecting the stress caused by nematodes; HI and PRI. Health index (HI) uses two spectral regions centred on 700 nm and 534 nm. Reflectance near 700 nm is a feature of green vegetation and chlorophyll content whereas reflectance around 534 nm is an indicator of photosynthetic function (Gamon et al. 1992; Gitelson and Merzlyak 1996). Thus, HI can be classified as a general stress index (Mahlein et al. 2013). Photochemical reflectance index (PRI), based on reflectance at 531 and 570 nm, reflects the light use efficiency (Trotter et al. 2002). Although HI and PRI are not nematode specific, they appear suitable in detecting nematode stress over the whole season under semi-field conditions.

Correlations between SVIs and final sugar beet biomass demonstrated the ability of spectrometry in predicting final yield on both susceptible and tolerant cultivars. In particular, CHLG and MCARI2 were the best SVIs to predict final yield on susceptible cultivars. Close relationship between beet fresh weight and nematode incidence make the correlation between SVIs and BCN populations evident. Correlations were higher for the susceptible cultivar compared to the tolerant cultivar because of the larger range of beet fresh weight that was observed. Cumulative canopy area was also correlated with the final sugar beet yield suggesting a close relationship between the early plant growth and the final yield of the sugar beet. Such relationship between early phenotyping parameters and final yield is not so clear with other crops such as maize or wheat where the early plant growth does not always reflect the final plant yield as reported by Tekrony and Egli (1991), Egli and Rucker (2012) and Sankaran et al. (2015). In this respect, sugar beet appears a suitable crop for early yield prediction using phenotyping measurements.

Our results obtained with visible phenotyping showed that a slight delay in plant growth during the first 30 days had a significant effect on the final yield. Similar results were highlighted in a previous field study by sowing seeds of sugar beets at different timings to simulate a delay in the plant development (Scott et al. 1973). The larger the canopy, the greater is the use of incident radiation. Olthof (1983) observed higher damage on the plant when seeds were sown directly in nematode infested soil than when the infestation occurred two weeks after sowing. Early growth delay observed for the nematode infested plants could not be compensated during later growth of the crop. Thus, it appears crucial to avoid stress during the first growth stages of the sugar beet (Griffin 1981). The *Fosthiazate* effect in 2015 supports this point. In this experiment, *Fosthiazate* nematicide was used as additional “positive control”. This nematicide acts by suppressing nematode hatching from the cysts and paralyzing juveniles and it is known to provide a strong root protection during the first month of the plant growth (Woods et al. 1999). According to the rate that was applied ( $30 \text{ kg}\cdot\text{ha}^{-1}$ ) and the concentration required for biological activity, it is likely that the *Fosthiazate* effect in the soil stopped after six to eight weeks (Woods et al. 1999; Pantelelis et al. 2006). However, the early protection enabled a good development of the seedlings and insured yield benefit compared to the nematode infested plants. This result is of interest for crop protection research. Under moderate nematode pressure, protection of sugar beet plants against nematode damage should occur from sowing to  $1200 \text{ }^\circ\text{Cd}$  (GS 25). Late nematode infestation did not significantly affect the plant growth of tolerant cultivars.

Given the complicated nature of the investigated nematode-plant interaction with belowground damage and unspecific symptoms displayed in the canopy, the phenotyping techniques evaluated here provided very encouraging results with potential applications in the area of sugar beet research. It can be stated that, visible imaging, thermography and spectrometry compared in the present investigation are complementary tools and are particularly suitable for automation. Field phenotyping platforms with multiple sensor systems will therefore be a valuable tool to improve crop performance via optimised management schedules (Kirchgessner et al. 2017; Virlet et al. 2017).

### 3.6 Conclusions

In conclusion, the study demonstrated that it was possible to use non-invasive and non-destructive technologies to characterise the dynamic of the plant growth and detect stress symptoms caused by BCN on nematode susceptible and tolerant sugar beets. While thermography only showed the ability to detect BCN stress on a susceptible cultivar, spectrometry and visible imaging technologies allowed the indirect observation of BCN damage on both susceptible and nematode tolerant cultivars and to give a prediction of the yield potential. In addition, the three different techniques have their specific strength at different points in time reflecting particular growth stages of the sugar beet. Visible imaging was the earliest stress indicator whereas spectrometry and thermography could identify the stress still when the canopy reached full coverage. Further applications of these tools could be developed for controlled environment and field situations. Under control conditions, canopy area has a great potential to be used as an early parameter to predict the degree of inhibition of the plant biomass caused by BCN and to quantify the degree of benefit from a new compound. Under field conditions visible image analysis, alone, may not be sufficiently specific to identify nematode damage because canopy area reduction can be caused by other types of stress. Therefore this technique would need to be combined with other approaches (e.g. spectrometry; thermography and/or soil sampling).

### 3.7 Acknowledgment

We would like to thank Dr. Roger Hall for his careful review of the manuscript and for his valuable suggestions and corrections as well as Beat Reber and Tobias Plec for the technical support in setting up the trials. We also thank Brigitte Slaats and Tobias Straumann for growing and providing the nematode inoculum and Cliff Watrin and Rita Kuznia for their technical advice through the project phases.



## Chapter 4.

### Application of a leaf segmentation method to detect stress caused by nematodes on sugar beet plants



**Samuel Joalland, Marco Pari, Alessandro Bevilacqua, Claudio Srepani**

This chapter is in preparation for submission to the peer-reviewed journal "Rhizosphere".

## 4.1 Abstract

The use of computer vision tools for image-based plant phenotyping has increased substantially in recent years, paving the way for numerous applications in plant science. Several of them have been developed to measure plant canopy area as a proxy for plant growth and plant response to environmental changes. Here we present a specific example, the development of a leaf segmentation method to count the number of sugar beet leaves and detect stress caused by a plant-parasitic nematode attack on sugar beet roots grown outdoor.

A leaf segmentation algorithm was built to analyse images of nematode infested and non-infested sugar beets grown in micro-plot during the early stage of plant development (from four to eight unfolded leaves). Results from the algorithm were compared with the true leaf number. The mean absolute error (MAE) of our system was 0.49 leaves. This precision allowed to conclude on a significant reduction in the number of leaves of nematode infested compared to non-infested plants at the four dates of measurement. An indirect estimation of the average leaf size showed that nematodes infection on the roots affected the two components of canopy area; leaf apparition and leaf expansion rates.

In conclusion, the developed leaf detection algorithm was demonstrated to be a promising tool to automatically count the sugar beet leaves under outdoor conditions during the early development of the sugar beet plants, with a MAE compatible with the application purposes. Moreover, the algorithm enabled the reliable differentiation of nematode infested and non-infested plants by detecting differences in the number of leaves. Thus, this work opens new opportunities for the use of high-throughput phenotyping tools to evaluate the efficacy of diverse nematode control approaches (i.e. breeding and chemical or biological control) in sugar beet during the early developmental stages.

## 4.2 Introduction

Plant growth has always been a trait of interest for plant performance evaluation since changes in plant biomass are very often related to changes in yield (Radford 1967). The fast development of image-based phenotyping applications allows the investigation of different components of the plant growth with a high level of precision. Sugar beet represents a valid crop model to study the relationships between plant growth, canopy development and final yield (Milford et al. 1985a; Joalland et al. 2016).

Twenty percent of the world's supply of sugar is derived from sugar beet (FAO 2009). The EU is the world's leading producer with a production of 102 million tons of sugar beet in 2015, which represented around 50% of the global production (Eurostat 2015). Sugar beet yield is formed by the beet, rich in sugar. Often the development of the beet is seriously affected by soil borne pathogens such as plant-parasitic nematodes. Belowground symptoms include a reduction of the beet growth and the appearance of many secondary roots to compensate for those infested by nematodes. Beet Cyst Nematodes (BCN) also cause diverse aboveground symptoms, like stunted growth, decreased chlorophyll content and wilting of the canopy due to water stress (Cooke 1987; Schmitz et al. 2006). Thus, non-destructive phenotyping methods appear to be appropriate for the detection of BCN related symptoms in sugar beet and for use as an early diagnosis of nematode infestations.

Among the different phenotyping approaches, visible imaging is a cheap technology, which is easy to handle and to calibrate (Li et al. 2014). The projected shoot area of the plants can be easily computed from visible images and has been widely used to estimate shoot biomass in different plant species (Lukina et al. 1999; Smith et al. 2000; Mizoue and Masutani 2003; Tackenberg 2007). Most notably in sugar beet, visible imaging showed promising results in discriminating at an early plant developmental stage, between BCN infested and non-infested plants in the greenhouse (Joalland et al. 2016). In this study, the “digital canopy area” parameter calculated was a suitable proxy for shoot and root biomass estimation during the first two months of growth.

The use of such simple phenotyping techniques has several potential applications in agricultural research: to obtain early indications on the efficacy of new crop protection products or to evaluate the degree of tolerance or resistance of new cultivars by studying the degree of inhibition of the canopy area under different nematode infestation levels. Yet, when studying the growth of sugar beet, the projected shoot area may not be the most suitable

parameter because it takes into account both growing and non-growing leaves. To improve the approach, an option consists to run analysis at the leaf level. Projected canopy area is a proxy, which integrates three fundamental parameters: number of leaves, size of leaves and leaf angle (Milford 1985b). In this paper, we focus on the number of leaves, which allows to determine the plant growth stage. More precisely, we investigate the ability of a leaf segmentation algorithm to count the number of leaves and detect stress caused by BCN.



### 4.3 Material and methods

#### 4.3.1 Sugar beet growing

Images of sugar beet plants were collected from an outdoor experiment conducted in 2015 on a polytunnel area equipped with 70 microplots of 150 litres (0.34 m<sup>2</sup>) and located in the Syngenta Research Centre in Stein (Switzerland). 20 microplots were used for this study.

The experiment consisted of two treatments: (i) non-infested soil (control); and (ii) soil infested with cysts of *H. schachtii* establishing the equivalent of 600 second stage juveniles per 100 cm<sup>3</sup> of soil at sowing (treated). This level of infestation can be considered as moderate and is realistic when compared to the level that can occur in open field. After the soil inoculation, three seeds of the nematode tolerant *Bluefox* cultivar (Syngenta, Switzerland) were sown per microplot in a sandy loam non-sterile soil (56% sand, 31% silt, 11% clay, pH 7.7, 2% organic matter). A complete randomised design was adopted and each treatment was replicated 10 times.

#### 4.3.2 Image capture

Visible images were captured using a digital camera Canon S100 (Canon, Tokyo, Japan) at four different times during the growth, that is 22, 27, 29 and 32 days after sowing (das) corresponding to growth stages (GS) BBCH 14, 15, 16 and 18 (Meier et al. 1993) (Fig. 1).

The camera was mounted on a mobile monopod and images were obtained from 1.8 m above the plant canopy with a resolution of 0.0029 cm<sup>2</sup>/pixel. The monopod was held vertically in order to position the camera centred above the centre of the pot. Photos were taken using the automatic settings of the camera. Three plants are visible per image. The dataset comprises a total of 80 images with 20 images per date of measurement.

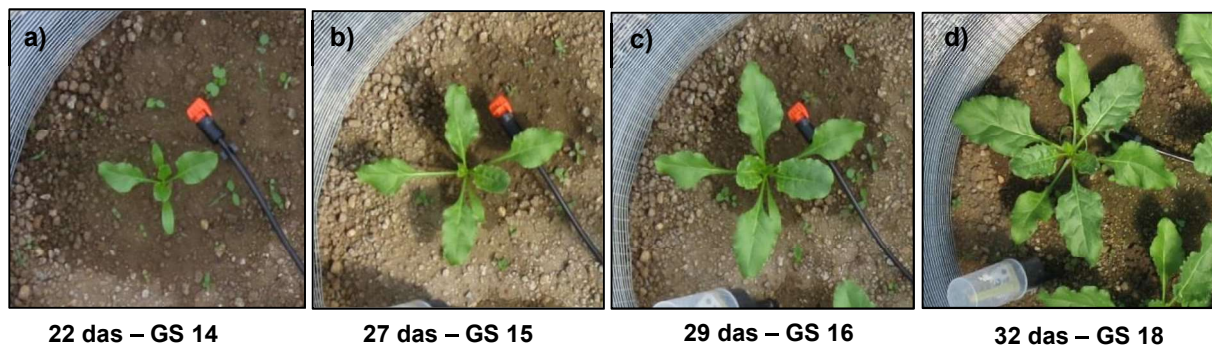


Figure 1. Top microplot images of one sugar beet plant at four timings: a) 22 das, b) 27 das, c) 29 das and d) 32 das.

### 4.3.3 Image analysis

The approach used to identify and count the number of leaves was inspired by different methods described by Scharr et al. (2016) in a collation study about leaf segmentation. Scharr's paper focused on single plants of *Arabidopsis thaliana* grown under controlled conditions. Our method was built for leaf detection on sugar beet grown under field-like conditions. To identify single leaves from each plant, the method consisted of three main steps that can be summarised in Fig. 2: plant segmentation, leaf identification and leaf segmentation. Canopy area was calculated using the protocol previously developed for sugar beet and described in detail by Joalland et al. (2016).

#### Plant segmentation

The first step was to select the region of interest and convert visible images to the lab colour space. This transformation compensates for the various lightning conditions observed between pots and timings. On the "a" channel, two separate peaks corresponding to soil and canopy could be observed which allowed the straightforward setting of the threshold for the "a" to 115. After applying the segmentation and separating the plant from the background, all the pixels not belonging to the plant canopy were removed and set to black.

#### Leaf identification

Erosion and dilatation were applied and combined to remove noise caused by small objects (opening) or to fill small holes (closing). Then, a distance map was computed using a distance transform function and a local maxima filter was subsequently applied to select the central part of each object.

#### Leaf segmentation

A blob centre detection method was used to connect pixels belonging to the same "blob". Finally, the ultimate erosion method was applied to separate overlapping leaves, thus achieving their total number (Dougherty 1994).

Image analysis was performed with the integrated development environment Xcode 7.2 on a MacBook Air endowed with four GB of RAM and a 1.7GHz dual-core Intel i5 processor. Libraries OpenCV version three were used to build and optimise the algorithm.

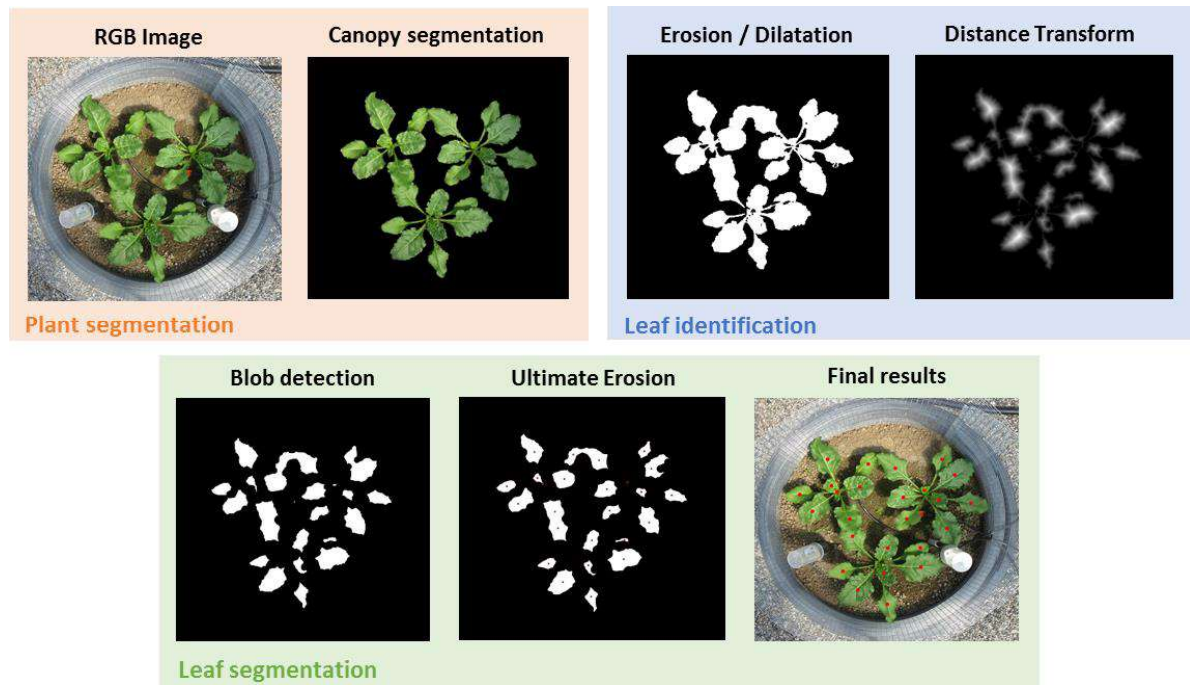


Figure 2. Example images illustrating the different steps in our approach (from left to right, top to bottom).

For each image, the ground truth number of leaves was evaluated. Phytomers longer than one cm were considered as leaves.

#### 4.3.4 Data analysis

At the start of measurement, cotyledons were considered and counted as leaves by the algorithm. It was not possible to automatically differentiate them from the true leaves because of their similarity in shape, size and colour (Fig. 1a). Thus, we subtracted two leaves from the leaf number count of each plant. For the other dates of evaluation, we did not apply this correction.

To evaluate the performance of the algorithm as well as the overall leaf segmentation accuracy, the residuals were computed. The Mean Error (ME) and the Mean Absolute Error (MAE) were computed accordingly.

The significance of the number of leaves between the two treatments was evaluated using the program *R* (version 3.2.3, The R Foundation for Statistical Computing). Results were exposed to a t-test at a probability level of 0.05 using the factor “nematode infestation”.

## 4.4 Results and discussion

### 4.4.1 Evaluation of the algorithm

The MAE of our algorithm was 0.49 of a leaf (Table 1). This error increased with the growth stage of the sugar beet. The higher the number of leaves, the larger the error. Overall, our algorithm tended to underestimate the real number of leaves (ME = -0.32). The underestimation increased substantially when plants reached eight to nine leaves. At this stage, the new developed leaves started to overlap the old ones. This was due to the particular sugar beet architecture which follows a specific 5:13 phyllotaxis (Stehlik 1938; Milford et al. 1985b). Thus, leaf number eight and nine slightly overlap leaf number three and four respectively. In addition, 32 das, largest leaves started to overlap adjacent ones. The ultimate erosion method was not always able to properly discriminate between overlapping leaves. The algorithm was accurate and robust in detecting leaves from BBCH 14 to 17 (four to seven leaves per plant) with ME of 0.3 leaves. Such high precision in counting leaves in the early growth stages is particularly suitable as the early sugar beet growth has a strong impact on the final yield (Scott et al. 1973).

**Table 1. ME and MAE of our algorithm at the different dates of measurements.**

Days after sowing	22	27	29	32	Average
Plant growth stages (BBCH)	14	16	17	18/19	-
ME	- 0.2	- 0.07	- 0.18	- 0.81	- 0.32
MAE	0.23	0.33	0.35	1.05	0.49

#### 4.4.2 Identification of nematode stress

##### Nematodes affect the growth of the canopy

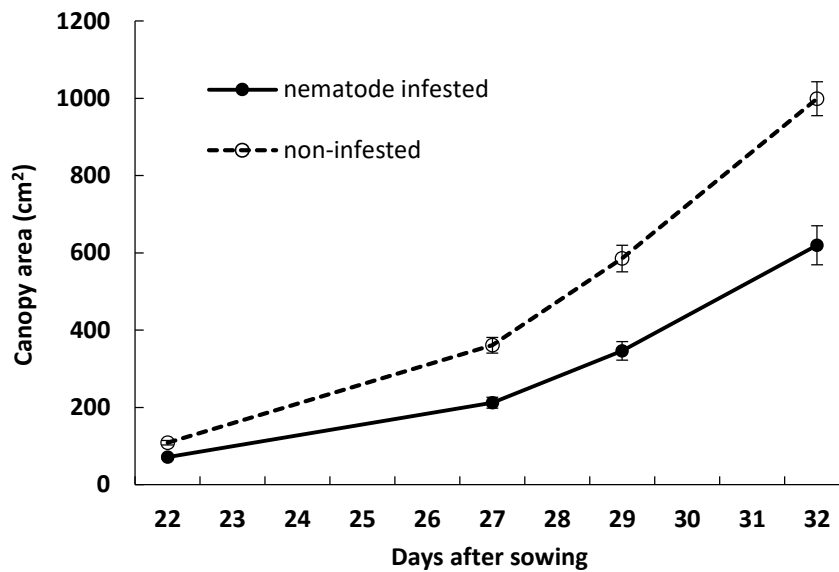


**Figure 3.** Evolution of the canopy area of BCN infested and non-infested sugar beets as a function of the time. Bars represent the standard error of the mean.

The first step in our image analysis workflow allowed the separation of plants from the background and to calculate their canopy area. From 22 to 32 das, canopy area of non-infested sugar beets was significantly larger than the canopy area of BCN infested sugar beets. Benefit from the non-infested treatment over the infested increased during the plant growth from 53% 22 das to 70% 29 das (Fig. 3). Such early canopy area reduction caused by nematodes has already been reported by Joalland et al. (2016) under greenhouse conditions on a nematode susceptible cultivar. In such controlled conditions they also demonstrated that at these early growth stages canopy area was a proxy for root biomass. In the present study we were able to observe a significant effect of the nematodes under outdoor conditions on a tolerant cultivar. Such early nematode effect on the canopy development of tolerant sugar beet cultivars could be expected under moderate nematode pressure in the soil. Tolerant cultivars did not prevent nematode penetration into the roots (Westphal 2013). Despite their ability to yield well under nematode infestation, tolerant cultivars still suffer from early infestation. Our results suggested that tolerance mechanism such as canopy recovery occur later in the growth.

## Nematodes delay the apparition of leaves

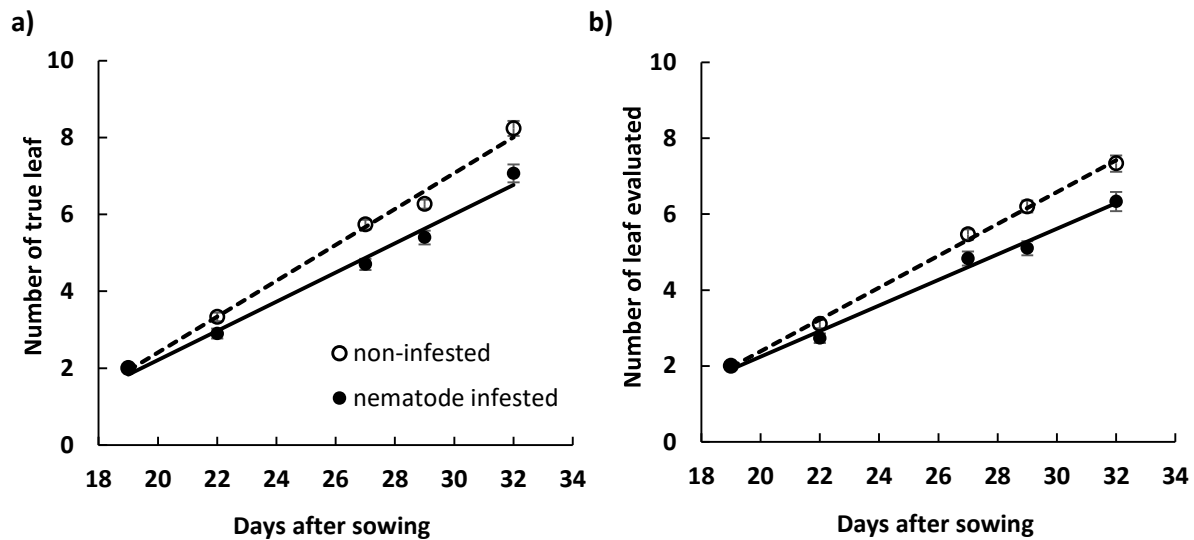


Figure 4. Number of true leaves a) and number of leaves identified with our algorithm b) as a function of the time. Bars represent the standard error.

From 22 to 32 das, a significant lower number of leaves was counted (ground truth) and identified (using the algorithm) on the BCN infested plants compared to the non-infested ones (Fig. 4). Average ground truth difference between the two treatments increased from 0.4 leaves 22 das to 1.1 leaves after 29 days (Fig. 4a) which showed that nematodes had a lasting effect in delaying the apparition of leaves during the first month of growth. For both counting methods, the slope of the linear trend line was significantly higher for the control (non-infested) compared to the nematode infested treatment ( $p < 0.01$ ). The thermal time interval that separates the appearance of two successive leaves (phyllochron), as defined by Milford et al. (1985a), was significantly longer for plants infested with nematodes (+ 12% and + 15% for the ground truth and algorithm method respectively). Cooke (1987) and Joalland et al. (2016) observed similar leaf apparition delay under greenhouse conditions. As soon as nematodes started to infest the plants, a recovery process was initiated which led to a production of secondary roots. Such a phenomenon decreases the leaf apparition rate. In this study we were able to detect this delay at the semi-field level by counting leaves using an automatic computer vision algorithm.

### Nematodes decrease the leaf expansion

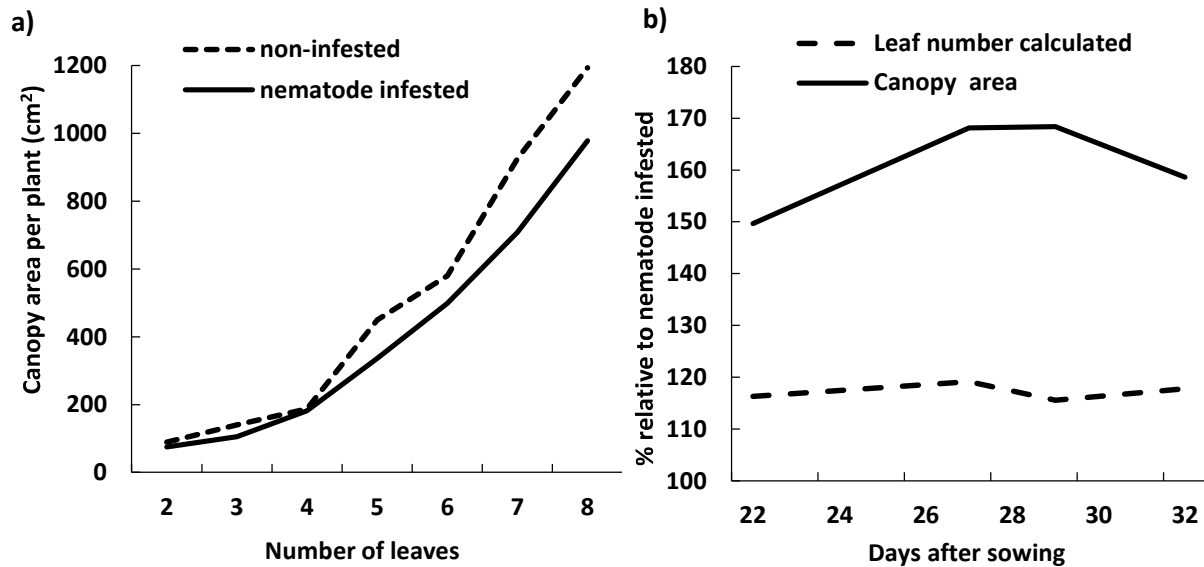


Figure 5. a) Canopy area as a function of the number of leaves (calculated). b) Leaf number (calculated) and canopy area as a percentage of the nematode infested treatment.

Fig. 5a displays the canopy area as a function of the number of leaves for both infested and non-infested treatments. For a given number of leaves, canopy area of non-infested sugar beets always appeared higher than the canopy area of the nematode infested plants. When plants reached BBCH 15 (five leaves), canopy area of the non-infested sugar beets was 34% larger than the canopy area of the infested plants. The average area of BCN infested leaves was smaller than non-infested ones. Stress caused by nematodes decreased the leaf expansion rate.

This observation was confirmed in Fig. 5b which presents the evolution of the canopy area and the number of leaves of the non-infested treatment as a percentage of the infested one. While the nematode effect on the leaf apparition appeared constant over time (+ 16% on average for the non-infested sugar beets), the effect on the canopy area increased between 22 and 27 das. During this time period, the increase in canopy area for the non-infested treatment over the infested treatment varied from 53 to 70%. This clearly demonstrated that nematodes also have a strong effect in decreasing the leaf expansion rates of the first growing leaves. The production of secondary roots to recover from the infestation as described by Cooke (1987) not only affects the leaf organogenesis but also the leaf growth.

## 4.5 Conclusions

In conclusion, the image analysis method developed in this study is fast, robust and accurate enough to detect significant differences in the number of leaves between nematode infested and non-infested sugar beets in a period of development from four to eight unfolded leaves. The method does not require any training and the number of parameters to setup is small. Threshold parameters can be easily tuned for each dataset or each image. The “ultimate erosion” method was very specific for the analysis of images taken under field like environment with realistic planting density. It displayed promising results in differentiating overlapping leaves from the same plant but also from adjacent sugar beets.

We investigated how nematodes affect the number of leaves. Evaluation of such a parameter using the computer vision approach highlighted that nematode stress delays the leaf organogenesis during the first month of growth. Indirect investigation on the size of the leaves showed that leaf expansion rate (morphogenesis) was also affected and decreased by nematodes. These new results support the evidence that leaf appearance can be a suitable proxy to detect in a non-destructive manner the stress below the ground. Both organogenesis and morphogenesis are components of the canopy area. This opens up opportunities for the further development of a computer vision tool to precisely identify and track the growth of single leaves over time. It will allow the potential use of a specific leaf as a proxy for nematode stress detection (by tracking its expansion rate over time). In the current context, where precision agriculture is playing a major role, this type of simple phenotyping tool has the potential to be integrated into a broader solution. Using an unmanned aerial vehicle our method can detect the degree of sugar beet canopy development in a large field area early and in a fast and efficient manner. Thus, it can highlight a planted area which is under stress and trigger more targeted and localised crop management actions.

## 4.6 Acknowledgment

We would like to thank Dr Chris Godfrey for his careful review of the manuscript and for his valuable suggestions and corrections.



## **Chapter 5.**

### **Multi sensors approach for the evaluation of sugar beet cultivar tolerance to the Beet Cyst Nematode in the field**



<http://blog.omex.co.uk>

**Samuel Joalland, Claudio Screpanti, Hubert Vincent Varella, Marie Reuther, Mareike Schwind, Christian Lang, Achim Walter, Frank Liebisch**

This chapter is in preparation for submission to the peer-reviewed journal "Remote Sensing".

## 5.1 Abstract

The fast development of digital phenotyping methods based on ground or unmanned aerial vehicle (UAV) platforms has increased our ability to evaluate traits of interest for crop breeding and crop management in the field. A field site infested with beet cyst nematode (BCN) and planted with four nematode susceptible cultivars and five tolerant cultivars was investigated with hyperspectral and thermal sensors at ground and airborne level, respectively at different times during the growing season. We compared the ability of spectral indices (SIs) and canopy temperature from the selected sensors to discriminate susceptible and tolerant cultivars and to predict the final sugar beet yield. Additionally, we compare the ground and airborne methods where applicable.

Results showed that SIs related to chlorophyll, nitrogen or water contents were able to differentiate nematode susceptible and tolerant cultivars from the same seed origin (seed provider). Discrimination between the types of cultivars was easier at very advanced stages when the nematode pressure was stronger and the plants and canopies further developed. Combinations of SIs in multivariate analysis allowed to better differentiate the response of the two types of cultivars and classify cultivars according to their groups of origin. Canopy temperatures allowed to rank cultivars according to their nematode tolerance. SIs and canopy temperature were suitable proxies for sugar yield prediction. Although in field spectral measurements and UAV hyperspectral images did not always show consistent results in the calculation of SIs, both tools led to the same conclusions.

Thus, UAV hyperspectral images appeared very promising to be used in the field for the evaluation of traits related to BCN tolerance. Chlorophyll, nitrogen and water contents were more affected on cultivars with a low tolerance to BCN. The high relationship between SIs and final sugar beet makes UAV hyperspectral imaging approach very suitable to be used for farming practices optimization through the establishment of yield potential or disease maps.

## 5.2 Introduction

Sugar beet is a root crop widely cultivated in Europe and North America for sugar production. Twenty percent of the world's supply of sugar is derived from sugar beet (FAO, 2009). One of the main soil borne parasites that limits sugar beet production worldwide is *Heterodera schachtii*. It is the most important pest of sugar beet (Müller, 1999). The Beet Cyst Nematode (BCN) causes severe damage and significant yield losses of up to 60% (Biancardi et al. 2010). In addition, this pathogen can infect more than 200 different plant species (Steele 1965; Harveson and Jackson 2008) making its management in the crop cycle a difficult task. Most of the nematode damage is caused belowground including reduction of the beet growth and the appearance of many secondary roots to compensate for those infested by nematodes. Nevertheless, BCN also causes symptoms on the shoot such as stunted growth, decreased chlorophyll content and wilting of the canopy due to water stress (Cooke 1987; Schmitz et al. 2006). In the field, nematodes occur in patches and have a very low mobility. This makes sugar beet breeding with respect to BCN infestation a good target for the use of non-destructive ground and aerial based phenotyping methodologies in the field.

Apart from direct observation of nematode-induced damage in excavated roots, an indirect observation of belowground damage via performance of the aboveground shoot performance is the only way to address the severity of deterioration. Such assessment can be done via remote sensing methods. For nematode-induced stress, several sensor based methods have been tested in a variety of crops such as potato, soybean or sugar beet using ground and airborne platforms (Heath et al. 2000, Nutter et al. 2002, Laudien 2005, Hillnhütter et al. 2012).

For differentiation of nematode infested and non-infested treatments under greenhouse and semi-field environment, ground based visible imaging has been successfully used on sugar beet (Joalland et al. 2016; Joalland et al. 2017). The canopy area of the plant can be robustly calculated and reflects root biomass in a variety of plant species (Sher-Kaul et al. 1995; Smith et al. 2000; Mizoue et Masutani 2003; Tackenberg 2007). Phenotyping methods based on multi- and hyper- spectral measurements showed promising results to evaluate the symptoms caused by BCN on sugar beet plants under field and semi-field conditions (Hillnhütter et al. 2012; Joalland et al. 2017). These methods are based on the calculation of spectral vegetation indices (SIs). In the field, the use of specific SIs has been reported to predict the final beet yield and the nematode population in the soil (Hillnhütter et al. 2011). Schmitz et al. (2004) reported the ability of aerial remote sensing thermography to detect changes in the canopy temperature

of sugar beet plants infested with nematodes in the field. This increase in canopy temperature of the nematode infested sugar beet plants was also observed at semi-field level under artificial nematode infestation on nematode susceptible and tolerant cultivars (Joalland et al. 2017).

The recent technological advances in unmanned aerial vehicles (UAV), miniaturization of sensors and developments of software and algorithms enabled the application of digital imaging methodology from aerial view potentially covering larger areas in shorter time (Colomina and Molina 2014; Araus and Cairns 2014; Walter et al. 2015). Recent work have demonstrated the ability of UAV coupled with a range of imaging sensors to provide suitable phenotype information for several purposes such as breeding support or precision farming and for different crops (Bendig et al. 2012; Guo et al. 2012; Primicerio et al. 2012; Tattaris et al. 2016; Akhtman et al. 2017). Very few studies have made use of the new technologies for investigation or detection of sugar beet BCN infestation in fields.

For aerial crop phenotyping, applied sensors and methodology contain usage of visible, multi to hyperspectral sensors (Constantin et al. 2015; Khanna et al. 2015; Liebisch et al. 2015; Burkart et al. 2017), thermal imaging (Jimenez-Bello et al. 2013; Liebisch et al. 2015), and extraction of crop height information (Diaz-Varela et al. 2015; Roth and Streit 2017). Among the applications of UAV based phenotyping are detection of weeds, soil characteristics, water status, diseases, pest management and fertilization support or yield estimation (Sankaran et al. 2015, Yang et al. 2017). Nevertheless, robust and reliable extraction of information from airborne sensors remains one of the biggest challenges.

For visible and spectral images, information can be extracted by band combination math (Burkart et al. 2017; Constantin et al. 2015) or other methods such as partial least square regression (Yu et al. 2014) or machine learning algorithms (Sa et al. 2018). Although SIs have been proven robust trait indicators in many studies, machine learning algorithms are not yet applied without task specific learning or calibration in agriculture. Thermal information can be retrieved from calibrated or non-calibrated cameras and often needs consideration of the actual weather conditions for correct interpretation. Crop or canopy height information can be extracted using “Structure from Motion” (SfM) algorithms subtracting the soil elevation model from the canopy elevation model. Although it is technically feasible, rarely combinations of sensors have been applied for phenotyping tasks. The combinations of different sensors and post processing methodology, SIs and SfM for instance offer a high

return of information for applications in crop phenotyping and large scale precision agriculture.

While for crop breeding or research such aerial based information retrieval offer faster and more frequent measurements with better spatial sampling for precision agriculture, larger areas can be measured and information more robustly used for crop management decisions.

For the sugar beet BCN infestation scenario, for instance aerial derived trait maps combined with a reduced number of soil samples in the field can confirm the presence of nematodes and allow exact determination of spatial distribution and density of nematode infestation in agricultural fields. Such knowledge may help to select the optimal sugar beet cultivar.

There is still a need to develop fast and reliable methods to evaluate the status of soil borne pathogen infestation such as BCN under realistic field conditions and give a first prediction of the yield potential. Applications would be profitable not only for breeding purposes but also for farmers to help in the selection of the best countermeasures such as crop rotation, use of appropriate cultivars or catch crops.

The present study therefore investigates the ability of thermography, spectrometry and aerial hyperspectral imaging to identify the stress caused by nematodes on susceptible and tolerant sugar beet cultivars in the field. More specifically, the main objectives were to:

- Compare the ability of thermography and spectrometry methods to discriminate and rank susceptible and tolerant sugar beet cultivars
- Evaluate the capability of the phenotyping methods to predict the sugar beet yield
- Validate the ability of aerial UAV based and hyperspectral imaging to discriminate and rank susceptible and tolerant sugar beet cultivars and predict nematode population and final yield.

## 5.3 Material and methods

### 5.3.1 Experimental site

Two sugar beet field trials were carried out side by side in 2016 in a field (0.4 ha) in Oberflörsheim (Rhineland-Palatinate, Germany) by the interest group for field experiments and Extension in sugar beet (“Arbeitsgemeinschaft für Versuchswesen und Beratung im Zuckerrübenanbau Südwest” - ARGE Zuckerrübe Südwest). The site is located 49°68'N, 8°15'E at an altitude of 244 m above sea level. The soil is sandy loam (pH 7.5) containing 29.5 kg P<sub>2</sub>O<sub>5</sub> ha<sup>-1</sup>, 45 kg K<sub>2</sub>O ha<sup>-1</sup>, 9.2 kg Mg ha<sup>-1</sup>. Fertilizer application followed best practice with a base fertilizer application of 159 kg N ha<sup>-1</sup>, 54 kg P<sub>2</sub>O<sub>5</sub> ha<sup>-1</sup>, 96 kg K<sub>2</sub>O ha<sup>-1</sup> and 24 kg Mg ha<sup>-1</sup> prior sowing.

Herbicide was applied during the first two months to avoid the influence of weeds on the plant growth (18<sup>th</sup> of April: 1.2 l ha<sup>-1</sup> Powertwin Plus + 1.5 l ha<sup>-1</sup> Goltix, (Feinchemie Schwebda GmbH, Eschwege, Germany); 2<sup>nd</sup> of May: 1.25 l ha<sup>-1</sup> Powertwin Plus + 1.5 l ha<sup>-1</sup> Goltix; 7<sup>th</sup> of May: 0.5 l ha<sup>-1</sup> Gallant, (Dow Agrosiences, US); 17<sup>th</sup> of May: 1.25 l ha<sup>-1</sup> Powertwin Plus + 1.5 l ha<sup>-1</sup> Goltix + 0.2 l ha<sup>-1</sup> Tramet (Bayer Cropscience, Monheim, Germany). Against fungal leaf pathogens, 1 l ha<sup>-1</sup> Spyrale (Syngenta AG, Switzerland) was applied twice during the season on the 19<sup>th</sup> of July and 18<sup>th</sup> of August.

The climate of the study area is temperate with a mean annual rainfall of around 611 mm. From sowing on March 24<sup>th</sup> until harvest on October 6<sup>th</sup>, mean minimum and mean maximum temperatures were 10.1 °C and 21.0 °C, respectively.

The field site was selected based on its natural infestation with BCN.

### 5.3.2 Experimental design

Two trials were sown on the 24<sup>th</sup> of March 2016 following two separate block designs (Table 1). Individual plots were three metres wide by eight metres long with a row distance of 0.5 m and a target sowing density of 10 seeds per m<sup>2</sup>. In experiment 1, one susceptible and two tolerant cultivars were planted (Sus A, Tol A1 and Tol A2 from the seed provider A). In the experiment 2, three susceptible and three tolerant cultivars were sown (Seed providers B, C and D). In the present manuscript, A, B, C, and D are groups of cultivars corresponding to five different seed providers (companies).

Sugar beet cultivars were randomised in a block design with 16 and eight replicates per treatment for experiment 1 and 2 respectively. Both experiments were located in the same field.

**Table 1. Summary of the experimental settings and the crop management operations during the two field experiments.**

<b>Sugar beet cultivars</b>	Susceptible	Tolerant
	Sus A	Tol A1
	Sus B	Tol A2
	Sus C	Tol B
	Sus D	Tol C
		Tol D
<b>Sowing</b>	March 24 <sup>th</sup> 2016	
<b>Fertilizer application</b>	Mid-March	
<b>Herbicide applications</b>	April 18 <sup>th</sup>	
	May 2 <sup>nd</sup>	
	May 7 <sup>th</sup>	
	May 17 <sup>th</sup>	
<b>Fungicide application</b>	July 19 <sup>th</sup>	
	August 18 <sup>th</sup>	
<b>Field spectrometry measurements</b>	June 20 <sup>th</sup> (88 das)	
	July 4 <sup>th</sup> (102 das)	
	August 23 <sup>rd</sup> (152 das)	
<b>Thermography measurements</b>	August 23 <sup>rd</sup>	
<b>Hyperspectral images acquisition</b>	July 4 <sup>th</sup>	
	August 23 <sup>rd</sup>	
<b>Harvest and sampling</b>	October 6 <sup>th</sup>	

### 5.3.3 Plant and nematode evaluation

Trials were harvested 196 days after sowing (das) on the 6th of October 2016. Three middle rows were harvested for each plot (17 m<sup>2</sup>). Final beet fresh weight and white sugar yield were determined for each single plot as described in Reuther et al. (2017).

The initial BCN population density (pi) in the different plots was assessed at the time of planting and the final BCN population (pf) was assessed at harvest. Soil cores were sampled

in each plot with a hydraulic soil sampler (Nietfeld, DUOPROB 60-UP, Quakenbrück, Germany). Ten samples were collected and automatically separated in topsoil (0-30 cm) and subsoil (30-60 cm) in the soil sampler. They were then mixed to obtain one topsoil and one subsoil sample of minimum 500 g each per plot. Samples were stored in the dark at 4 °C before analysis. Nematode population was evaluated using a method described by Grosse et al. (1985). Based on the observation that 60% of the dormant nematodes hatched, the nematode infestation levels were determined by multiplying the observed infestation levels by a correction factor of two (Grosse and Decker 1989). Infestation level was expressed as the number of juveniles (J2s) of *H. schachtii* per 100 g of soil.

#### **5.3.4 In field thermography and spectrometry**

Thermal images were acquired 152 das using an infrared camera (Testo 885, Testo Ltd, UK). The thermal device was calibrated prior to taking pictures by setting up the emissivity to 96% and the reflected temperature compensation parameter to the current air temperature (Oerke and Steiner 2010). One picture was taken from the side of each plot with an angle of 45°. Canopy temperature ( $T_c$ ) was determined by combining both thermal and visible images generated by the thermal camera. Temperature fluctuation in the field was measured by evaluating the naked soil ( $T_s$ ) temperature between rows with the thermal camera ten times during the measurements. On average,  $T_s$  was 28.7 °C ( $\pm 0.4$  °C) and relative humidity was 54 % at the time of measurement. Because of the stable ambient temperature (fluctuating less than 1.5%) during measurements no normalization to ambient temperatures was applied.

Spectral measurements in the field were performed at das 88, 102 and 152 during the plant development using a non-imaging spectroradiometer (ASD FieldSpec® 4, Analytic Spectral Devices, Boulder, CO, USA) with a spectral range of 350-2500 nm. Spectra were acquired from the top of the plots at a height of one m above canopy and a 25° field of view. For each plot, five spectra were randomly taken at different positions consisting of five spectral samples and overall averaged. Instrument radiometric optimization and reflectance calibration were performed before spectral sampling every three plots using a Zenith Polymer® (SphereOptics, Germany) 99% reflectance target as white reference.

#### **5.3.5 Hyperspectral imaging**

Aerial image spectroscopy was acquired 102 and 152 das with a Gamaya OXI VNIR 40 camera system (Gamaya, SA, Lausanne, CH) consisting of two individual sensors measuring 16 bands in the visible (VIS) and 25 bands in the near-infrared (NIR) range, respectively. The



system was mounted on a Solo drone (3D Robotics, Inc, USA). The camera system provides a total of 40 spectral bands between 475nm and 875nm with a full width half maximum (FWHM) ranging from approximately 15 to 25 nm. It was equipped with 25 mm-focal length optics. The images were captured from an altitude of 80 m with at least 75% overlap and 60% sidelap. VIS and NIR images were deconvolved with the Sprocket software provided by Gamaya, using the raw images and a camera specific calibration profile resulting in 2 megapixels images (2048x1088 pixels) for each camera. Both sets of images were processed in Agisoft Photoscan Professional (v. 1.26, Agisoft, LLC, Petersburg Russia) resulting in a digital elevation model (DEM) and an orthophoto for VIS and NIR, respectively. Reflectance computation and final hypercube generation in .bil was also done with the Sprocket software. Three in field reflectance targets of different and known reflectance were used to estimate the atmospheric correction (Fig. 1).

Regions of interest (ROI) reflecting individual plots were manually identified on the hyperspectral images using the ENVI software (v. 5.1, Exelis, US). For each ROI, the average spectrum was extracted.

### **5.3.6 Spectral vegetation indices**

SIs are combinations of spectral bands that enhance the sensitivity to specific canopy characteristic while reducing the effect of non-desirable factors such as soil background for example (Baret and Guyot 1991). For each date of measurement and each plot, 123 published SIs were computed using the field spectrometer measurements. Seventy-seven SIs (reduced spectral range) were calculated from the hyperspectral images using the closest available channels for the calculation. The number of SIs was reduced subsequently for both spectral devices using a correlation matrix as described by Joalland et al. (2017) to a small number of SIs, reflecting a range of traits, selected for further analysis (Table 2).

**Table 2. Selected SVIs, their respective equations (field spectrometer), the aimed detection trait and references.**

SVIs	Equation	Traits	Reference
NDVI	$(R_{800} - R_{680}) / (R_{800} + R_{680})$	Biomass, coverage	Rouse et al. 1974
780/740	$R_{780} / R_{740}$	Nitrogen content	Mistele et al. 2004
780/700	$R_{780} / R_{700}$	Nitrogen content	Mistele et al. 2004
TCARI	$3 * [(R_{700} - R_{670}) - 0.2 * (R_{700} - R_{550}) * (R_{700} / R_{670})]$	Chlorophyll content	Haboudane et al. 2002
TGI	$-0.5 [(W_{670} - W_{480})(R_{670} - R_{550}) - (W_{670} - W_{550})(R_{670} - R_{480})]$	Chlorophyll content	Hunt et al. 2011
ANTH	$R_{760} - R_{800} * (1 / R_{540} - R_{560} - 1 / R_{690} - R_{710})$	Anthocyanins	Gitelson et al. 2006
CHLG	$(R_{760} - R_{800}) / (R_{540} - R_{560})$	Chlorophyll content	Gitelson et al. 2006
PRI	$(R_{531} - R_{570}) / (R_{531} + R_{570})$	Stress	Gamon et al. 1992
NDWI	$(R_{860} - R_{1240}) / (R_{860} + R_{1240})$	Plant water status	Gao 1996
NDWI1650	$(R_{840} - R_{1650}) / (R_{840} + R_{1650})$	Plant water status	Clay et al. 2006
WI	$(R_{900} / R_{970})$	Plant water status	Penuelas et al. 1997
HI	$(R_{534} - R_{698}) / (R_{534} + R_{698}) - R_{704} / 2$	Plant health	Mahlein et al. 2013

### 5.3.7 Statistical data analysis

Data were analysed with the statistical program *R*. Beet fresh weight, white sugar yield and BCN population were exposed to analysis of variance (ANOVA) at a probability level of 0.05. ANOVA was also used to compare and differentiate the cultivars for the computed or measured traits. PCA (Principal component analysis) were performed using the main selected phenotyping parameters computed from the thermal images and the field spectrometer.

We used the WEKA software (The Waikato Environment for Knowledge Analysis v. 3.8, 2016) and the J48 algorithm to build decision trees (Witten et al. 2016). The decision trees were calibrated and cross-validated using an n-fold approach with n=10 (Weiss and Kulikowski 1991). This cross-validation can be considered as a conservative estimation of model accuracy. The total dataset was partitioned into 10 groups and 10 new subsets of the total were created using nine out of the 10. Ten test trees are then built using the reduced datasets, the unused 10% in each case is then run through each test tree and the classification error for each tree is

computed. Once the 10 test trees have been built, their classification error rate as a function of tree size is averaged. Finally, the reference tree is pruned to the number of nodes matching the size that produces the minimum cross validation cost (Breiman et al. 1984).

## 5.4 Results

### 5.4.1 Spatial BCN distribution in the field

The spatial distribution of the initial BCN population density varied strongly throughout the experimental field (Fig. 1). At sowing, BCN population densities ranged from 306 to 2284 J2s per 100 g of the topsoil and from 320 to 3457 J2s per 100 g in the subsoil. Overall, BCN population distribution was relatively even and high with 90% of the plots infested with more than 600 J2s per 100 g of soil (Fig. 1c).

c

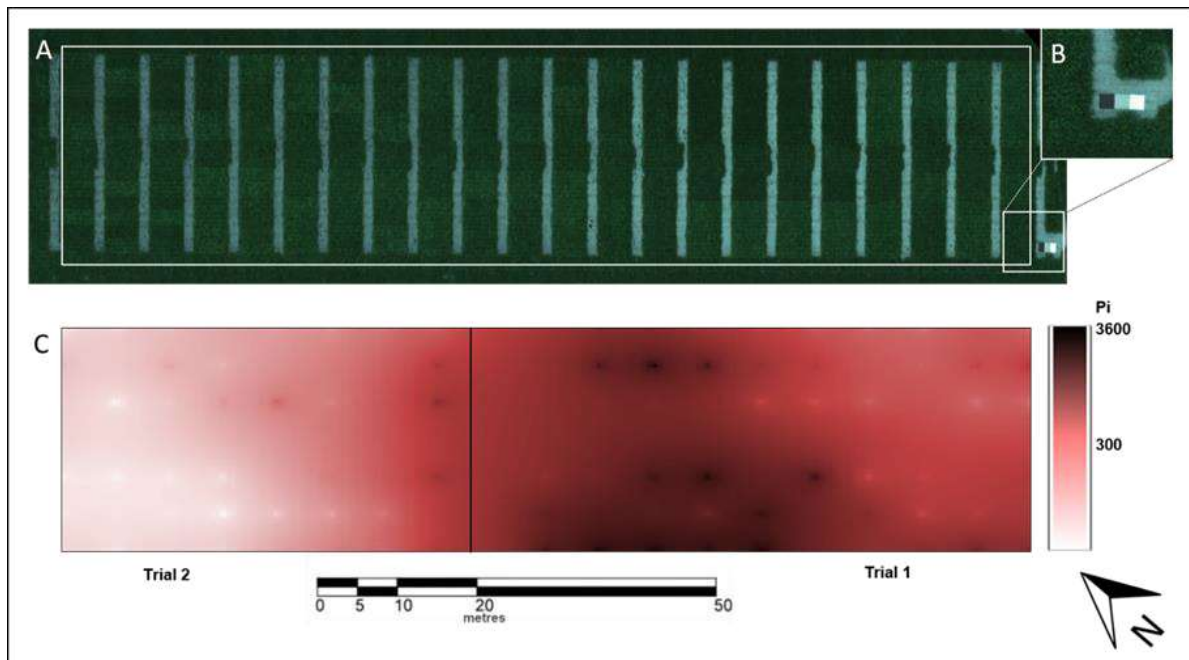


**Figure 1.** Orthophoto of the experimental field extracted from the hyperspectral imager (A) and detail of the used reflectance plates in the field (B). Map of the initial BCN population density in the topsoil (0-30cm) (C). The nematode density map was extrapolated from 108 data points representing 108 plots using the inverse distance weighting method.

The initial BCN population density per treatment (cultivar) varied from 814 to 1283 J2s per 100 g soil on average in the topsoil (CV of 15%) (Table 3). There was no significant difference between the initial BCN infestations of the treatments which were all affected by a high BCN pressure on average.

The reproduction index  $pf/pi$  in the topsoil was on average 1.1 for the tolerant cultivars and 8.6 for the susceptible cultivars (Fig. 2). Tolerant cultivars B and D performed the best with an average  $pf/pi$  ratio below one (0.65 and 0.55 respectively).

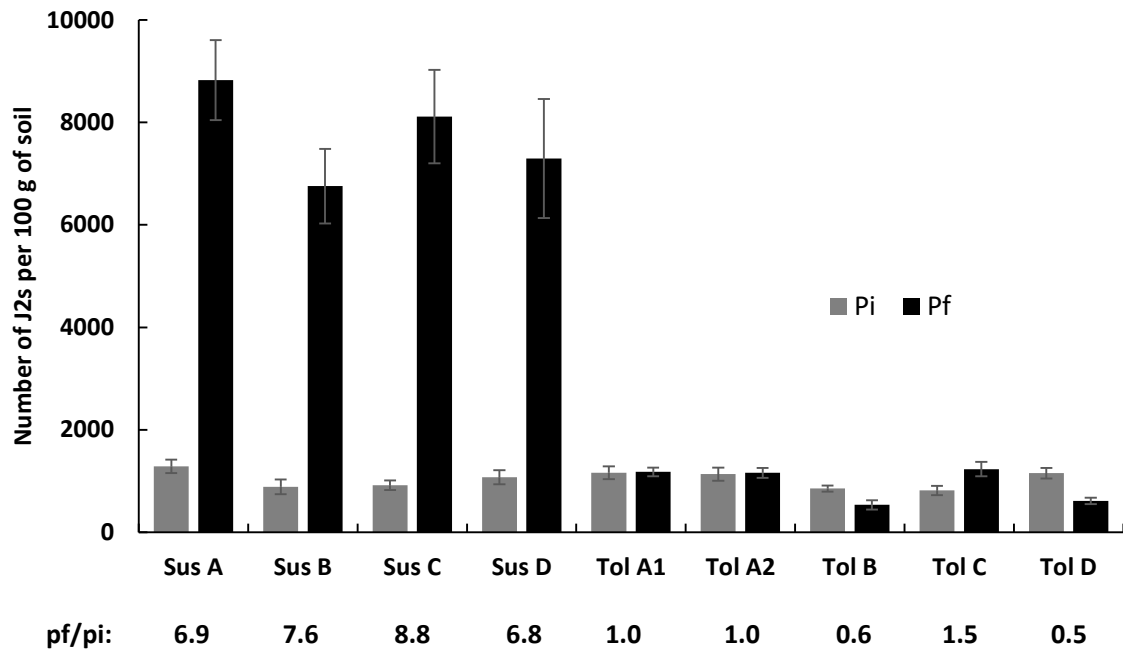


Figure 2. Average initial (pi) and final (pf) BCN population in the topsoil (0-30cm) for the nine different cultivars.

#### 5.4.2 Beet fresh weight and nematode population

The tolerant cultivars produced higher beet fresh weight (BFW) than the susceptible cultivars. The highest white sugar yield (WSY) was observed for the tolerant cultivar D with a WSY of 17.7 t/ha. On average, BFW and WSY were significantly higher for the tolerant cultivars compared to the susceptible ones (on average + 18% and + 17% respectively). There was no significant correlation between the initial BCN population density and the yield of the different cultivars. Thus, yield differences between cultivars were not caused by differences in initial BCN population density but by differences in the cultivar response to nematodes.

**Table 3. Beet fresh weigh, white sugar yield and initial BCN population density of each sugar beet cultivar. Displayed, are the mean  $\pm$  standard error of each treatment. Different letters within each column indicate significant differences ( $p < 0.05$ ).**

		Beet fresh weight (t)	White Sugar Yield (t)	Initial BCN population (number of J2s per 100 g soil)
Susceptible cultivars	Susceptible A	73.27 $\pm$ 1.39 <sup>a</sup>	12.13 $\pm$ 0.23 <sup>a</sup>	1283 $\pm$ 131 <sup>a</sup>
	Susceptible B	78.08 $\pm$ 2.30 <sup>a</sup>	13.63 $\pm$ 0.44 <sup>b</sup>	886 $\pm$ 144 <sup>a</sup>
	Susceptible C	69.10 $\pm$ 1.18 <sup>c</sup>	13.00 $\pm$ 0.22 <sup>b</sup>	919 $\pm$ 94 <sup>a</sup>
	Susceptible D	83.56 $\pm$ 2.05 <sup>a</sup>	15.14 $\pm$ 0.38 <sup>cd</sup>	1073 $\pm$ 140 <sup>a</sup>
	<i>Average Susceptible</i>	76.00 $\pm$ 1.09	13.48 $\pm$ 0.22	1031
Tolerant cultivars	Tolerant A1	91.41 $\pm$ 1.01 <sup>bf</sup>	15.52 $\pm$ 0.17 <sup>c</sup>	1160 $\pm$ 126 <sup>a</sup>
	Tolerant A2	85.48 $\pm$ 0.97 <sup>d</sup>	14.80 $\pm$ 0.14 <sup>d</sup>	1134 $\pm$ 128 <sup>a</sup>
	Tolerant B	87.99 $\pm$ 1.53 <sup>ef</sup>	15.60 $\pm$ 0.30 <sup>c</sup>	1512 $\pm$ 62 <sup>a</sup>
	Tolerant C	87.30 $\pm$ 0.80 <sup>de</sup>	15.81 $\pm$ 0.22 <sup>c</sup>	814 $\pm$ 90 <sup>a</sup>
	Tolerant D	94.66 $\pm$ 1.13 <sup>b</sup>	17.17 $\pm$ 0.19 <sup>e</sup>	1154 $\pm$ 103 <sup>a</sup>
	<i>Average Tolerant</i>	89.37 $\pm$ 0.63	15.78 $\pm$ 0.13	1026

For both susceptible and tolerant cultivars, final beet fresh weight was not significantly correlated with the pf/pi ratio (Fig. 3). However, there was a trend showing that the more nematodes reproduce in the roots, the higher is the yield reducing effect. This trend was higher for the susceptible cultivars ( $R^2=0.58$ ) than for the tolerant ones ( $R^2=0.28$ ).

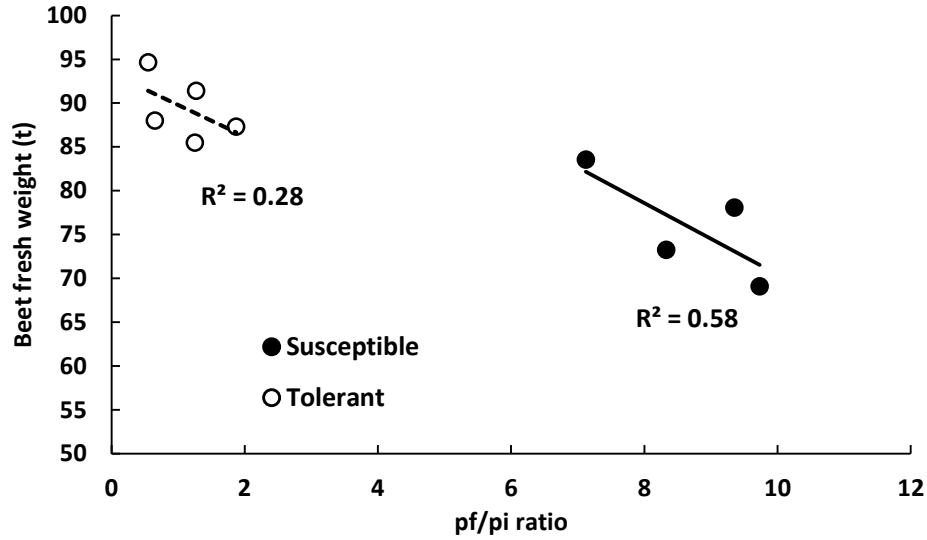


Figure 3. Beet fresh weight at harvest as a function of the nematode multiplication factor in the soil for the four susceptible and five tolerant treatments. Correlations were not significant.

### 5.4.3 Thermography

Air temperature ( $T_{AIR}$ ) was very stable during the measurements in the field, fluctuating less than 1.5%. Canopy temperature ( $T_C$ ) allowed to rank cultivars according to their ability to cool down under moderate environmental stress ( $T_{AIR}$  28.7 °C, RH 54%). Average  $T_C$  of the susceptible cultivars was significantly higher than the tolerant ones ( $24.7\text{ °C} \pm 0.1$  vs.  $23.8 \pm 0.1$  on average). The average cooling effect of the tolerant cultivars was 5.4% higher than that of the susceptible cultivars (data not shown). Three susceptible cultivars displayed the highest  $T_C$  (Fig. 4). Susceptible cultivar D displayed a canopy temperature similar to the tolerant cultivars.

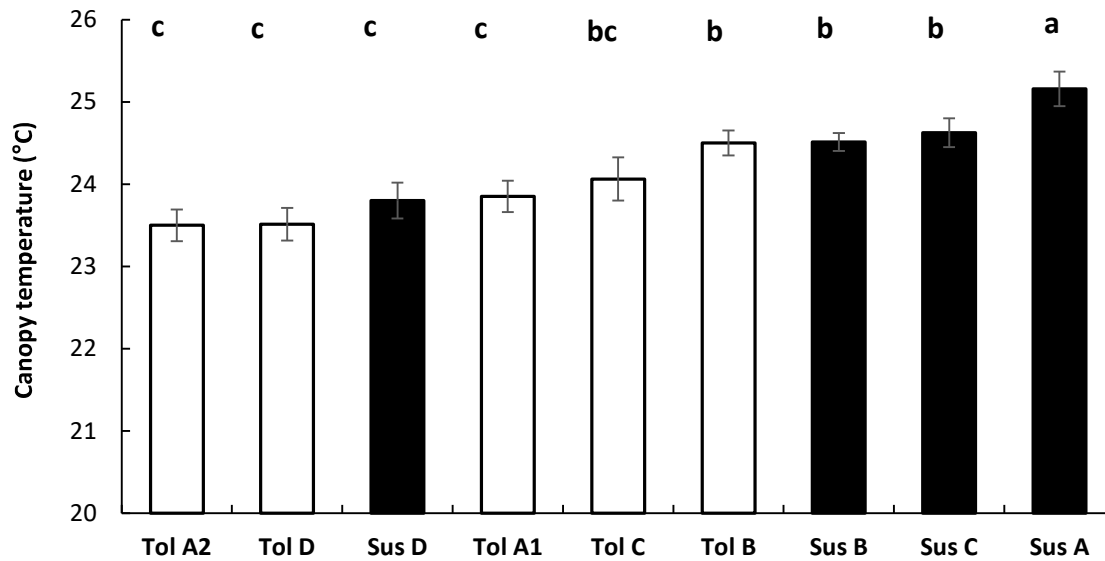


Figure 4. Average canopy temperatures of five tolerant and four susceptible cultivars on the 23<sup>rd</sup> of August. Bars represent the standard error. Different letters indicate significant differences.

Relationships between  $T_c$  and sugar yield are presented at the plot and cultivar levels in Fig. 5a and 5b respectively. At the plot level, high correlations could be observed between the canopy temperature and the white sugar yield for the susceptible cultivars ( $R^2=0.40$ ,  $p<0.01$ ). The correlation was very high at the cultivar level ( $R^2=0.99$ ,  $p<0.01$ ). In contrary, no correlation between  $T_c$  and final yield could be observed for the tolerant cultivars.

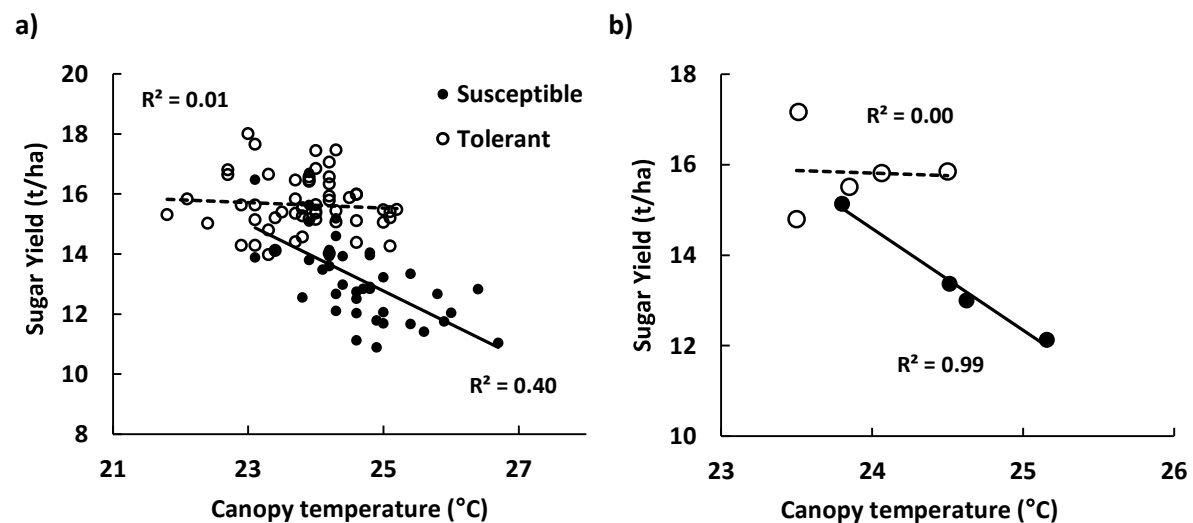


Figure 5. White sugar yield at harvest as a function of the canopy temperature (152 das - 23<sup>rd</sup> of August) at the a) plot and b) treatment (cultivar) levels.



#### **5.4.4 Spectrometry and UAV hyperspectral imaging**

##### **Discrimination of susceptible and tolerant cultivars**

We found several SIs suitable to discriminate susceptible and tolerant cultivars of each group for both field spectroscopy and UAV hyperspectral imaging (Table 4). Surprisingly, it was not possible to find SIs to significantly discriminate susceptible and tolerant cultivars after 88 days, likely related to the subtle or small differences related to small plants in early growth stages. For later stages, the SIs HI, CHLG or 780/700 were particularly suitable in differentiating susceptible and tolerant cultivars over two dates of measurements and three different cultivars. After 102 days, main differences between susceptible and tolerant cultivars were related to biomass (NDVI), chlorophyll content of the leaves (780/700, CHLG) and general stress (HI). 152 das, susceptible cultivars could also be differentiated from the tolerant ones using the SIs related to water content (NDWI1650, NDWI). The range of the hyperspectral imager on the UAV did not include short wave infrared bands which prevented the calculation of spectral indices related to the water absorption bands. SIs extracted from the UAV hyperspectral device were not able to differentiate the two types of cultivar from the group C.

**Table 4. SIs that allow to statistically discriminate susceptible and tolerant cultivars in each group ( $p < 0.05$ ). a) Field spectrometer b) UAV hyperspectral imager. SIs in common between both tools are highlighted in bold.**

a)	Experiment 1		Experiment 2	
	Sus A / Tol A1- Tol A2	Sus B / Tol B	Sus C / Tol C	Sus D / Tol D
88 das				
102 das	780/700 <b>HI</b> <b>CHLG</b> <b>PRI</b> NDVI	780/700 <b>CHLG</b> HI <b>PRI</b> TGI	ANTH HI	NDWI1650 NDWI <b>HI</b>
152 das	780/700 <b>HI</b> <b>TGI</b> PRI <b>CHLG</b> TCARI NDWI1650	<b>CHLG</b> NDWI NDWI1650 PRI TCARI TGI	ANTH HI NDWI1650	780/700 <b>ANTH</b> <b>CHLG</b> NDVI NDWI NDWI1650
<b>b)</b>				
b)	Experiment 1		Experiment 2	
	Sus A / Tol A1- Tol A2	Sus B / Tol B	Sus C / Tol C	Sus D / Tol D
102 das	<b>CHLG</b> <b>HI</b> <b>ANTH</b> <b>PRI</b>	<b>CHLG</b> ANTH PRI		<b>CHLG</b> HI ANTH PRI
152 das	<b>CHLG</b> ANTH <b>TGI</b> <b>HI</b> 785/705 NDVI	<b>CHLG</b> ANTH HI		<b>CHLG</b> <b>ANTH</b> TGI HI 785/705

### Correlations with the yield on susceptible and tolerant cultivars

Best correlations between SIs and the final sugar yield were obtained for susceptible cultivars (Table 5). Correlations were higher using SIs from the field spectrometer than from the hyperspectral imager. For the imager significant correlations to sugar yield were only found after 102 days. Already after 88 days, SIs related to chlorophyll content (780\_700, CHLG) or water content (NDWI1650, WI) allowed to predict the final sugar yield for the susceptible cultivars (Table 4a). Correlations between SIs and final yield were lower for the tolerant cultivars at the two first dates of measurements. At 152 das prediction of yield was good for both types of cultivars.

**Table 5. Coefficient of determination  $R^2$  for the relationship between SIs and white sugar yield for susceptible and tolerant cultivars at different measurement times. a) Field spectrometer b) UAV hyperspectral imager. \* indicates significant correlations (n=56 for the susceptible and n=40 for the tolerant cultivar,  $p<0.05$ ).**

Spectral Vegetation index	88 das		102 das		152 das	
	Susceptible	Tolerant	Susceptible	Tolerant	Susceptible	Tolerant
780/740	0.47*	0.12	0.73*	0.40*	0.70*	0.62*
780/700	0.62*	0.42*	0.67*	0.39*	0.63*	0.62*
CHLG	0.46*	0.38*	0.66*	0.37*	0.64*	0.62*
HI	0.22	.	0.61*	0.33	0.32	0.20
NDVI	0.57*	0.42*	0.59*	0.49*	0.61*	0.49*
NDWI1650	0.71*	.	.	0.27	0.56*	0.52*
WI	0.71*	.	.	0.28	0.57*	0.56*

b) Spectral Vegetation index	102 das		152 das	
	Susceptible	Tolerant	Susceptible	Tolerant
785_555	0.62*	0.34*	0.21	0.21
ANTH	0.64*	0.34*	0.20	0.21
CHLG	0.61*	0.34*	0.20	0.21
HI	0.36*	0.23		0.13

### 5.4.5 Field spectrometer versus UAV hyperspectral imager

Table 6. Coefficient of determination  $R^2$  for the relationship between SIs computed from the field spectrometer and from the UAV hyperspectral imager

	102 das	152 das
780_700	0.09	0.60*
ANTH	0.13	0.57*
CHLG	0.53*	0.69*
HI	-	0.05
NDVI	0.03	0.16
PRI	0.12	-
TGI	0.06	0.30*

\* Significant correlations (n=96, p<0.05)

Good correlations were observed for the determination of the CHLG index between both spectrometers at the two dates of measurements (Table 6). Other indices related to chlorophyll (780\_700, ANTH) or photosynthesis (TGI) were well correlated after 152 das. Surprisingly, the two methods differed a lot in the evaluation of HI. 102 das, calculation of most of the indices was not consistent between both methods.

### 5.4.6 Multivariate analysis

Studying single parameters allowed to differentiate susceptible and tolerant cultivars from the same group and to predict yield with a fair good accuracy. To go further and discriminate the type of cultivars independently from the group, we use multivariate analysis. Since both field spectrometry and hyperspectral imaging led to similar results, multivariate analysis was conducted with the field spectrometer indices.

## Principal Component Analysis

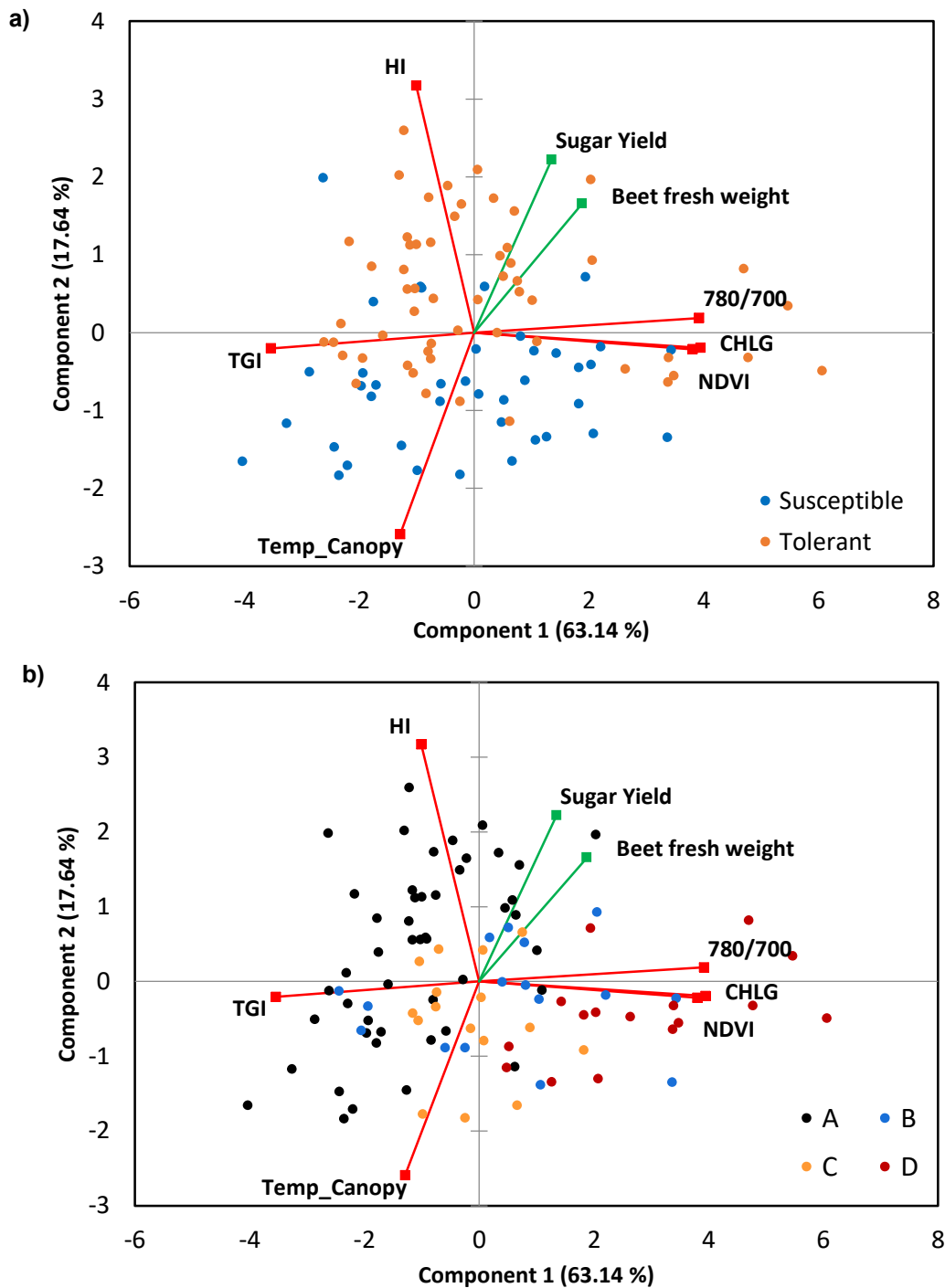


Figure 6. Principal component analysis of the main phenotyping parameters 152 das. The percentage of variance explained by each component is displayed in parentheses. a) The susceptible and tolerant cultivars are represented in blue and orange, respectively. b) The groups of cultivars are represented in different colours. Each data point represents one field plot (n=96).

A PCA was built using the mains SIs identified and the canopy temperature parameter on the 3<sup>rd</sup> date of measurements 152 das (Fig. 6). Sugar yield was used as an explanatory variable. 81% of the variance is explained by the two first principal components. Results confirmed that high canopy temperature is correlated with lower yield. Canopy temperature and HI appeared particularly suitable in differentiating susceptible and tolerant cultivars (Fig. 6a). Cultivars from groups A and D could be easily discriminated using indices related to chlorophyll (CHLG, 780/700) biomass (NDVI) and water (NDWI1650) (Fig. 6b). The two other companies showed a similar profile in terms of canopy reflectance. Overall, principal component #2 represents the ability of the sugar beets to tolerate nematodes while principal component #1 is more related with intrinsic genetic characteristic of the plants.

### Decision Tree

The univariate decision trees (UDT) were used to classify sugar beet according to the type of cultivar (susceptible or tolerant) or the genetic background by using multiple traits. All the 123 and 77 SIs computed using the field spectra data and the hyperspectral images respectively were included in the analysis. The cross validation technique used has been demonstrated to produce accurate results without requiring an independent dataset for assessing the accuracy of the model (Sherrod 2008).

We found that decision trees could classify cultivar type (susceptible, tolerant) and genetic background (seed provider) using few parameters (Table 7). Model accuracy was the same for the spectrometry and the UAV hyperspectral images. Cultivar classification accuracy was on average 74% 102 das and 78% 152 das. The same orders of magnitude were observed for the classification of the plot according to the seed provider.

**Table 7. Decision tree classification accuracy (10-fold cross-validation) for cultivar type and group of cultivars using field spectrometer and UAV based imager data.**

	das	Classification accuracy "Cultivars"	Classification accuracy "Group of cultivars"
Field spectrometer	102	0.74	0.76
	152	0.78	0.76
UAV based imager	102	0.73	0.72
	152	0.83	0.68

In table 8, the decision tree misclassified nine plots of susceptible cultivars as tolerant cultivars and 12 plots of tolerant cultivars as susceptible. Kappa coefficient was 0.55, which can be

considered as “moderate” agreement (Landis and Koch 1977). The decision tree was developed using five SIs out of the 124 parameters used as input in the model. 780/740 and NDWI1650 were already used above for cultivar discrimination. LCI (Datt 1999), SIPI (Penuelas et al. 1995) and RGR (Gamon and Surfus 1999) are indices related to pigment content in the leaves such as chlorophyll and anthocyanins. They appeared suitable for cultivar type discrimination.

**Table 8. Classification and mis-classification matrix for “types of cultivar” using field spectrometer data 152 das. Kappa: 0.55. Kappa coefficient represents the degree of beyond-chance agreement.**

		Predicted classification	
		Susceptible	Tolerant
Actual classification	Susceptible	<u>31</u>	9
	Tolerant	12	<u>44</u>

**SIs selected by the model to split the data: 780/740, LCI, SIPI, NDWI1650, RGR.**

Decision tree classified very well plots with cultivars belonging to groups A and D (accuracy of 94% and 75% respectively) with a kappa coefficient of 0.63 that can be considered as “substantial” agreement (Table 9). Classification of plots with cultivars belonging to groups B and C was less accurate (44% and 56% accuracy respectively). Physiological indices related to photosynthesis such as PRI and canopy temperature or related to water content (WI, WI\_NDVI) were selected to build the model. NPCI (Penuelas et al. 1994), ANSI (Lewis et al 2006) and NDNI (Serrano et al. 2002) related to carotenoids content, residue cover and nitrogen content respectively were also appropriate to differentiate genetic backgrounds.

**Table 9. Classification and mis-classification matrix for “group of cultivars” using field spectrometer data 152 das. Kappa: 0.63.**

		Predicted classification			
		A	B	C	D
Actual classification	A	<u>45</u>	1	1	1
	B	2	<u>7</u>	4	3
	C	1	4	<u>9</u>	2
	D	1	3	0	<u>12</u>

**SIs selected by the model to split the data: WI, PRI, NPCI, WI\_NDVI, Canopy T, ANSI, NDNI.**

## 5.5 Discussion

The results of this study demonstrated that ground based and airborne spectrometry and thermometry can be used in the field to evaluate the level of BCN tolerance of several cultivars and predict the final sugar beet yield.

Infestation levels observed in the field can be considered as moderate to high. The tolerance limit, which is the population below which no damage is detectable, could not be precisely evaluated in this study. However, it could be estimated to be between 300 and 1000 J2s per 100 g of soil for the nine cultivars according to the field location and soil temperatures observed during the season (Seinhorst 1965; Cooke and Thomason 1979). Under such nematode stress, it was possible to rank cultivars according to their ability to withstand or recover from the nematode attack and yield well. As expected, the five cultivars described as tolerant showed higher yield than the ones known to be susceptible (Hauer et al. 2015). The  $pf/pi$ , an indicator for reproduction, represents the ability of the cultivar to prevent nematode reproduction in the roots (Oostenbrink 1966). The high multiplication factor observed for the four susceptible cultivars is aligned with the lower yield observed for these cultivars. Interestingly two tolerant cultivars (B and D) presented a multiplication factor below one indicating them as resistant since they decreased the nematode population in the field (Trudgill 1991; Reuther et al. 2017). Cultivar D combines high tolerance (high yield under nematode infestation) and high resistance (prevention of nematode multiplication), which is of advantage for use in infested fields. No significant correlation could be found between the initial number of BCN and the final yield. This was also shown by Reuther et al. (2017). This can eventually be explained by the range of initial BCN population in the field which was too narrow and above the damage threshold.

The canopy temperature showed high potential for classifying cultivars according to their susceptibility or tolerance to nematodes. Three out of four susceptible cultivars had the highest  $T_c$ , reflecting the lower ability of these plants to transpire water and cool down.  $T_c$  is closely correlated with the temperature of the environment, the leaf transpiration rate and the stomatal conductance (Inoue et al. 1990; Jones and Schofield 2008; Oerke and Steiner 2010; Liebisch et al. 2015). BCN damage in the roots decreases water uptake which reduces the leaf transpiration rate and results in a higher canopy temperature (Trudgill 1980; Haverkort et al. 1991; Jones 2004). High correlations were observed between  $T_c$  and final sugar yield for the susceptible cultivars. Schmitz et al. (2004) and Joalland et al. (2017) observed similar results



on susceptible cultivars under field and semi-field conditions respectively. The higher the BCN damage on the roots is, the higher is the  $T_c$ . That no correlation between  $T_c$  and sugar yield was observed for tolerant cultivars is likely related to the less affected, water uptake and transpiration rate than in susceptible cultivars (Evans and Franco 1979; Trudgill 1986; Radcliffe 1990). Thus  $T_c$  is not suitable to determine the level of tolerance or to predict the final yield.

SIs are useful indicators for quantitative and qualitative evaluation of the plant canopy. Under moderate to high BCN infestation, single SIs related to chlorophyll content (CHLG), photosynthetic activity (PRI), plant biomass (NDVI) or general stress (HI) were able to discriminate tolerant and susceptible cultivars from the same seed provider (same genetic background). For crop genetic improvement, spectrometry and/or spectral imaging could be implemented as a fast screening method to characterise and rank different sugar beet cultivars from the same genetic background according to their ability to tolerate nematodes. For large variation in genetic background (cultivars from different seed companies), it was not possible to use a single SI to robustly discriminate the tolerant and susceptible cultivars. Here, only the use of several relatively independent SIs helped to identify the type of cultivars under BCN infestation. Combining SIs allow to integrate different aspects of the plant growth and development such as biomass, pigment- and water content, photosynthetic activity and therefore classify cultivars properly, even in experiments incorporating high genetic diversity.

UDT techniques allow to identify indicators such as SIs to classify plots according to their susceptibility or tolerance to nematodes and their genetic background. After 152 days, chlorophyll and water content related indices (780/740, LCI, NDWI1650) were essential to discriminate the two types of cultivars which demonstrates the high diversity and non-specificity of nematode symptoms (Cooke 1987). Interestingly, cultivars from group A and group D could be classified with a high accuracy. This is clearly reflected in the PCA where plots from both groups were separated and clustered. Such results illustrate the high variability caused by the intrinsic genetic background of each seed provider which is clearly reflected in the plant physiology (water content, pigment concentration) and plant performance (photosynthetic activity). Cultivars that were bred using different germplasm pools may display very different reflectance spectra although depicting a similar tolerance level.

SIs related to leaf chlorophyll showed high correlations with the final sugar yield at the three dates of measurements for the susceptible cultivars. This observation is consistent with the observation that more nematode damage on the roots triggers more visible symptoms on the shoots and thus causes yield reduction. As early as 88 das, SIs related to nitrogen status and water content such as 780/700 and NDWI respectively could be used to predict yield with high precision. Hillnhütter et al. (2011) also showed correlations between water content or leaf pigment related SIs and beet fresh weight in an infested field. Yield prediction on tolerant cultivars was the best after 152 days when environmental conditions were more constraining (air temperature 28.7 °C, RH 54 %). Such moderate environmental stress increased the nematode stress and allowed to differentiate tolerant cultivars and better predict final yield. Stronger symptoms were also observed on a tolerant cultivar under semi-field conditions when vapour pressure deficit stress was present (Joalland et al. 2017).

The data obtained from the field spectrometer and the hyperspectral imager were not always consistent. SIs calculated by the two instruments were not perfectly correlated. Such mismatch can be explained by several differences of the sensors and the measurement procedure. The used instruments use different sensor and filter technology causing different spectral resolution and slight differences in the spectral response reflected by slightly altered shape of the spectrum. The field spectrometer had a very high resolution while the hyperspectral imager had a lower spectral resolution. As a consequence, some SIs were computed using non-optimal bands, which resulted in low correlation between them (Hillnhütter et al. 2011). In addition, the used spatial resolution differed between the two measurement approaches. Whereas the average spectra per plot for the field spectrometer is the average of five point measurements with a footprint of about 50 cm diameter at random locations in each plot, the plot spectra obtained from the hyperspectral imaging was an average of hundreds of pixels with an instantaneous field of view (ifov) of two cm. Further, the processing and calibration steps of both instruments differ. While the measurements of the field spectrometer is calibrated every three measurements using a white reference, the hyperspectral images are stitched using structure from motion procedures in Agisoft and orthomosaiced in this process before to be subsequently calibrated to reflectance with a partial least squares regression using three reflectance panels differing in absolute reflectance intensity (Fig. 1). Better understanding of the sensors used procedures and the consequences for the resulting measurements will surely improve the use of aerial imaging methods in the

future. First attempts can be seen in the standardization of calibration methodology and cross validation (Aasen and Bolten 2018).

Although SIs computed from the field spectrometer and from the spectral imager were not fully consistent, results and conclusions were similar. Both tools were able to detect stress caused by nematodes and predict the final yield. This showed the great potential of UAV hyperspectral imagery to be used to generate maps of nematode symptoms and yield potential of sugar beets with a high throughput. Such maps, combined with a reduced number of soil samples in the field to confirm the presence of nematodes, allow the exact determination of spatial distribution and density of nematode infestation in agricultural fields. Such knowledge may help to select the right countermeasure such as optimised crop rotations or use of catch crops or appropriate tolerant sugar beet cultivars. For breeding purposes, such technology has the potential to make selection monitoring more efficient and thus to accelerate crop improvement (Shakoor et al. 2017). In our experimental field, tolerant and susceptible cultivars could be classified with an accuracy of 75%. Specific SIs alone or combined have the ability to quantify traits related to BCN damage and final sugar yield. Cultivar response to nematodes could be compared in a fast and efficient manner on different physiological aspects such as chlorophyll and water content, plant biomass or photosynthesis rate. This will significantly improve the efficiency of sugar beet breeding for nematode tolerance and resistance.

## 5.6 Conclusions

Remote sensing methods in the field were able to identify BCN symptoms on sugar beet plants and discriminate the type of cultivars. While thermography appeared suitable for yield prediction on susceptible cultivars only, field spectrometry and aerial UAV hyperspectral imaging were able to predict yield on susceptible and tolerant cultivars. Despite disparities in spectral and spatial resolution, both spectral tools can be used to characterise nematode symptoms and classify varieties. Multivariate methods were precious tools to identify genetic backgrounds of the sugar beet cultivars and their ability to tolerate nematodes using a diversity of spectral indices. The UAV equipped with a hyperspectral imager proved to be a great tool for BCN stress diagnosis in the field and for improving breeding efficiency facilitating the monitoring of multiple traits at the same time at multiple sites at short sequence.

## 5.7 Acknowledgment

We would like to thank the technical support of the “Arbeitsgemeinschaft für Versuchswesen und Beratung im Zuckerrübenanbau Südwest” - ARGE Zuckerrübe Südwest (Germany) in setting up the field trial. We also thank Marc Bonfils for leading the collaboration with Ruebe and making feasible the phenotyping measurements. The authors would like to thank Lukas Roth for the great support in hyperspectral data process.

## **Chapter 6.**

### **General discussion**

Agriculture productivity has to be increased to cope with climate change and with the growing human population (FAO 2009; OECD/FAO 2012; Tilman et al. 2011). New genotypes, crop technologies and farming systems need to be developed (Neumann et al. 2010; Ray et al. 2013). This can be achieved by further developing plant phenotyping tools to efficiently characterise plant traits under controlled and field conditions (Yang et al. 2014; Campbell et al. 2015; Nagel et al. 2015, Neilson et al. 2015).

The present thesis focused on a specific case study. It compared the ability of several parameters computed from different sensing devices to evaluate phenotypic changes on sugar beet plants caused by nematodes. Sugar beet was used as a model crop to demonstrate the ability of remote sensing methods to investigate the root biomass accumulation, the plant responses to nematode infestation and the root-pathogen-chemical interaction over the plant growth. Comparison was done in three different platforms (greenhouse, semi-field and field), which form a continuity of environments with a decreasing control of environmental factors (Table 6.1) (Araus and Cairns 2014).

Digital and thermal images as well as field spectrometry and hyperspectral images were evaluated for their potential Research and Development (R&D) applications both in area of new crop protection technologies and crop genotypes. These techniques are very sensitive to changes in illumination. They are based on the evaluation of the intensity of light reflected or emitted by the plant canopy at a certain range of the electromagnetic spectrum.

**Table 6.1. Overview of the phenotyping methods tested at three different scales and their respective sensitive spectral range in the electromagnetic spectrum.**

Phenotyping methods	Range in the electromagnetic spectrum	Greenhouse	Semi-Field	Field
Digital images	400 – 700 nm	X	X	
Thermal images	9,000 – 14,000 nm		X	X
Spectrometry	350 – 2,500 nm		X	X
UAV hyperspectral images	475 – 875 nm			X

Overall, results obtained during the PhD thesis demonstrated that parameters extracted from the canopy reflectance of sugar beet plants are powerful indicators to characterise the sugar beet growth and status, identify the BCN stress and predict the final yield. Such information

has practical agronomical implications. Under controlled conditions, digital images allowing for the calculation of canopy area can be applied for the research and development of new crop protection technologies and new genetics. In the field, spectral information and thermography can support the development and evaluation of new sugar beet varieties and the optimization of farming practices such as application of nematicides on sugar beet seeds or directly into the soil prior sugar beet cultivation based on maps.

## **6.1 Sugar beet phenotyping under controlled conditions**

In the greenhouse and semi-field, part of the environmental conditions can be regulated. Nematode pressure and soil conditions can be fully controlled, which is of great interest for experiment accuracy and repeatability (Schaeffer et al. 2010). In addition, the use of control non-infested plants as reference allows the evaluation of the nematode effect. In the greenhouse, digital nadir images were taken from plants grown in 3 l pots while in the semi-field, a population of three plants, in 150 l microplots, mimicking the field density, was evaluated using a digital red green blue (rgb) camera, thermal camera and field spectrometer. Specific precautions were taken to minimise the lighting fluctuations during data acquisition. Digital images were acquired in the early morning within a five minutes period to minimise changes in light intensity between measurements. For the semi-field spectrometry measurements, a mobile dark box combined with a halogen lamp was used to ensure constant illumination. The thermal camera was used on cloudy days and calibrated with the current air temperature. Canopy area and canopy temperature traits were extracted from digital and thermal images using specifically developed macros. Spectral indices (SIs) were computed from the spectral data via software R. In total, in the semi-field, data acquisition and processing required ten minutes for digital images, 30 minutes for thermography and an hour the spectral measurements.

### **6.1.1 Nematode stress detection**

The most suitable parameter to evaluate the sugar beet biomass accumulation during the early plant development (from emergence until growth stage (GS) 25 (Meier et al. 1993)), under controlled conditions, was canopy area determined in nadir view images (Granier et al. 2006; Tackenberg 2007; Wiese et al. 2007). Canopy area is a simple morphological and performance related parameter that reflects the fraction of the ground covered by the canopy (Gerard et al. 1999; Liebisch et al. 2015). Results obtained in chapter 2 demonstrated that canopy area of single sugar beet plants can be used as a proxy for shoot and root biomass

until GS 25 (Joalland et al. 2016). Such relationship between above and belowground biomass on sugar beet was first described by Green et al. (1986) and Milford et al. (1988). They revealed the existence of a biomass allocation ratio between shoots and roots, which was confirmed in our study. The use of canopy area in the semi-field in chapter 3 was very appropriate to evaluate the homogeneity of growth in between pots, collect data of the plant growth over time and evaluate the net primary production (Tackenberg 2007). In addition, we revealed that nematode damage could be identified by evaluating the degree of shoot and root biomass inhibition compared to control non-infested plants. Plant growth reduction could be detected after the apparition of the second leaf (Chapter 3). Interestingly, such early decrease in plant growth was observed on both susceptible and tolerant cultivars, which confirmed the inability of both types of cultivar to prevent BCN penetration into the roots (Westphal 2013). Decrease of plant growth during the first month can be explained by the high nematode infestation level applied (600 eggs and larvae per 100 cm<sup>3</sup> of soil) that was already above the damage threshold even for a tolerant cultivar (Trudgill 1986). The main difference between susceptible and tolerant cultivar responses was in the ability of the plant to recover from the infestation. Tolerant cultivars initiated a canopy growth recovery almost two weeks before the susceptible one demonstrating the ability of the tolerant cultivar to better withstand nematode stress (Chapters 2 and 3; Joalland et al. unpublished data).

In chapter 4 we demonstrated that the use of sophisticated and specific image analysis methods enables to extract more information from nadir canopy images. Canopy area could be split up into basic elements such as leaf area and number of leaves, which is a direct assessment of the sugar beet growth stage (Milford et al. 1985; Scharr et al. 2016). The presented algorithm was precise enough to detect a significant reduction of leaves caused by nematodes in a period of development from four to eight unfolded leaves. In addition, we indirectly showed that nematode infestation also affects the leaf expansion rate. Thus, the combination of digital imaging with an advanced computer vision algorithm resulted in a powerful tool enabling the identification of nematode effects in delaying leaf apparition rate and leaf expansion rate (morphogenesis). With the fast progress in image analysis for leaf identification techniques and the use of very advanced computer vision methods such as neural networks (Chaki et al. 2015; Scharr et al. 2016), great opportunities arise, not only to investigate canopy growth but also leaf growth. Overall, more features could be extracted from digital images (leaf number, leaf area, leaf geometry, leaf colour, leaf angle), which



makes the use of image analysis very powerful for morphological, physiological and performance related traits evaluation (Li et al. 2014, Perez-Sanz et al. 2017).

Previous studies on the use of phenotyping tools to detect BCN under controlled conditions focused on more advanced growth stages (BBCH 25+) with the use of sophisticated technologies such as hyperspectral images (Hillnhütter et al. 2012). After GS 30 in the semi-field, leaf overlapping is high, which prevents canopy area to be used to estimate the plant biomass on sugar beets. At these stages, measurement of SIs gave a suitable evaluation of both morphological and physiological aspects of the plants (Thenkabail et al. 2000). NDVI correlated well with the early evaluation of the canopy area (chapter 3). CHLG index gave an evaluation of the chlorophyll content of the leaves (Gitelson et al. 2006).

Overall, under semi-field conditions, spectrometry and thermography did not bring any additional benefit over digital images for the BCN damage characterisation. Specific SIs were suitable to detect physiological stress caused by nematodes such as biomass reduction (NDVI), decrease in chlorophyll content (CHLG, HI, TGI) and water content (NDWI). Canopy temperature is closely related with stomatal conductance and transpiration rate of the plants (Leinonen et al. 2006; Guillioni et al. 2008; Rebetzke et al. 2013). It enabled the discrimination of non-infested and infested sugar beets on both susceptible and tolerant cultivars.

Despite the ability of spectrometry and thermography to investigate BCN symptoms, both tools had the disadvantage of requiring a substantial canopy area to be used. They could only be used at advanced stages in the plant growth when the diagnostic had already been done using digital images (Berni et al. 2009, Joalland et al. 2017). Spectrometry integrates the spectrum over a large area of the plots, which includes both vegetal canopy and soil. In particular in the early growth stages when the canopy area is still limited, there is a high proportion of the spectrum coming from the soil and therefore the spectral point measurements are difficult to interpret with respect to properties of the small leaves. Canopy temperature measurement itself is difficult to analyse. Canopy temperature is highly correlated with the ambient temperature making comparison through time very difficult. The use of references (air temperature) therefore is necessary to compare the ability of different plants to cool down and transpire more (Munns et al. 2010). Moreover, most of the physiological symptoms can only be detected once the nematode infestation is strong at late growth stages under constrained conditions. This makes spectrometry and thermography less suitable than digital images to be used under controlled conditions for nematode detection.

### 6.1.2 Applications in the research context – Challenges and opportunities

Digital imaging appears to be a convenient and informative technique in the research context, when environmental conditions are controlled (e.g. soil moisture, level of infestation in the soil) and sample plants are small, to evaluate the efficacy of chemical or biological methods for controlling nematode infestation. Our results demonstrated the value of protecting roots from BCN infestation during the first month of growth. We showed that an efficient soil applied nematicide, such as *Fosthiazate*, prevented nematodes from root infection by suppressing the first generation of nematodes hatching from the cysts during the first four weeks of growth. As a result, canopy area of *Fosthiazate* treated sugar beets was the same than in the non-infested ones (Chapter 3). This treatment resulted in a comparable final sugar beet yield. On the contrary, control infested sugar beets exhibited smaller canopy area and a lower final yield. These findings support the work done by Scott et al. (1973) and Jaggard et al. (1983) who found that any delay in the emergence and early growth of the sugar beet plant significantly affected the final sugar beet yield by decreasing the photosynthetic efficiency. Chapter 3 corroborated these results. Significant correlations were observed between the integral of the canopy area, which represents the net primary production, and the final sugar beet yield. Late BCN infestation and reproduction in the roots do not have significant effects on the beet biomass. These findings are of particular interest regarding the way nematode strategies are conceived in crop protection research. Similarly to other indications such as weed control, these results clearly demonstrates how early control is essential and sufficient for nematodes. A six week soil persistent nematicide should be sufficient to prevent a sugar beet yield reduction.

Evaluating canopy area during the first month is sufficient to evaluate the nematicide activity and have a first prediction of the final sugar beet yield. Such digital evaluation tools have a high potential to replace the time consuming and labour intensive plant biomass evaluation and manual assessment of the number of nematodes that penetrate each root system. It could be easily implemented in a nematicide screening test (in-furrow or seed treatment applications) on a susceptible variety using a nematode infestation level above the damage threshold. Fig. 6.1 illustrated the potential use of canopy area as ranking criteria for nematicide screening.

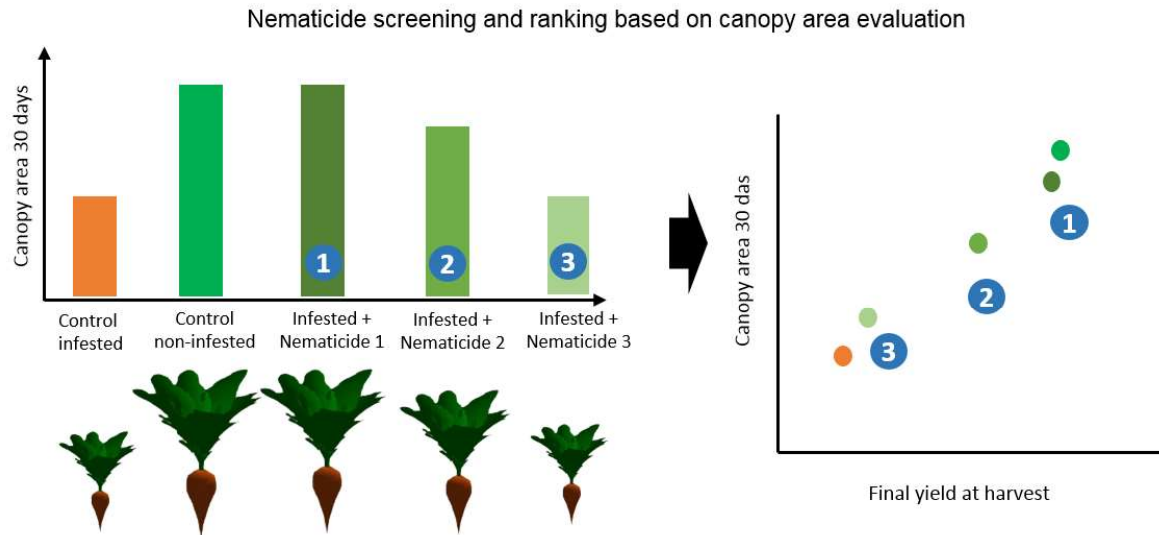


**Figure 6.1.** Schematic representation on how application of canopy area could be used for screening the biological efficacy of different hypothetical new nematicides. The evaluation of the canopy area after one month shows a full nematode control for the nematicide number one. Nematicides number two and three are less efficient in preventing nematode penetration in the roots. Canopy area differences result in final yield differences.

## 6.2 Sugar beet phenotyping in the field

In the field, nematode pressure and environmental conditions cannot be controlled. In this complex environment, plant growth can be affected by a large variety of biotic and abiotic stresses. Dealing with a soil pest and its non-specific symptoms is very challenging. However, the patchy distribution of nematodes in the field and their low mobility make them perfect targets for plant phenotyping and precision farming. The use of remote sensing methods requires important calibration steps to correct temporal and spatial fluctuations in illumination and environmental conditions. In the framework of this thesis, field spectrometry, thermography and UAV based hyperspectral imagery were tested in a nematode infested sugar beet field at advanced growth stages, when the soil was fully covered by the canopy, to detect BCN symptoms and discriminate the response of different cultivars (Chapter 5).

### 6.2.1. Sugar beet cultivar characterisation and classification

The measurement and evaluation of several spectral indices related to biomass, chlorophyll/nutrient content, water content and transpiration rate (canopy temperature) allowed to discriminate the response of susceptible and tolerant cultivars from each seed

provider and to predict the final yield in a moderate to highly infested field. Differences in leaf reflectance between both types of cultivar already exist when grown under non-stressed conditions because of natural genetic differences. However, in the same way as for yield, response of susceptible and tolerant cultivars is modified and strongly amplified under nematode stress. The discrimination and yield prediction was more accurate after five months when nematode stress was stronger on the plants because of the subsequent infection cycles, which constantly weaken the growing plants (Cooke 1987). We observed a relationship between SIs such as CHLG, 780/700, NDWI1650 related to chlorophyll, nitrogen and water contents of the sugar beets, respectively, and the final yield for susceptible and tolerant cultivars, illustrating the genetic diversity existing inside cultivar types. Such relationships between nitrogen and water content related SIs have already been suggested by Hillnhütter et al. (2011) in a field study using a nematode susceptible cultivar.

Applying multivariate analysis increased the power of cultivar discrimination since the method takes into account many SIs and wavebands and thus better estimates overall crop performance. A high precision was obtained in the classification of infested field plots planted with susceptible or tolerant cultivars. Interestingly, genetic background of the cultivars (seed providers) could be differentiated using decision tree techniques. This was the first report on the use of a remote sensing approach in the field to discriminate cultivars with different genetic background under nematode infestation. These results highlighted the diversity of genetic backgrounds in between seed providers and the specificity of their spectral signature. SIs obtained from the field spectrometer and the hyperspectral UAV imager led to the same conclusions demonstrating the great potential of UAV hyperspectral imagery to be used to generate maps of BCN symptoms and yield potential with a high throughput and a complete field/plot coverage (Araus and Cairns 2014).

### **6.2.2. Applications in the field – Challenges and opportunities**

For crop genetic improvement under nematode stress, few suitable SIs could be used to characterise the ability of a population of germplasms to tolerate BCN. Field plots could be ranked by comparing SIs related to chlorophyll content, water content or photosynthetic activity at different times during the growth. These remote evaluations could be performed high throughput by UAV and assist or partly replace the labour intensive manual assessment of several traits (Ghanem et al. 2015). Repeated measurements would generate dynamic and robust evaluation of traits and help to assess the ability of the cultivars to withstand or cope

with the nematode infestation over the season. Canopy temperature was also appropriate to classify varieties and predict yield under nematode infestation confirming the close link between nematode damage, low water uptake ability, stomatal closure, and high canopy temperature (Schmitz et al. 2006). However, thermography presents some practical limitations for regular use in the field related to its sensor spatial resolution, the generally changing meteorological conditions, the sensor calibrations and the viewing angles (Khanal et al. 2017).

Under normal farming situations, identifying nematode stress is a difficult task. As there are no specific nematode symptoms and no known nematode free area of reference, few soil samples will always be required to confirm a remote sensing diagnostic. Improving the remote sensing diagnostic requires deep investigation on the nematode effect on the spectral reflectance and the development of specific spectral disease indices (SDIs). SDIs consist in the combination of a single and a normalised wavelength difference and they aim to detect specific disease (Delalieux et al. 2009). Mahlein et al. (2013) developed the Health-Index using a feature selection algorithm. This index uses wavelengths at 704, 534 and 698 nm, which take into account nitrogen and chlorophyll contents. Both are strongly affected by nematodes, which makes this index particularly suitable for detection of nematode stress and potentially similar soil borne disease stresses such as *Rhizoctonia solani*. However, this SDI is not sufficient to identify BCN fully certainly. Using a large dataset of UAV hyperspectral images on several nematode infested fields could support the development of nematode specific SDIs or advanced algorithms to identify nematode stress with a high accuracy on susceptible and tolerant cultivars.

In situations, in which farmers are aware that a field could be prone to nematode infestation based on historical records or soil analysis, SIs such as NDVI, CHLG, TGI, and NDWI will provide a first indication about possible distribution and extension of the infested areas in the field. Maps of yield potential can be built to determine temporal and spatial distribution of nematodes, which will help to select the best crop management practices and countermeasures for the coming years (use of tolerant cultivars, crop rotation, nematicide in-furrow or seed treatment applications).

The visible imaging technique was not tested in the field in this project. However, nadir view digital imaging could be improved and deployed for sugar beet growth characterisation. Main challenges are image resolution and changes in the illumination and soil properties,

which will affect the image analysis process and can make the identification of single leaves difficult. Early growth assessment in the field would require imaging technologies with high resolution and a very efficient segmentation algorithm since a high proportion of the image will be occupied by the soil background (Yu et al. 2017). Canopy area will inform on the homogeneity of the field in term of plant growth and reveal areas where the plant development is delayed. To precisely diagnose stress caused by nematodes, the specific agronomical context should be known and additional soil sampling might be necessary.

### **6.3 Semi-field platforms for phenotyping tools development and crop modelling**

Three sugar beet trials were carried out on the microplot semi-field platform during the PhD thesis. The ability to control soil conditions and the level of disease pressure combined with the natural and realistic growth conditions, make semi-field platform particularly suitable for the development and optimization of phenotyping methods. The semi-field platform enabled the test of three phenotyping techniques from emergence to harvest. Measurements are very convenient on the platform since it is protected by a rain shelter and one can move easily around the plots. Results obtained with digital images were highly correlated with the ones generated in the greenhouse. Similarly, indices computed from near range spectrometry and thermography could be used in the semi-field and in the field to characterise sugar beets under nematode infestation and predict yield.

Unlike some concerns that have been raised by White et al. (2012) and Araus and Cairns (2014), this work demonstrated that it is possible to extrapolate observations from controlled environment to phenotypic traits that can be observed under field conditions. This suggested that semi-field platforms could be used more extensively for the test and development of shoot and root phenotyping methods and trait indicators to be used in greenhouses and in fields. Since imaging technologies are becoming the norm in plant phenomics, there is a need to develop standardised experimental protocols with proper sensor calibration and repeatable measurements (Rahaman et al. 2015). Semi-field experiments could be an appropriate type of platform to establish such standards and technologies and further use them.

Another benefit of semi field platforms stands in the chance to perform deep environmental characterisation. Soil and air conditions can be easily evaluated at high spatial and temporal scales. Therefore, there is a high potential to combine environmental and phenotyping data

to improve existing crop models and predict the degree of nematode infestation and reproduction in the root system. Such information would help to better diagnose nematode stress and better quantify the impact on the yield.

#### **6.4 Conclusion and outlook**

In this thesis, I bring an innovative approach for plant phenotyping method development. The thesis focuses on one model crop that was studied at three different scales, in presence of BCN, using three different phenotyping techniques allowing a fair evaluation of the different approaches. It illustrates how digital phenotyping methods can help to improve the approach used in R&D and support a more effective and sustainable agriculture.

The three methods have different abilities to characterise the sugar beet plants and detect BCN damage. Under controlled conditions, digital imaging is sufficient for early evaluation of the root biomass, for early discrimination of infested and non-infested plants and for early assessment of nematicide activity. In the field, UAV derived hyperspectral images have great potential in predicting final yield, identifying nematode infestation and differentiating germplasm pools for the purpose of nematode tolerance breeding. Overall, under controlled conditions, this thesis balanced the current vision of plant phenotyping based on the use of innovative, advanced and complex tools requiring partly expensive sensors, specific calibration and very precise protocols. We demonstrated that digital cameras supported by specific computer vision tools can be sufficient for early nematode stress detection and nematicide selection.

The main remaining challenge is in the data processing and analysis (Kim et al. 2017). Computer vision approaches have the potential to extract meaningful information from digital images. Advanced phenotyping tools like hyperspectral imagers, thermal cameras and laser scanners are getting cheaper and gain better spatial and spectral resolution. Data storage has been facilitated by the fast development of cloud solutions and wireless networks. Therefore, the main bottleneck is the efficient use of the big amount of data generated and the computation of the right plant trait indicators to better understand the relationships between plant phenotype, genotype and environment. To achieve this, more intensive campaigns of measurements should be carried out in the field and in the semi-field together with the development of sophisticated data mining and analysing tools.

An optimal UAV set up can be proposed based on the results from this thesis. Three on-board sensors should be considered: a high resolution rgb digital camera for canopy cover

measurements in early stages; a thermal camera for canopy temperature evaluation and a hyperspectral camera for SIs and SDIs measurements. With the fast improvement of drone and robotic technologies, one could imagine to develop such UAV system that would take off and fly autonomously when weather conditions are optimal and crop growth stages appropriate. The UAV would automatically recharge batteries on its base and upload data to the cloud for processing. Data would be analysed and integrated with other agronomical information (meteorological data, crop model, crop management practices) to generate suitable traits, maps and farming practices recommendations.



## 7. List of abbreviations

### 7.1 General abbreviations

2D: Two dimensional

3D: Three dimensional

ANOVA: Analysis of variance

BCN: Beet cyst nematodes

°C: Degrees Celsius

das: days after sowing

FAO: Food and Agriculture Organization of the United Nations

GS: Growth stages

Ha: hectare

*H. schachtii*: *Heterodera schachtii*

J2 or J2s: Second stage juveniles

K<sub>2</sub>O: Potassium oxide

kg: kilogram

MAE: Mean absolute error

ME: Mean error

Mg: Magnesium

N: Nitrogen

NIR: Near infrared

P<sub>2</sub>O<sub>5</sub>: Phosphate

PAR: Photosynthetically active radiation

PCA: Principal component analysis

R&D: Research and Development

SDIs: Spectral disease indices

SIs: Spectral indices

SVIs: Spectral vegetation indices

UAV: Unmanned aerial vehicle

VIS: Visible

VPD: Vapour pressure deficit

## **7.2 Spectral indices**

ANSI: ASTER Normalised shortwave index

CHLG: Chlorophyll index

HI: Health index

LCI: Leaf chlorophyll index

MCARI2: Modified chlorophyll absorption ratio index 2

NDNI: Normalised difference nitrogen index

NDVI: Normalised difference vegetation index

NDWI1650: Normalised difference water index 1650

NPCI: Normalised pigment chlorophyll ratio index

PRI: Photochemical reflectance index

SIPI: Structural independent pigment index

RGR: Red green ratio

TCARI: Transformed carotenoid index

TGI: Triangular greenness index

WI\_NDVI: WI/NDVI ratio

WI: Water index

## 8. Literature

**Aasen H, Bolten A (2018)** Multi-temporal high-resolution imaging spectroscopy with hyperspectral 2D imagers—From theory to application. *Remote Sens Environ* 205: 374-389.

**Anderson DB (1936)** Relative humidity or vapor pressure deficit. *Ecology* 17: 277-282.

**Akhtman Y, Golubeva E, Tutubalina O, Zimin M (2017)** Application of hyperspectral images and ground data for precision farming. *Geography, Environment, Sustainability* 10: 117-128.

**Anon (2016)** Anbauinformationen 2016. Arbeitsgemeinschaft für Versuchswesen und Beratung im Zuckerrübenanbau in Baden-Württemberg, Hessen und Pfalz. Worms. [http://www.ruebe.info/uploads/media/Anbauinformationen\\_2016.pdf](http://www.ruebe.info/uploads/media/Anbauinformationen_2016.pdf).

**Araus JL, Cairns JE (2014)** Field high-throughput phenotyping: the new crop breeding frontier. *Trends Plant Sci* 19: 52-61.

**Arvidsson S, Pérez-Rodríguez P, Mueller-Roeber B (2011)** A growth phenotyping pipeline for *Arabidopsis thaliana* integrating image analysis and rosette area modeling for robust quantification of genotype effects. *New Phytol* 191: 895-907.

**Avendano F, Pierce FJ, Schabenberger O, Melakeberhan H (2004)** The spatial distribution of soybean cyst nematode in relation to soil texture and soil map unit. *Agron J* 96: 181-194.

**Bajwa SG, Mishra AR, Norman RJ (2010)** Canopy reflectance response to plant nitrogen accumulation in rice. *Precis Agric* 11: 488-506. doi:10.1007/s11119-009-9142-0.

**Baret F, Guyot G (1991)** Potentials and limits of vegetation indices for LAI and APAR assessment. *Remote Sens Environ* 35: 161-173. doi:10.1016/0034-4257(91)90009-U.

**Bauriegel E, Giebel A, Herppich WB (2011)** Hyperspectral and chlorophyll fluorescence imaging to analyse the impact of *Fusarium culmorum* on the photosynthetic integrity of infected wheat ears. *Sensors* 11: 3765-3779.

**Bendig J, Bolten A, Bareth G (2012)** Introducing a low-cost mini-UAV for thermal- and multispectral-imaging. *Int. Arch. Photogramm. Remote Sens Spat Inf Sci* 39: 345-349.

**Bengough AG, Gordon DC, Al-Menaie H, Ellis RP, Allan D, Keith R, Thomas WTB, Forster BP (2004)** Gel observation chamber for rapid screening of root traits in cereal seedlings. *Plant Soil* 262: 63-70.

**Berg A (1980)** Remote sensing techniques applied to sugar beet diseases in Germany and Italy: Introduction to the results of a European project. *Int Arch Photogramm* 23: 457-462.

**Berni JA, Zarco-Tejada PJ, Suárez L, Fereres E (2009)** Thermal and narrowband multispectral remote sensing for vegetation monitoring from an unmanned aerial vehicle. *IEEE T Geosci Remote* 47: 722-738.

**Biancardi E, McGrath JM, Panella LW, Lewellen RT, Stevanato P (2010)** Sugar Beet In: "Root and Tuber Crops", (Ed.): Bradshaw, JE. *Handbook of Plant Breeding*, Dordrecht Heidelberg London, New York 173-221.

**Breiman L, Friedman J, Olshen R, Stone C (1984)** Classification and regression trees. Belmont, CA: Wadsworth International Group.

**Brodrick HT, Gilbertson B, Kreitzer MH (1971)** Advances in aerial photography. *SA Citrus J* 449: 9-1.

**Bucksch A, Burrige J, York LM, Das A, Nord E, Weitz JS, Lynch JP (2014)** Image-based high-throughput field phenotyping of crop roots. *Plant Physiol* 166: 470-86.

**Burkart A, Hecht VL, Kraska T, Rascher U (2017)** Phenological analysis of unmanned aerial vehicle based time series of barley imagery with high temporal resolution. *Precis Agric* 1-13.

**Campbell MT, Knecht AC, Berger B, Brien CJ, Wang D, Walia H (2015)** Integrating image-based phenomics and association analysis to dissect the genetic architecture of temporal salinity responses in rice. *Plant physiol* 168: 1476-1489.

**Chaki J, Parekh R, Bhattacharya S (2015)** Plant leaf recognition using texture and shape features with neural classifiers. *Pattern Recogn Lett* 58: 61-68.

**Chloupek O, Forster BP, Thomas WTB (2006)** The effect of semi-dwarf genes on root system size in field-grown barley. *Theor Appl Genet* 112: 779-86.

**Clark RT, MacCurdy RB, Jung JK, Shaff JE, McCouch SR, Aneshansley DJ, Kochian LV (2011)** Three-dimensional root phenotyping with a novel imaging and software platform. *Plant physiol* 156: 455-465.

**Clay DE, Kim KI, Chang J, Clay SA, Dalsted K (2006)** Characterizing water and nitrogen stress in corn using remote sensing. *Agron J* 98: 579-587.

**Cobb JN, DeClerck G, Greenberg A, Clark R, McCouch S (2013)** Next-generation phenotyping: Requirements and strategies for enhancing our understanding of genotype–

phenotype relationships and its relevance to crop improvement. *Theor Appl Genet* 126: 867-887.

**Cohen Y, Alchanatis V, Meron M, Saranga Y, Tsipris J (2005)** Estimation of leaf water potential by thermal imagery and spatial analysis. *J Exp Bot* 56: 1843-1852.

**Colombi T, Kirchgessner N, Le Marié CA, York L, Lynch J, Hund A (2015)** Next generation shovelomics: set up a tent and REST. *Plant Soil* 1-20.

**Colomina I, Molina P (2014)** Unmanned aerial systems for photogrammetry and remote sensing: A review. *ISPRS J. Photogramm. Remote Sens* 92: 79-97.

**Constantin D, Rehak M, Akhtman Y, Liebisch F (2015)** Detection of crop properties by means of hyperspectral remote sensing from a micro UAV. In *Bornimer Agrartechnische Berichte* (Vol. 88, No. EPFL-CONF-218662, pp. 129-137). Leibniz-Institut für Agrartechnik Potsdam-Bornim eV.

**Cooke DA, Thomason IJ (1979)** The relationship between population density of *Heterodera schachtii*, soil temperature, and sugarbeet yields. *J Nematol* 11: 124.

**Cooke DA (1984)** The relationship between numbers of *Heterodera schachtii* and sugar beet yields on a mineral soil, 1978-81. *Ann App Biol* 104: 121-129.

**Cooke DA (1987)** Beet cyst nematode (*Heterodera schachtii* Schmidt) and its control on sugar beet. *Agric Zool Rev* 2: 135-183.

**Cooke DA (1991)** The effect of beet cyst nematode, *Heterodera schachtii*, on the yield of sugar beet in organic soils. *Ann App Biol* 118: 153-160.

**Curi J, Zmoray I (1966)** The relation of climatic factors to the duration of the development of *Heterodera schachtii* in Slovakia (CSSR). *Helminthologica* 7: 49-63.

**Curran PJ, Dungan JL, Macler BA, Plummer SE (1991)** The effect of a red leaf pigment on the relationship between red edge and chlorophyll concentration. *Remote Sens Environ* 35: 69-76.

**Datt B (1999)** A new reflectance index for remote sensing of chlorophyll content in higher plants: tests using *Eucalyptus* leaves. *Journal of Plant Physiology* 154: 30-36.

**Davy de Virville J, Person-Dedryver F (1989)** Growth and respiratory activity of roots of various Triticeae tolerant or resistant to *Heterodera avenae* Woll. with or without infection by the nematode. *Rev Nematol* 12: 379-86.

- Decker H (1969)** Biology and control of plant parasitic nematodes. *Phytonematology*. Brill.
- Delalieux S, Somers B, Verstraeten WW, Van Aardt JAN, Keulemans W, Coppin P (2009)** Hyperspectral indices to diagnose leaf biotic stress of apple plants, considering leaf phenology. *Int J Remote Sens* 30: 1887-1912.
- Devienne-Barret F, Richard-Molard C, Chelle M, Maury O, Ney B (2006)** Ara-rhizotron: An effective culture system to study simultaneously root and shoot development of *Arabidopsis*. *Plant Soil* 280: 253-266.
- Diaz-Varela RA, de la Rosa R, Leon L, Zarco-Tejada PJ (2015)** High-resolution airborne UAV imagery to assess olive tree crown parameters using 3D photo reconstruction: application in breeding trials. *Remote Sens* 7: 4213-4232.
- Dietrich RC, Bengough AG, Jones HG, White PJ (2013)** Can root electrical capacitance be used to predict root mass in soil? *Ann Bot* 112: 457-64.
- Dobermann A, Nelson R (2013)** Opportunities and solutions for sustainable food production. United Nations sustainable development solutions network – sustainable agriculture and food systems. Available: [http://unsdsn.org/thematicgroups/tg7/tg7\\_resources](http://unsdsn.org/thematicgroups/tg7/tg7_resources).
- Dougherty (1994)** Digital image processing methods. CRC Press 2: 70-76.
- Duan LF, Yang WN, Huang CL, Liu Q (2011)** A novel machine-vision-based facility for the automatic evaluation of yield-related traits in rice. *Plant Methods* 7: 1-13.
- Egli DB, Rucker M (2012)** Seed vigor and the uniformity of emergence of corn seedlings. *Crop Sci* 52: 2774-82.
- Ellenby C (1954)** Environmental determination of the sex ratio of a plant parasitic nematode. *Nature Lond* 174: 1016-1017.
- Evans K, Franco J (1979)** Tolerance to cyst-nematode attack in commercial potato cultivars and some possible mechanisms for its operation. *Nematologica* 25: 153-162.
- Evans K, Webster RM, Halford PD, Barker AD, Russell MD (2002)** Site-specific management of nematodes-pitfalls and practicalities. *J Nematol* 34: 194-199.
- FAO (2009)** Global agriculture towards 2050. Rome, FAO.
- FAO (2017)** FAOSTAT Online Database. Available: <http://faostat.fao.org/> (accessed November, 2017)

**Frank E, Hall MA, Witten IH (2016)** The WEKA Workbench. Online Appendix for "Data Mining: Practical Machine Learning Tools and Techniques", Morgan Kaufmann, Fourth Edition.

**Franke W (1997)** Nutzpflanzenkunde: nutzbare Gewächse der gemäßigten Breiten, Subtropen und Tropen. Thieme, Stuttgart & New York.

**Furbank RT, Tester M (2011)** Phenomics—technologies to relieve the phenotyping bottleneck. Trends Plant Sci 16: 635-644.

**Gamon JA, Penuelas J, Field CB (1992)** A narrow-waveband spectral index that tracks diurnal changes in photosynthetic efficiency. Remote Sens Environ 41: 35-44.

**Gamon JA, Surfus JS (1999)** Assessing leaf pigment content and activity with a reflectometer. New Phytol 143: 105-117.

**Gardner M, Verma A, Mitchum G (2015)** Emerging roles of cyst nematode effectors in exploiting plant cellular processes. In: Escobar, C.; Fenoll, C. (2015): Advances in botanical research, plant nematode interactions: A view on compatible interrelationships. Academic Press 259–292.

**Gausman HW, Heald CM, Escobar DE (1975)** Effect of *Rotylenchulus reniformis* on reflectance of cotton plant leaves. J Nematol 7: 368-374.

**Gerard B, Buerkert A (1999)** Aerial photography to determine fertiliser effects on pearl millet and *Guiera senegalensis* growth. Plant Soil 210: 167–77.

**Ghanem ME, Marrou H, Sinclair TR (2015)** Physiological phenotyping of plants for crop improvement. Trends Plant Sci 20: 139-144.

**Gitelson AA, Merzlyak MN (1996)** Signature analysis of leaf reflectance spectra: algorithm development for remote sensing of chlorophyll. J Plant physiol 148: 494-500.

**Gitelson AA, Keydan GP, Merzlyak MN (2006)** Three-band model for noninvasive estimation of chlorophyll, carotenoids, and anthocyanin contents in higher plant leaves. Geophys Res Lett 33.

**Glenn OF, Sivasithamparam K (1990)** The effect of soil compaction on the saprophytic growth of *Rhizoctonia solani*. Plant Soil 286: 282-286.

**Golzarian MR, Frick RA, Rajendran K, Berger B, Roy, S, Tester M, Lun DS (2011)** Accurate inference of shoot biomass from high-throughput images of cereal plants. *Plant Methods* 7: 1-11. doi:10.1186/1746-4811-7-2.

**Granier C, Tardieu F (1998)** Is thermal time adequate for expressing the effects of temperature on sunflower leaf development? *Plant Cell Environ* 21: 695-703. doi:10.1046/j.1365-3040.1998.00319.x.

**Granier C, Aguirrezabal L, Cookson SJ, Dauzat M, Hamard P, Thioux JJ, Rolland G, Bouchier-Combaud S, Lebaudy A, Muller B, Simonneau T, Tardieu F (2006)** PHENOPSIS, an automated platform for reproducible phenotyping of plant responses to soil water deficit in *Arabidopsis thaliana* permitted the identification of an accession with low sensitivity to soil water deficit. *New Phytol* 169: 623-635. doi:10.1111/j.1469-8137.2005.01609.x.

**Green CF, Vaidyanatham LV, Ivins JD (1986)** Growth of sugar-beet crops including the influence of synthetic plant growth regulators. *J Agr Sci* 107: 285-297. doi:10.1017/S0021859600087098.

**Grieder C, Hund A, Walter A (2015)** Image based phenotyping during winter: A powerful tool to assess wheat genetic variation in growth response to temperature. *Funct Plant Biol* 42: 387-396.

**Griffin GD (1981)** The relationship of plant age, soil temperature, and population density of *Heterodera schachtii* on the growth of sugarbeet. *J nematol* 13: 184-190.

**Grift TE, Novais J, Bohn M (2011)** High-throughput phenotyping technology for maize roots. *Biosyst Eng* 110: 40-48.

**Grosse E, Banasiak L, Lyr H, Jock M (1985)** Neuer Labortest zum Nachweis des Rübennematoden (*Heterodera schachtii*). *Nachr.-Bl. Pflanzenschutz DDR* 39: 111-112.

**Grosse E, Decker H (1989)** Untersuchungen zur Eignung von Biotest und Schlupftest für den quantitativen Nachweis des Rübenezystenälchen (*Heterodera schachtii*) in Bodenproben. *Nachr.-Bl. Pflanzenschutz DDR* 43: 227-230.

**Guilioni L, Jones HG, Leinonen I, Lhomme JP (2008)** On the relationships between stomatal resistance and leaf temperatures in thermography. *Agr Forest Meteorol* 148: 1908-1912.



**Guo T, Kujirai T, Watanabe T (2012)** Mapping crop status from an unmanned aerial vehicle for precision agriculture applications. In International Archives of the Photogrammetry, Remote Sens Spat Inf Sci 39 (B1), Melbourne, Australia.

**Haboudane D, Miller JR, Pattey E, Zarco-Tejada PJ, Strachan IB (2004)** Hyperspectral vegetation indices and novel algorithms for predicting green LAI of crop canopies: Modeling and validation in the context of precision agriculture. *Remote Sens Environ* 90: 337-352.

**Hafez SL, Sundararaj P (2009)** Evaluation of suppressive effect of trap crops on *Heterodera schachtii* and *Meloidogyne chitwoodi* under greenhouse conditions. *Nematol Mediterr* 37: 245-248.

**Hartmann A, Czauderna T, Hoffmann R, Stein N, Schreiber F (2011)** HTPPheno: An image analysis pipeline for high-throughput plant phenotyping. *BMC Bioinformatics* 12: 148.

**Harveson RM, Jackson TM (2008)** Sugar Beet Cyst Nematode. University of Nebraska, USA.

**Hauer M, Koch HJ, Märlander B (2015)** Water use efficiency of sugar beet cultivars (*Beta vulgaris* L.) susceptible, tolerant or resistant to *Heterodera schachtii* (Schmidt) in environments with contrasting infestation levels. *Field Crop Res* 183: 356-364.

**Haverkort, AJ, Fasan T, Van de Waart M (1991)** The influence of cyst nematodes and drought on potato growth. 2. Effects on plant water relations under semi-controlled conditions. *Neth J Plant Pathol* 97: 162-170.

**Heald CM, Thames WH, Wiegand CL (1972)** Detection of *Rotylenchulus reniformis* infestations by aerial infrared photography. *J Nematol* 4: 298-300.

**Heath WL, Haydock PPJ, Wilcox A, Evans K (2000)** The potential use of spectral reflectance from the potato crop for remote sensing of infection by potato cyst nematodes. *Asp Appl Biol* 60: 185-188.

**Herr L (1996)** Sugar Beet Diseases Incited by *Rhizoctonia* Spp. In: Sneh B, Jabaji-Hare S, Neate S, Dijst G (eds) *Rhizoctonia Species: Taxonomy, Molecular Biology, Ecology, Pathology and Disease Control*. Springer Netherlands, pp 341-349. doi:10.1007/978-94-017-2901-7\_31.

**Hillnhütter C, Schweizer A, Kühnhold V, Sikora RA (2010)** Remote Sensing for the Detection of Soil-Borne Plant Parasitic Nematodes and Fungal Pathogens. *Precision Crop Protection - the Challenge and Use of Heterogeneity*. Oerke EC, Gerhards R, Menz G and Sikora RA. Dordrecht, Springer Netherlands 151-16.

**Hillnhütter C, Mahlein AK, Sikora RA, Oerke EC (2011)** Remote sensing to detect plant stress induced by *Heterodera schachtii* and *Rhizoctonia solani* in sugar beet fields. *Field Crop Res* 122: 70-77.

**Hillnhütter C, Sikora RA, Oerke EC, Van Dusschoten D (2011)** Nuclear magnetic resonance: a tool for imaging belowground damage caused by *Heterodera schachtii* and *Rhizoctonia solani* on sugar beet. *J Exp Bot* 63: 319-327.

**Hillnhütter C, Mahlein AK, Sikora RA, Oerke EC (2012)** Use of imaging spectroscopy to discriminate symptoms caused by *Heterodera schachtii* and *rhizoctonia solani* on sugar beet. *Precis Agric* 13: 17-32. doi:10.1007/s11119-011-9237-2.

**Holen CD, Dexter AGA (1996)** Growing degree day equation for early sugarbeet leaf stages. *Research and extension Reports* 27:152-157.

**Hoyos-Villegas V, Houx J, Singh S, Fritschi F (2014)** Ground-Based digital imaging as a tool to assess soybean growth and yield. *Crop Sci* 54: 1756-1768. doi:10.2135/cropsci2013.08.0540.

**Hunt ER, Daughtry CST, Eitel JU, Long DS (2011)** Remote sensing leaf chlorophyll content using a visible band index. *Agron J* 103: 1090-1099.

**Inoue Y, Kimball BA, Jackson RD, Pinter PJ, Reginato RJ (1990)** Remote estimation of leaf transpiration rate and stomatal resistance based on infrared thermometry. *Agric For Meteorol* 51: 21-33.

**Iyer-Pascuzzi AS, Symonova O, Mileyko Y, Hao Y, Belcher H, Harer J, Weitz JS, Benfey PN (2010)** Imaging and analysis platform for automatic phenotyping and trait ranking of plant root systems. *Plant Physiol* 152: 1148-1157. doi:10.1104/pp.109.150748.

**Jaggard KW, Wickens R, Webb DJ, Scott RK (1983)** Effects of sowing date on plant establishment and bolting and the influence of these factors on yields of sugar beet. *J Agr Sci* 101: 147-161. Doi: 0.1017/S0021859600036479.

**Jahnke S, Menzel MI, Van Dusschoten D, Roeb GW, Bühler J, Minwuyelet S, Blümmer P, Temperton VM, Hombach T, Streun M, Beer S, Khodaverdi M, Ziemons K, Coenen HH, Schurr U (2009)** Combined MRI–PET dissects dynamic changes in plant structures and functions. *Plant J* 59: 634-644.

**Jansen M et al (2009)** Simultaneous phenotyping of leaf growth and chlorophyll fluorescence via GROWSCREEN FLUORO allows detection of stress tolerance in *Arabidopsis thaliana* and other rosette plants. *Funct Plant Biol* 36: 902-914. doi:<http://dx.doi.org/10.1071/FP09095>.

**Jimenez-Bello MA, Royuela A, Manzano J, Zarco-Tejada PJ, Intrigliolo D (2013)** Assessment of drip irrigation sub-units using airborne thermal imagery acquired with an Unmanned Aerial Vehicle (UAV). In *Precision agriculture 13*; Wageningen Academic Publishers, Wageningen pp. 705-711.

**Joalland S, Screpanti C, Gaume A, Walter A (2016)** Belowground biomass accumulation assessed by digital image based leaf area detection. *Plant Soil* 398: 257-266.

**Joalland S, Screpanti C, Liebisch F, Varella HV, Gaume A, Walter A (2017)** Comparison of visible imaging, thermography and spectrometry methods to evaluate the effect of *Heterodera schachtii* inoculation on sugar beets. *Plant Methods* 13: 73.

**Johnson MG, Tingey DT, Phillips DL, Storm MJ (2001)** Advancing fine root research with minirhizotrons. *Environ Exp Bot* 45: 263-89.

**Jones FGW (1980)** Some aspects of the epidemiology of plant parasitic nematodes. *Comparative epidemiology, a tool for better disease management* Ed. J Palti and J Kranz 71-92.

**Jones HG (2004)** Application of thermal imaging and infrared sensing in plant physiology and ecophysiology. *Adv Bot Res* 41: 107-163.

**Jones HG, Schofield P (2008)** Thermal and other remote sensing of plant stress. *Gen Appl Plant Physiol* 34: 19-32.

**Kämpfe L, Kerstan U (1964)** Die Beeinflussung des Geschlechtsverhältnisses in der Gattung *Heterodera* Schmidt. *Nematologica* 10: 388-398.

**Khanal S, Fulton J, Shearer S (2017)** An overview of current and potential applications of thermal remote sensing in precision agriculture. *Comput Electron Agr* 139: 22-32.

**Khanna R, Möller M, Pfeifer J, Liebisch F, Walter A, Siegwart R (2015)** Beyond point clouds-3d mapping and field parameter measurements using uavs. In *Emerging Technologies and Factory Automation (ETFA)*, Proceedings of the IEEE 20th Conference on IEEE, pp. 1-4.

**Kim SL, Solehati N, Choi IC, Kim KH, Kwon TR (2017)** Data management for plant phenomics. *J Plant Biol* 60: 285-297.

- Kirchgessner N, Liebisch F, Yu K, Pfeifer J, Friedli M, Hund A, Walter A (2017)** The ETH field phenotyping platform FIP: A cable-suspended multi-sensor system. *Funct Plant Biol* 44: 154-168.
- Koch DW, Gray FA, Krall JM (1999)** Trap crops: A promising alternative for sugar beet nematode control. Cooperative Extension Service, University of Wyoming, Department of Plant Sciences.
- Koyanagi T, Imai O, Yoshida K (1998)** Development of a new nematicide, fosthiazate. *J Pestic Sci* 23: 174-183.
- Laemmlen F (2010)** Sugarbeet Cyst Nematode - Biology and Management.
- Landis JR, Koch GG (1977)** The measurement of observer agreement for categorical data. *Biometrics* 159-174.
- Laudien R (2005)** Entwicklung eines GIS-gestützten schlagbezogenen Führungsinformationssystems für die Zuckerrwirtschaft. (Development of a field- and GIS-based management information system for the sugar beet industry). PhD thesis University of Hohenheim. Germany.
- Lee YJ (1989)** Aerial photography for the detection of soil-borne disease. *Can J Plant Pathol* 11: 173-176.
- Leinonen I, Grant OM, Tagliavia CPP, Chaves MM, Jones HG (2006)** Estimating stomatal conductance with thermal imagery. *Plant Cell Environ* 29: 1508-1518.
- Leister D, Varotto C, Pesaresi P, Niwergall A, Salamini F (1999)** Large-scale evaluation of plant growth in *Arabidopsis thaliana* by non-invasive image analysis. *Plant Physiol Bioch* 37: 671-678. doi:[http://dx.doi.org/10.1016/S0981-9428\(00\)80097-2](http://dx.doi.org/10.1016/S0981-9428(00)80097-2).
- Le Marié CA, Kirchgessner N, Marschall D, Walter A, Hund A (2014)** Rhizoslides: paper-based growth system for non-destructive, high throughput phenotyping of root development by means of image analysis. *Plant Methods* 10: 13-29.
- Lewis D, Yao H, Fridgen J, Kincaid R (2006)** Investigation on the potential of using ASTER image for corn plant residue coverage estimation in three Indiana counties. In *Geoscience and Remote Sensing Symposium, 2006. IGARSS 2006. IEEE International Conference on* (pp. 2092-2094). IEEE.

**Li L, Zhang Q, Huang D (2014)** A review of imaging techniques for plant phenotyping. *Sensors* 14: 20078-20111.

**Li Y, Chen D, Walker CN, Angus JF (2010)** Estimating the nitrogen status of crops using a digital camera. *Field Crop Res* 118: 221-227. doi:<http://dx.doi.org/10.1016/j.fcr.2010.05.011>.

**Liebisch F, Küng G, Damm A, Walter A (2014)** Characterization of crop vitality and resource use efficiency by means of combining imaging spectroscopy based plant traits. Workshop on hyperspectral image and signal processing: Evolution in remote sensing. 24-27 June 2014, Lausanne, Switzerland, IEEE International. 6.

**Liebisch F, Kirchgessner N, Schneider D, Walter A, Hund A (2015)** Remote, aerial phenotyping of maize traits with a mobile multi-sensor approach. *Plant Methods* 11: 9.

**Luc M, Sikora RA, Bridge J (2005)** Plant parasitic nematodes in subtropical and tropical agriculture. CABI Bioscience, Egham.

**Lukina EV, Stone ML, Raun WR (1999)** Estimating vegetation coverage in wheat using digital images. *J Plant Nutr* 22: 341-350. doi:[10.1080/01904169909365631](https://doi.org/10.1080/01904169909365631).

**Ma BL, Dwyer LM, Costa C, Cober ER, Morrison MJ (2001)** Early Prediction of Soybean Yield from Canopy Reflectance Measurements ECORC Contrib. no. 11618 *Agron J* 93: 1227-1234. doi:[10.2134/agronj2001.1227](https://doi.org/10.2134/agronj2001.1227).

**Mahlein AK, Steiner U, Dehne HW, Oerke EC (2010)** Spectral signatures of sugar beet leaves for the detection and differentiation of diseases. *Precis Agric* 11: 413-431.

**Mahlein AK, Oerke EC, Steiner U, Dehne HW (2012)** Recent advances in sensing plant diseases for precision crop protection. *Eur J Plant Pathol* 133: 197-209.

**Mahlein AK, Rumpf T, Welke P, Dehne HW, Plümer L, Steiner U, Oerke EC (2013)** Development of spectral indices for detecting and identifying plant diseases. *Remote Sens Environ* 128: 21-30.

**Mathieu L, Lobet G, Tocquin P, Périlleux C (2015)** "Rhizoponics": A novel hydroponic rhizotron for root system analyses on mature *Arabidopsis thaliana* plants. *Plant methods* 11: 3.

**Meier U, Bachmann E, Buhtz H, Hack H, Klose R, Märländer B, Weber E (1993)** Phenological growth stages of beta beets (*Beta vulgaris* L. spp.). *Nachrichtenbl Deut Pflanzenschutzd* 45: 37-41.

**Metzner R, van Dusschoten D, Bühler J, Schurr U, Jahnke S (2014)** Belowground plant development measured with magnetic resonance imaging (MRI): Exploiting the potential for non-invasive trait quantification using sugar beet as a proxy. *Front Plant Sci* 5.

**Milford GFJ, Pocock TO, Riley J (1985a)** An analysis of leaf growth in sugar-beet. I. Leaf appearance and expansion in relation to temperature under controlled conditions. *Ann Appl Biol* 106: 163-172. doi:10.1111/j.1744-7348.1985.tb03106.x.

**Milford GFJ, Pocock TO, Riley J (1985b)** An analysis of leaf growth in sugar beet. II. Leaf appearance in field crops. *Ann Appl Biol* 106: 173-185. doi:10.1111/j.1744-7348.1985.tb03107.x.

**Milford GFJ, Pocock TO, Riley J, Messem AB (1985)** An analysis of leaf growth in sugar beet. *Ann Appl Biol* 106: 187-203.

**Milford GFJ, Travis KZ, Pocock TO, Jaggard KW, Day W (1988)** Growth and dry-matter partitioning in sugar beet. *J Agr Sci* 110: 301-308. doi:10.1017/S0021859600081326.

**Mistele B, Gutser R, Schmidhalter U (2004)** Validation of field-scaled spectral measurements of the nitrogen status in winter wheat. In *Seventh international conference on precision agriculture and other precision resources management, Minneapolis, Minnesota, USA* (Ed D Mulla) (pp. 1187-1195).

**Mizoue N, Masutani T (2003)** Image analysis measure of crown condition, foliage biomass and stem growth relationships of *Chamaecyparis obtusa*. *Forest Ecol Manag* 172: 79-88. doi:http://dx.doi.org/10.1016/S0378-1127(02)00281-5.

**Mooney SJ, Pridmore TP, Helliwell J, Bennett MJ (2012)** Developing X-ray computed tomography to non-invasively image 3-D root systems architecture in soil. *Plant soil* 352: 1-22.

**Mullan DJ, Reynolds MP (2010)** Quantifying genetic effects of ground cover on soil water evaporation using digital imaging. *Funct Plant Biol* 37: 703-712.

**Müller J (1979)** Über die Generationenzahl von *Heterodera schachtii* unter Feldbedingungen an Zuckerrüben. *Nachrichtenblatt Deutscher Pflanzenschutzdienst* 31: 92-95.

**Müller J (1999)** The economic importance of *Heterodera schachtii* in Europe. *Helminthologia* 36: 205-213.

**Munns R, James RA, Sirault XR, Furbank RT, Jones HG (2010)** New phenotyping methods for screening wheat and barley for beneficial responses to water deficit. *J Exp Bot* 61: 3499–3507.

**Nagel KA, Kastenholz B, Jahnke S, van Dusschoten D, Aach T, Mühlich M, Truhn D, Scharr H, Terjung S, Walter A, Schurr U (2009)** Temperature responses of roots: Impact on growth, root system architecture and implications for phenotyping. *Funct Plant Biol* 36: 947–959.

**Nagel KA, Putz A, Gilmer F, Heinz K, Fischbach A, Pfeifer J, Faget M, Blossfeld S, Ernst M, Dimaki C, Kastenholz B, Kleinert AK, Galinski A, Scharr H, Fiorani F, Schurr U (2012)** GROWSCREEN-Rhizo is a novel phenotyping robot enabling simultaneous measurements of root and shoot growth for plants grown in soil-filled rhizotrons. *Funct Plant Biol* 39: 891–904. doi: 10.1071/fp12023.

**Nagel KA, Bonnett D, Furbank R, Walter A, Schurr U, Watt M (2015)** Simultaneous effects of leaf irradiance and soil moisture on growth and root system architecture of novel wheat genotypes: implications for phenotyping. *J Exp Bot* 66: 5441–5452.

**Neilson EH, Edwards AM, Blomstedt CK, Berger B, Møller BL, Gleadow RM (2015)** Utilization of a high-throughput shoot imaging system to examine the dynamic phenotypic responses of a C<sub>4</sub> cereal crop plant to nitrogen and water deficiency over time. *J Exp Bot* 66: 1817–1832.

**Neumann K, Verburg PH, Stehfest E, Müller C (2010)** The yield gap of global grain production: A spatial analysis. *Agricultural Systems* 103: 316–326.

**Norman GG, Fritz NL (1965)** Infrared photography as an indicator of disease and decline in citrus trees. *Proc Florida State Hort Soc* 78: 59–63.

**Nutter FW, Tylka GL, Guan J, Moreira AJD, Marett CC, Rosburg TR, et al (2002)** Use of remote sensing to detect soybean cyst nematode-induced plant stress. *J Nematol* 34: 222–231.

**OECD/FAO (2012)** OECD-FAO Agricultural Outlook 2012–2021, OECD Publishing and FAO. Available: [http://dx.doi.org/10.1787/agr\\_outlook-2012-en](http://dx.doi.org/10.1787/agr_outlook-2012-en).

**Oerke EC (2005)** Crop losses to pests. *J Agric Sci* 144: 31–43.

**Oerke EC, Steiner U (2010)** Potential of digital thermography for disease control. In *Precision Crop Protection-the Challenge and Use of Heterogeneity*. Springer Netherlands. 167–182.

**Olthof HA (1983)** Effect of plant age and transplanting damage on sugar beets infected by *Heterodera schachtii*. *J Nematol* 15: 555-559.

**Oostenbrink M (1966)** Major characteristics of the relations between nematodes and plants. Reports of the 8th International Symposium of nematology 8-10.

**Paez-Garcia A, Motes CM, Scheible WR, Chen R, Blancaflor EB, Monteros MJ (2015)** Root traits and phenotyping strategies for plant improvement. *Plants* 4: 334-355.

**Pantelalis I, Karpouzas DG, Menkissoglu-Spiroudi U, Tsiropoulos N (2006)** Influence of Soil Physicochemical and Biological Properties on the Degradation and Adsorption of the Nematicide Fosthiazate. *J Agr Food Chem* 54: 6783-6789.

**Paruelo JM, Lauenroth WK, Roset PA (2000)** Estimating Aboveground Plant Biomass Using a Photographic Technique. *J Range Manage* 53: 190-193.

**Penuelas J, Gamon JA, Fredeen AL, Merino J, Field CB (1994)** Reflectance indices associated with physiological changes in nitrogen-and water-limited sunflower leaves. *Remote Sens Environ* 48: 135-146.

**Penuelas J, Baret F, Filella I (1995)** Semi-empirical indices to assess carotenoids/chlorophyll a ratio from leaf spectral reflectance. *Photosynthetica* 31: 221-230.

**Penuelas J, Pinol J, Ogaya R, Filella I (1997)** Estimation of plant water concentration by the reflectance water index WI (R900/R970). *Int J Remote Sens* 18: 2869-2875.

**Perez-Sanz F, Navarro PJ, Egea-Cortines M (2017)** Plant phenomics: An overview of image acquisition technologies and image data analysis algorithms. *GigaScience* gix092.

**Pfeifer J, Kirchgessner N, Colombi T, Walter A (2015)** Rapid phenotyping of crop root systems in undisturbed field soils using X-ray computed tomography. *Plant methods* 11: 41.

**Pfeifer J, Khanna R, Constantin D, Popovic M, Galceran E, Kirchgessner N, Walter A, Siegwart R, Liebisch F (2016)** Towards automatic UAV data interpretation for precision farming. CIGR-AgEng conference. Aarhus, Denmark.

**Pingali PL (2012)** Green Revolution: Impacts, limits, and the path ahead. *P Natl A Sci* 109: 12302-12308.

**Primicerio J, Di Gennaro SF, Fiorillo E, Genesio L, Lugato E, Matese A, Vaccari FPA (2012)** Flexible unmanned aerial vehicle for precision agriculture. *Precis Agric* 13: 517-523.



**R Development Core Team (2008)** R: A language and environment for statistical computing. R Foundation for Statistical Computing, Vienna, Austria. ISBN 3-900051-07-0, URL <http://www.R-project.org>

**Radcliffe DE, Hussey RS, McClendon RW (1990)** Cyst nematode vs. tolerant and intolerant soybean cultivars. *Agron J* 82: 855-60.

**Radford PJ (1967)** Growth Analysis Formulae - Their Use and Abuse1. *Crop Sci* 7: 171-175.

**Rahaman MM, Chen D, Gillani Z, Klukas C, Chen M (2015)** Advanced phenotyping and phenotype data analysis for the study of plant growth and development. *Front Plant Sci* 6.

**Rao NS, Laxman RH, Shivashankara KS (2016)** Physiological and Morphological Responses of Horticultural Crops to Abiotic Stresses. *Abiotic Stress Physiology of Horticultural Crops*. Springer India 3-17.

**Ray DK, Mueller ND, West PC, Foley JA (2013)** Yield trends are insufficient to double global crop production by 2050. *PLoS one* 8:e66428. doi: 10.1371/journal.pone.0066428.

**Rebetzke GJ, Rattey AR, Farquhar GD, Richards RA, Condon ATG (2013)** Genomic regions for canopy temperature and their genetic association with stomatal conductance and grain yield in wheat. *Func Plant Bio* 40: 14-33.

**Reuther M, Lang C, Grundler FMW (2017)** Nematode-tolerant sugar beet varieties – resistant or susceptible to the Beet Cyst Nematode *Heterodera schachtii*? *Sugar industry* 142: 277-284.

**Rezbová H, Belová A, Skubna O (2013)** Sugar beet production in the European Union and their future trends. *Agris On-line Papers in Economics and Informatics* 5: 165.

**Roessner U, Willmitzer L, Fernie AR (2001)** High-resolution metabolic phenotyping of genetically and environmentally diverse potato tuber systems. Identification of phenocopies. *Plant physiol* 127: 749-764.

**Roth L, Streit B (2017)** Predicting cover crop biomass by lightweight UAS-based RGB and NIR photography: an applied photogrammetric approach. *Precis Agric* 1-22. doi:10.1007/s11119-017-9501-1.

**Rouse JW, Haas RH, Schell JA, Deering DW (1974)** Monitoring vegetation systems in the Great Plains with ERTS. *NASA special publication* 351: 309.

- Sa I, Chen Z, Popovic M, Khanna R, Liebisch F, Nieto J (2018)** Siegwart, R. weedNet: Dense Semantic Weed Classification Using Multispectral Images and MAV for Smart Farming. *IEEE Robot Autom Lett* 3: 588-595.
- Sankaran S, Khot LR, Espinoza CZ, Jarolmasjed S, Sathuvalli VR, Vandemark GJ, Miklas PN, Carter AH, Pumphrey MO, Knowles NR, Pavek MJ (2015)** Low-altitude, high-resolution aerial imaging systems for row and field crop phenotyping: A review. *Eur J Agron* 70: 112-123.
- Schäffer A, van den Brink P, Heimbach F, Hoy S, de Jong F, Römlke J, Sousa JP, Roß-Nickoll (2008)** Semi-field methods are a useful tool for the environmental risk assessment of pesticides in soil. *Env Sci Pollut Res* 15: 176–177.
- Schaeffer A., van den Brink PJ, Heimbach F, Hoy SP, de Jong FM, Rombke J, Sousa JP (Eds.) (2010)** Semi-field methods for the environmental risk assessment of pesticides in soil. CRC Press.
- Scharr H, Minervini M, French AP, Klukas C, Kramer DM, Liu X, Luengo I, Pape JM, Polder G, Vukadinovic D, Yin X, Tsaftaris SA (2016)** Leaf segmentation in plant phenotyping: A collation study. *Mach Vision Appl* 27: 585-606.
- Schmitz A, Kiewnick S, Schlang J, Sikora RA (2004)** Use of high resolution digital thermography to detect *Heterodera schachtii* infestation in sugar beets. *Commun Agric Appl Biol Sci* 69: 359-363.
- Schmitz A, Tartachnyk II, Kiewnick S, Sikora RA, Kühbauch W (2006)** Detection of *Heterodera schachtii* infestation in sugar beet by means of laser-induced and pulse amplitude modulated chlorophyll fluorescence. *Nematology* 8: 273-286.
- Schulz H, Postma JA, van Dussloten D, Scharr H, Behnke S (2013)** Plant Root System Analysis from MRI Images. *Comm Com Inf Sc* 359: 411-425.
- Scott RK, English SD, Wood DW, Unsworth MH (1973)** The yield of sugar beet in relation to weather and length of growing season. *J Agri Sci* 81: 339-347. doi:10.1017/S0021859600059001.
- Seinhorst JW (1965)** The relation between nematode density and damage to plants. *Nematologica* 11: 137-154. doi:doi:10.1163/187529265X00582.

**Serrano L, Penuelas J, Ustin SL (2002)** Remote sensing of nitrogen and lignin in Mediterranean vegetation from AVIRIS data: Decomposing biochemical from structural signals. *Remote Sens Environ* 81: 355-364.

**Shakoor N, Lee S, Mockler TC (2017)** High throughput phenotyping to accelerate crop breeding and monitoring of diseases in the field. *Curr Opin Plant Biol* 38: 184-192.

**Sher-Kaul S, Oertli B, Castella E, Lachavanne JB (1995)** Relationship between biomass and surface area of six submerged aquatic plant species. *Aquat Bot* 51: 147-154. doi:[http://dx.doi.org/10.1016/0304-3770\(95\)00460-H](http://dx.doi.org/10.1016/0304-3770(95)00460-H).

**Sherrod PH (2008)** DTREG Predictive Modeling Software. Users Manual. [www.dtregh.com/DTREG.pdf](http://www.dtregh.com/DTREG.pdf).

**Siddique S, Radakovic Z, De La Torre CM, Chronis T, Novák O, Raireddy W, Holbein J, Matera C, Hütten M, Gutbrod P, Anjam MS, Rozanska E, Habash S, Elashry A, Sobczak M, Kakimoto T, Strnad M, Schmülling T, Mitchum MG, Grundler FMW (2015)** A parasitic nematode releases cytokinin that controls cell division and orchestrates feeding site formation in host plants. *PNAS* 112: 12669-12674.

**Smith SM, Garrett PB, Leeds JA, McCormick PV (2000)** Evaluation of digital photography for estimating live and dead aboveground biomass in monospecific macrophyte stands. *Aquat Bot* 67: 69-77. doi:[http://dx.doi.org/10.1016/S0304-3770\(99\)00085-6](http://dx.doi.org/10.1016/S0304-3770(99)00085-6).

**Steele AE (1965)** The host range of the sugar beet nematode, *Heterodera schachtii* Schmidt. *J Am Soc Sugar Beet* 13: 573-603.

**Stehlik V (1938)** La feuille de betterave sucrière. In: Communication au VIIIème congrès de l'IIRB janvier 1938.

**Stelter H (1963)** Die Vermehrung der Rasse B des Kartoffelnematoden, *Heterodera rostochiensis* Woll., an der A-anfälligen Sorte Aquila und der Aresistenten Sorte Spekula. *Nematologica* 9: 237-240.

**Tackenberg O (2007)** A new method for non-destructive measurement of biomass, growth rates, vertical biomass distribution and dry matter content based on digital image analysis. *Ann Bot London* 99: 777-783.

**Tattaris M, Reynolds MP, Chapman SC (2016)** A Direct Comparison of Remote Sensing Approaches for High-Throughput Phenotyping in Plant Breeding. *Front. Plant Sci* 7: 1131.

**Taubenhaus JJ, Ezekiel WN, Neblette CB (1929)** Airplane photography in the study of cotton root rot. *Phytopathology* 19: 1025-1029.

**Tekrony DM, Egli DB (1991)** Relationship of seed vigor to crop yield: A review. *Crop Sci* 31: 816-22.

**Thenkabail PS, Smith RB, De Pauw E (2000)** Hyperspectral vegetation indices and their relationships with agricultural crop characteristics. *Remote Sens Environ* 71: 158-182.

**Tilman D, Balzer C, Hill J, Befort BL (2011)** Global food demand and the sustainable intensification of agriculture. *Proc Natl Acad Sci USA* 108: 20260-20264.

**Trachsel S, Kaeppler SM, Brown KM, Lynch JP (2011)** Shovelomics: High throughput phenotyping of maize (*Zea mays* L.) root architecture in the field. *Plant Soil* 341: 75-87.

**Trotter GM, Whitehead D, Pinkney EJ (2002)** The photochemical reflectance index as a measure of photosynthetic light use efficiency for plants with varying foliar nitrogen contents. *Int J Remote Sens* 23: 1207-1212.

**Trudgill DL (1980)** Effects of *Globodera rostochiensis* and fertilisers on the mineral nutrient content and yield of potato plants. *Nematologica* 26: 243-54.

**Trudgill, D. L. (1986)** Concepts of resistance, tolerance and susceptibility in relation to cyst nematodes. In *Cyst nematodes* (pp. 179-189). Springer US.

**Trudgill DL (1991)** Resistance to and tolerance of plant parasitic nematodes in plants. *Ann Rev Phytopathol* 29: 167-192.

**Trudgill DL (1992)** Mechanisms of damage and of tolerance in nematode infested plants. *Nematology from molecule to ecosystem*. European Society of Nematologists Invergowrie, Dundee 133-145.

**Tuberosa R, Sanguineti MC, Landi P, Giuliani MM, Salvi S, Conti S (2002)** Identification of QTLs for root characteristics in maize grown in hydroponics and analysis of their overlap with QTLs for grain yield in the field at two water regimes. *Plant Mol Biol* 48: 697-712.

**Van Dusschoten D, Metzner R, Kochs J, Postma JA, Pflugfelder D, Bühler J, Schurr U, Jahnke S (2016)** Quantitative 3D analysis of plant roots growing in soil using magnetic resonance imaging. *Plant Physiol* 170: 1176-1188.

**Virlet N, Sabermanesh K, Sadeghi-Tehran P, Hawkesford MJ (2017)** Field Scanalyzer: An automated robotic field phenotyping platform for detailed crop monitoring. *Funct Plant Bio* 44: 143-153.

**Wallace HR (1988)** A perception of tolerance. *Nematologica* 33: 419-32.

**Walter A, Silk WK, Schurr U (2009)** Environmental effects on spatial and temporal patterns of leaf and root growth. *Annu Rev Plant Biol* 60: 279-304.

**Walter A, Studer B, Kölliker R (2012)** Advanced phenotyping offers opportunities for improved breeding of forage and turf species. *Ann Bot* 110: 1271-1279. doi:10.1093/aob/mcs026.

**Walter A, Liebisch F, Hund A (2015)** Plant phenotyping: From bean weighing to image analysis. *Plant Methods* 11: 14.

**Watt M, Moosavi S, Cunningham SC, Kirkegaard JA, Rebetzke GJ, Richards RA (2013)** A rapid, controlled-environment seedling root screen for wheat correlates well with rooting depths at vegetative, but not reproductive, stages at two field sites. *Ann Bot* 112: 447-55.

**Weiss SM, Kulikowski CA (1991)** Computer systems that learn. Kaufmann Publishers, San Mateo, CA, USA.

**Westphal A (2013)** Vertical distribution of *Heterodera schachtii* under susceptible, resistant, or tolerant sugar beet cultivars. *Plant Dis* 97: 101-106.

**White JW, Andrade-Sanchez P, Gore MA, Bronson KF, Coffelt TA, Conley MM, Feldmann KA, French AN, Heun JT, Hunsaker DJ, Jenks MA, Kimball BA, Roth RL, Strand RJ, Thorp KR, Wall GW, Wang G (2012)** Field-based phenomics for plant genetics research. *Field Crop Res* 133: 101-112.

**Wiese A, Christ MM, Virnich O, Schurr U, Walter A (2007)** Spatio-temporal leaf growth patterns of *Arabidopsis thaliana* and evidence for sugar control of the diel leaf growth cycle. *New Phytol* 174: 752-761.

**Wishart J, George T, Brown L, White P, Ramsay G, Jones H, Gregory P (2014)** Field phenotyping of potato to assess root and shoot characteristics associated with drought tolerance. *Plant Soil* 378: 351-363. doi:10.1007/s11104-014-2029-5.

**Witten IH, Frank E, Hall MA, Pal CJ (2016)** Data Mining: Practical machine learning tools and techniques. Morgan Kaufmann.

**Woebbecke DM, Meyer GE, Von Bargen K, Mortensen DA (1995a)** Color indices for weed identification under various soil, residue and lighting conditions. *Transactions of the ASAE* 38: 259-269.

**Woods SR, Haydock PJ, Edmunds C (1999)** Mode of action of fosthiazate used for the control of the potato cyst nematode *Globodera pallida*. *Ann Appl Biol* 135: 409-415.

**Wyse-Pester DY, Wiles LJ, Westra P (2002)** The potential for mapping nematode distributions for site-specific management. *J Nematol* 34: 80-87.

**Wyss U, Grundler FMW, Munch A (1992)** The parasitic behaviour of second-stage juveniles of *Meloidogyne incognita* in roots of *Arabidopsis thaliana*. *Nematologica* 38: 98-111.

**Yang C, Everitt JH (2002)** Relationships between yield monitor data and airborne multirate digital imagery for grain sorghum. *Precis Agric* 3: 373-388. doi:10.1023/a:1021544906167.

**Yang W, Guo Z, Huang C, Duan L, Chen G, Jiang N, Fang W, Geng H, Xie W, Lian X, Wang G, Luo Q, Zhang Q, Liu Q, Xiong L (2014)** Combining high-throughput phenotyping and genome-wide association studies to reveal natural genetic variation in rice. *Nat Commun* 5.

**Yang G, Liu J, Zhao C, Li Z, Huang Y, Yu H, Xu B, Yang X, Zhu D, Zhang X, Zhang R, Feng H, Zhao X, Li Z, Li H, Yang H (2017)** Unmanned Aerial Vehicle Remote Sensing for Field-Based Crop Phenotyping: Current Status and Perspectives. *Front Plant Sci* 8.

**Yu K, Lenz-Wiedemann V, Chen X, Bareth G (2014)** Estimating leaf chlorophyll of barley at different growth stages using spectral indices to reduce soil background and canopy structure effects. *ISPRS J Photogramm* 97: 58-77.

**Yu K, Kirchgessner N, Grieder C, Walter A, Hund A (2017)** An image analysis pipeline for automated classification of imaging light conditions and for quantification of wheat canopy cover time series in field phenotyping. *Plant Methods* 13: 15.

**Zhu J, Ingram PA, Benfey PN, Elich T (2011)** From lab to field, new approaches to phenotyping root system architecture. *Curr Opin Plant Biol* 14: 310-317.

## 9. Acknowledgement

This thesis would not have been possible without the help of many persons.

First of all, I would like to express my gratitude to Dr. Claudio Screpanti for offering me the opportunity to do my PhD in Syngenta. I am very grateful for his constant support, advice and the confidence he has placed in me. These three and a half years of PhD thesis were a great journey where I learnt a lot, not only about sciences but also about myself. I also would like to say thank you to Dr. Alain Gaume, Cliff Watrin and Rita Kuznia for their sponsorship and scientific advice all along my PhD thesis in Syngenta.

Second - but not less - I would like to thank Prof. Achim Walter for his supervision and for giving me the chance to do my PhD thesis in his group. Your advice were always relevant and helpful.

I would like to thank Dr. Frank Liebisch for the great support and help during the last three years and for agreeing being my co-examiner. Our discussion were always very fruitful. We spent some good time in the field for sugar beet phenotyping. You really passed me your passion for agriculture and remote sensing.

I also would like to thank Prof. Jeremie Lecoer for his availability when I had questions and for agreeing being my co-examiner.

Next, I would like to thank Dr. Hubert Varella for the precious support regarding data analysis and statistics but even more for his friendship and the great time spent playing basketball or drinking beers.

In five years in Syngenta, I have met a lot of people. I have spent very pleasant times within my team in a very stimulating working environment. I am very happy to have worked with so many colleagues. Especially, I would like to thank Nuria Bonilla, Laure Castelli, Brigitte Slaats, Beat Reber, Jan Werthmüller, Tobias Plec and Alain Jost for their support and enthusiasm and for contributing in this thesis with smaller and bigger proportions. Many thanks also to all colleagues from Biology and Chemistry with whom I enjoyed my work and my time in Stein.

Special thanks go to Marco Pari for his excellent job as an MSc student.

I would also like to thank my colleagues from the group of Crop Sciences. As an external PhD student, I only spent a few time there but I have always enjoyed being in Zürich and discussing with you.

The support of my long-term friends cannot be underestimated and I would like to thank you all for the great time we always spent together.

I am grateful to my parents and my two brothers for their constant support and encouragement and for always being there for me.